Radio resource allocation in relay based OFDMA cellular networks

Xiao, Lin

Radio Resource Allocation in Relay Based OFDMA Cellular Networks

Lin Xiao

Submitted for the degree of Doctor of Philosophy

School of
Electronic Engineering and Computer Science
Queen Mary, University of London

January 2010

To all the people I love

Abstract

Adding relay stations (RS) between the base station (BS) and the mobile stations (MS) in a cellular system can extend network coverage, overcome multi-path fading and increase the capacity of the system.

This thesis considers the radio resource allocation scheme in relay based cellular networks to ensure high-speed and reliable communication. The goal of this research is to investigate user fairness, system throughput and power consumption in wireless relay networks through considering how best to manage the radio resource.

This thesis proposes a two-hop proportional fairness (THPF) scheduling scheme fair allocation, which is considered both in the first time subslot between direct link users and relay stations, and the second time subslot among relay link users.

A load based relay selection algorithm is also proposed for a fair resource allocation. The transmission mode (direct transmission mode or relay transmission mode) of each user will be adjusted based on the load of the transmission node.

Power allocation is very important for resource efficiency and system performance improvement and this thesis proposes a two-hop power allocation algorithm for energy efficiency, which adjusts the transmission power of the BS and RSs to make the data rate on the two hop links of one RS match each other.

The power allocation problem of multiple cells with inter-cell interference is studied. A new multi-cell power allocation scheme is proposed from non-cooperative game theory; this coordinates the inter-cell interference and operates in a distributed manner. The utility function can be designed for throughput improvement and user fairness respectively.

Finally, the proposed algorithms in this thesis are combined, and the system performance is evaluated. The joint radio resource allocation algorithm can achieve a very good tradeoff between throughput and user fairness, and also can significantly improve energy efficiency.

Acknowledgement

I would like to express my gratitude to all those who helped me to complete this research.

The first person I want to say "thank you" to is my supervisor Prof Laurie Cuthbert. During my PhD time, he gave me the strongest support and guidance for both my study and daily life. He gave me lots of freedom to study an area that interested me and he encouraged every small progress I have ever made. His selflessness, goodness to students, and passion for the work is the treasure that I value for the rest of my life.

I would also like to express my appreciation to Dr Yue Chen and Dr John Schormans for their helpful suggestions and comments on my research. Yue Chen, who is my second supervisor, is a nice, beautiful, and smart woman who gave me a lot of useful advice during my study. John Schormans gave me his support and encouragement, boosting my confidence and helping me to finish the study well.

Finishing a PhD degree abroad is not easy, but because of the company of my lovely friends, the memory of the last three years is so beautiful and colourful. Thanks Keijing Zhang, Luo Liu, Dapeng Zhang, Xiaojing Wang, and so many others. You are my best friends forever.

In my life, there are so many people I should thank. The love they have given me is enormous and selfless. With my love and gratitude, I want to dedicate this thesis to all the people who have ever helped me.

Contents

List of Figures

List of Abbreviations

3G	Third Generation
3GPP	The 3rd Generation Partner Project
AF	Amplify and Forwarding
ART	Above Roof Top
AWGN	Additive White Gaussian Noise
BER	Bit Error Rate
BRT	Below Roof Top
BS	Base Station
BW	Bandwidth
CDF	Cumulative distribution Function
CP	Cyclic Prefix
CQI	Channel Quality Indicator
CSI	Channel State Information
DACs	Digital-to-Analogue Converters
DF	Decode and Forwarding
DFT	Discrete Fourier Transform
DL	Downlink
DMPA	Distributed Multi-cell Power Allocation
EQPA	Equal Power Allocation
EU	European Union
E-UTRAN	Evolved UMTS Terrestrial Radio Access Network
FDD	Frequency Division Duplex
FDM	Frequency-Division Multiplexing
FFT	Fast Fourier Transform

FP 6	Framework Programmes 6
FRF	Frequency Reuse Factor
HDR	High Data Rate
ICI	Inter-carrier Interference
IDFT	Inverse Discrete Fourier Transform
IEEE	The Institute of Electrical and Electronics Engineers
IFFT	Inverse Fast Fourier Transform
ITU-R	International Telecommunications Union Radio communication sector
LBRS	Load Based Relay Selection
LOS	Line-of-Sight
LRTN	Joint Algorithm of LBRS, RR, THPA, NPAG
LRTN-F	Joint Algorithm of LBRS, RR, THPA, NPAG-F
LTE	Long Term Evolution
LTE-A	Long Term Evolution Advanced
LTTN	Joint Algorithm of LBRS, THPF, THPA, NPAG
LTTN-F	Joint Algorithm of LBRS, THPF, THPA, NPAG-F
Max C/I	Maximum carrier to interference ratio
MIMO	Multiple Input Multiple Output
MS	Mobile Station
NLOS	Non-Line-of-Sight
NPAG	Non-cooperative Power Allocation Game
NPAG-F	Non-cooperative Power Allocation Game for Fairness
NP-hard	Non-deterministic Polynomial-time hard
OFDM	Orthogonal Frequency Division Multiplexing
OFDMA	Orthogonal Frequency Division Multiplexing Access

PBRS	Pathloss Based Relay Selection
PF	Proportional Fairness
PPF	Partial Proportional Fairness
PREQ	Joint algorithm of PBRS, RR, EQPA
PRNG	Joint algorithm of PBRS, RR, NPAG
PRNG-F	Joint algorithm of PBRS, RR, NPAG-F
PSK	Phase Shift Keying
PTEQ	Joint algorithm of PBRS, THPF, EQPA
PTNG	Joint algorithm of PBRS, THPF, NPAG
PTNG-F	Joint algorithm of PBRS, THPF, NPAG-F
QAM	Quadrature Amplitude Modulation
QoS	Quality of Service
RAOS	Relay Aided Opportunistic Scheduling
RR	Round Robin scheduling algorithm
RRM	Radio Resource Management
RS	Relay Station
SINR	Signal to Interference plus Noise Ratio
TDD	Time Division Duplex
TG	Time Guard
THPA	Two-Hop Power Allocation scheme
THPF	Two-Hop Proportional Fairness scheme
TTI	Transmission Time Interval
UL	Uplink

Chapter 1 Introduction

1.1 Background/Motivation

As wireless communication develops, higher requirements are demanded of wireless networks. In 2003, the International Telecommunication Union Radio communication sector (ITU-R) proposed that next generation networks should achieve a total cell capacity of up to 1 Gbps for slow-moving users and 100 Mbps for fast moving mobile stations (MS). However, the limitation on radio resource is the real bottleneck for developing higher-speed wireless networks. Research on future wireless systems to provide higher capacity, yet retaining efficient use of the frequency spectrum, can be divided into two aspects:

i. Advanced technology in the physical layer，such as orthogonal frequency division multiplexing (OFDM) [1] which can be used to reduce multi-path interference, and multiple input multiple output (MIMO) [2], which provides spatial reuse.

ii. New network architectures, such as adding relay stations between the base station (BS) and MS [3], or with MESH networks [4].

In future wireless systems, each user will expect a high throughput so they can access different multimedia services regardless of their location and mobility. However, the traditional cellular architecture is not well-suited to provide uniform data rate coverage. Additionally, if the radio propagation is non-line-of-sight (NLOS) (as is likely) the pathloss will be higher than line-of-sight (LOS), so that the effect on an MS near the cell boundary will be worse, making it more difficult to achieve a spectral efficiency comparable to that seen by an MS near the BS that does have LOS transmission.

A simple way to handle the pathloss problem is to divide a long path into multiple shorter hops and to use relay stations (RS) for data forwarding. RSs can also be used

for temporary coverage in applications such as disaster relief as well as being deployed in hotspot areas.

Whatever techniques are used for increasing available bit rate, radio resource management (RRM) is an increasingly important problem and one that faces new challenges. In addition, the spectral efficiency and the energy efficiency should be considered in the RRM. The addition of relay stations in the wireless cellular network creates new research issues for the RRM, including relay station allocation, handover between RSs, and new considerations in frequency planning. In addition, channel allocation and power allocation between relays need to be considered.

1.2 Research Scope

This thesis describes research into the radio resource allocation scheme in relay based cellular networks. OFDMA [5] will be the modulation and multiple access method for future wireless networks and hence it is the only multiple access method considered in this thesis.

Adding fixed relays into the cellular network adds new research considerations:

- which users will have their data forwarded through a relay;
- which relay will be selected to serve a user;
- the allocation of subchannels to the RS and MS in the first hop link;
- the allocation of subchannels to the MS in the second hop link;
- how to allocate transmission power between links; and
- how to allocate transmission power among cells.

The goal of this research is to investigate fairness, throughput and power consumption of wireless relay networks through considering how best to manage the radio resource.

Initially fairness is considered as it is important that available resources are shared equitably between users. The user fairness is considered in the subchannel allocation

and relay selection, which will give the best tradeoff between system throughput and user fairness.

Power allocation is very important for resource efficiency and system performance. Determining how transmission power will be allocated between the two hop links and among different cells is important to increase the power efficiency while maintaining system performance.

1.3 Research Contributions

The work reported in this thesis is novel. The main contributions are:

1. Two-hop proportional fairness algorithm

This thesis proposes a two-hop proportional fairness (THPF) scheduling scheme for relay based OFDMA cellular systems. The fairness allocation problem is considered both in the first time subslot between direct link users and relay stations, and the second time subslot among relay link users. The proportional fairness scheduling algorithm [6] is extended to a two-hop scenario, so the long-term fairness between the relay link user and the direct link user is guaranteed, and the radio resource is fully exploited.

2. Load based relay selection algorithm

A load based relay selection algorithm (LBRS) is proposed for a fair resource allocation. The transmission mode (direct transmission mode or relay transmission mode) of each user will be adjusted based on the load of the transmission node, which will make the long-term average data rate of relay link users and direct link users equal so that user fairness is enhanced.

3. Two-hop power allocation algorithm

An adaptive power allocation algorithm (called two-hop power allocation - THPA) is proposed for energy efficiency in relay based OFDMA cellular systems. The base

station or relay station adjusts power adaptively in terms of the difference between the first hop link data rate and the second hop link data rate of each RS. In this way, the data rate on the two hop links of one RS will be matched so that the total transmission power will be reduced while the system throughput does not decrease.

4. Multi-cell non-cooperative power allocation game

A multi-cell non-cooperative power allocation game (NPAG) is proposed to improve the system throughput and reduce the transmission power. This is applied to the first time subslot for BSs and the second time subslot for RSs. In all the cells, each transmitter (BS or RS) controls the power allocation on each subchannel to maximize its own utility in a distributed way. As the Nash equilibrium is used to determine the solution of this problem, the existence and uniqueness of the Nash equilibrium are also studied.

5. Multi-cell non-cooperative power allocation game for fairness

The multi-cell non-cooperative power allocation game is modified by adding a novel utility function defined for user fairness, since cell-edge users will suffer from larger inter-cell interference. This is known as NPAG-F. The pricing factors for BS and RS are adjusted adaptively as a function of the average data rate and it is shown that this improves fairness greatly with only a small impact on system throughput and reduces the transmission power of the BS and the RSs greatly.

6. Joint radio resource allocation algorithm

The proposed algorithms in this thesis improve the system performance by relay selection, subchannel allocation and power allocation. The proposed LBRS, THPF, THPA and NPAG (NPAG-F) are combined, and the system performance (throughput, the user fairness and energy efficiency) is evaluated. The joint radio resource allocation algorithm can achieve a very good tradeoff between throughput and user fairness, and also can significantly improve energy efficiency.

1.4 Author's Publications

[1] Lin Xiao, Laurie Cuthbert. "A Two-hop Proportional Fairness Scheduling Algorithm for Relay Based OFDMA Systems", in *IEEE WICOM 2008*, Oct.10, 2008, pp. 1-4.

[2] Lin Xiao, Laurie Cuthbert. "Improving Fairness in Relay-based Access Networks", in *ACM MSWIM 2008*, Nov. 2008, pp. 18-22.

[3] Lin Xiao, Laurie Cuthbert. "Power Allocation Scheme in Regenerative Relay-based OFDMA Systems", in *IEEE ICCS 2008*, Nov. 2008, pp. 637-641.

[4] Lin Xiao, Laurie Cuthbert. "Load Based Relay Selection Algorithm for Fairness in Relay Based OFDMA Cellular Systems", in *IEEE WCNC 09*, Apr. 2009, pp. 1-6.

[5] Lin Xiao, Laurie Cuthbert. "Multi-cell Non-cooperative Power Allocation Game in Relay Based OFDMA Systems", in IEEE *VTC2009-Spring*, Apr. 2009, pp. 1-5.

[6] Lin Xiao, Laurie Cuthbert, Tiankui Zhang. "Distributed Multi-cell Power Allocation Algorithm for Energy Efficiency in OFDMA Relay Systems", in IEEE *ICC Workshops '09*, Jun. 2009, pp. 1-5.

[7] Lin Xiao, Laurie Cuthbert, Tiankui Zhang. "User Fairness Analysis of a Game Theory Based Power Allocation Scheme in OFDMA Relay Systems", in *European Wireless* 2009, May 2009, pp. 173-177.

[8] Lin Xiao, Tiankui Zhang, Yutao Zhu, Laurie Cuthbert. "Two-Hop Subchannel Scheduling and Power Allocation for Fairness in OFDMA Relay Networks", in *ICWMC 2009*, Aug. 2009, pp. 267-271.

[9] Lin Xiao, Yue Chen, Tiankui Zhang, Laurie Cuthbert. "Multi-cell Non-cooperative Power Allocation Game for User Fairness in OFDMA Relay Systems", in *WPMC'09*, 2009.

1.5 Thesis Organisation

The remainder of this thesis is organised as follows.

Chapter 2 introduces the relevant concepts in relay networks, including the basic concept of a relay based cellular network, usage model, relay classification and network configuration; it also introduces relevant research in relay networks.

Chapter 3 discusses the simulator used for relay based OFDMA systems. The overall design of the simulation platform and the system parameters are given in the first part of this chapter with the detailed function of the main modules being given in the second part. The chapter also discusses validation of the simulator.

Chapter 4 surveys radio resource allocation in relay networks. The basic concept and content of resource management is introduced first, and then the relevant work of relay selection, channel allocation and power allocation is discussed in turn.

Chapter 5 investigates the fairness issue for resource allocation in two-hop relay based cellular systems. A two-hop proportional fairness scheduling algorithm and a load based relay selection algorithm are proposed to give fair resource allocation.

Chapter 6 researches the power allocation problem. First, a two-hop power allocation scheme for energy saving is given that balances the date rates on the two hop links. Second, the power allocation problem with co-channel interference is studied in multi-cell systems. Based on game theory, a multi-cell non-cooperative power allocation game for throughput and fairness is proposed respectively. Besides, the joint power allocation algorithm which considered power allocation between multi-cell and between two hop links is given and the performance is discussed.

Chapter 7 gives the system performance evaluation of the proposed radio resource allocation algorithms in this thesis.

Chapter 8 concludes the works in this thesis, and the direction of the future work is discussed.

Chapter 2 Relay based OFDMA Cellular Networks

2.1 Basic Concept of Relay

In future wireless systems, the requirement for high data rate and spectral efficiency means that the conventional cellular architecture is not feasible for the following reasons:

- Much higher transmission power is needed to maintain the same coverage because the required transmission rate is much higher to support applications.
- The frequency spectrum will be higher than the 2GHz band and as a result the radio propagation will be significantly more vulnerable to NLOS conditions [7].

To overcome these problems, some fundamentally new technologies are needed to satisfy the requirement of throughput and coverage: these include modification of wireless network architecture as well as advanced transmission techniques.

Increasing the density of base stations is one potential solution for these two problems but it will greatly increase the deployment costs; an alternative is deploying RS which has drawn much attention [7] and is considered to be a most promising architecture for the very high throughput and coverage requirements of future systems. Adding RS in a cellular system can extend network coverage, overcome multi-path fading and increase the capacity of the system.

RSs, which can be either network elements or user terminals, are more intelligent than repeaters and are capable of storing and forwarding data, making scheduling and routing decisions, supporting radio resource assignment and MS handover [8]. The cost of a relay network is much lower compared with one that just adds more BSs because RSs have more limited functionality. Compared with single-hop cellular networks in which data is transmitted directly between BS and MS, information can

be routed from source to destination via multiple hops in relay based cellular networks.

2.2 Usage Model of Relay

Different models can be devised for how relay networks can be used; all of those mentioned are from [9].

In the **fixed usage model**, fixed RSs can be sited on towers, poles, buildings, lamp posts, or other similar locations. Figure 2.1 (Figure 1 from [9]) illustrates some of the cases that appear in this usage model:

- deployment of RSs to provide coverage extension at the edge of the cell;
- coverage for indoor locations;
- coverage for users in "holes" that exist due to shadowing and in areas between buildings; and
- access for clusters of users outside the coverage area of the BS.

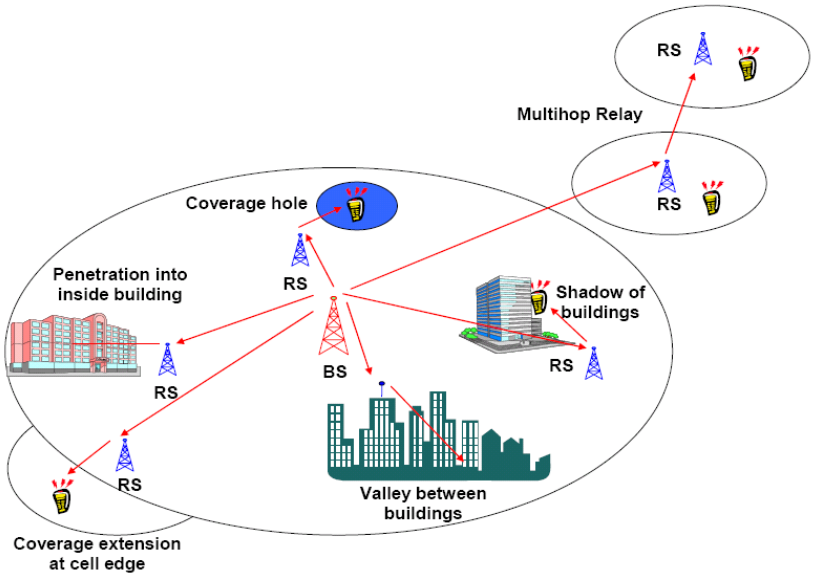

Figure 2.1 Example fixed infrastructure usage model (from [9])

Another model is for **in-building coverage** where RSs are used to provide better coverage and higher throughput inside a closed area, like a building or shopping mall; RSs can be fixed or nomadic and can be inside or outside the building.

In the **temporary coverage** model, nomadic RSs are put in temporary locations, to provide capacity where the BS and fixed RS will not suffice. Some examples of this usage model are (i) emergency or disaster recovery; (ii) temporary coverage for event, which is illustrated in Figure 2.2 (Figure 3 from [9]).

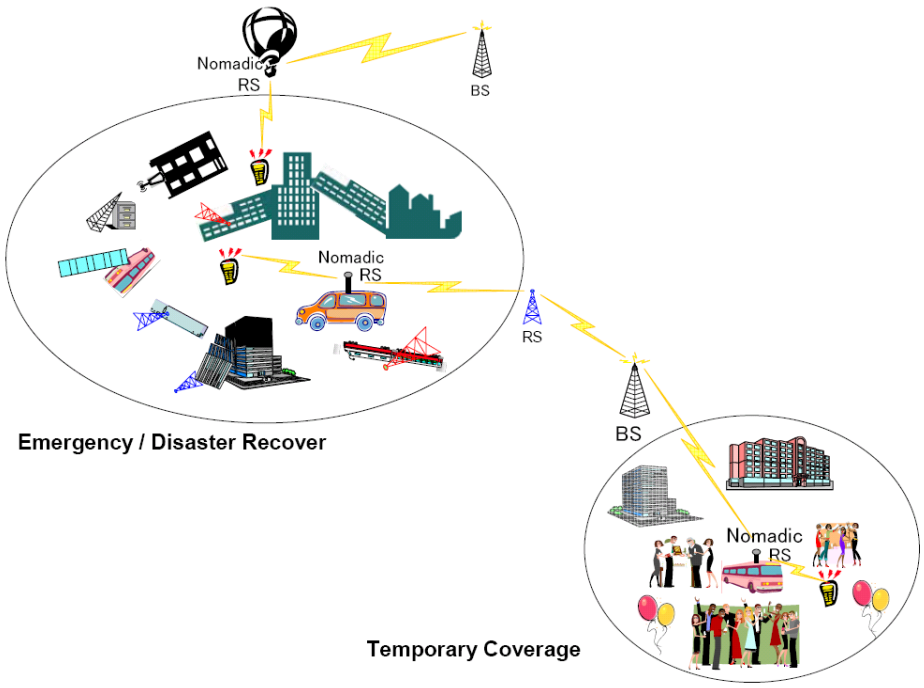

Figure 2.2 Examples of temporary coverage (from [9])

Mobile RSs can also be located on a **mobile vehicle**, such as a bus, train or ferry and provide service directly to a number of MSs which are travelling together with the mobile vehicle. In this case the RSs are mobile in the sense that they are moving with the vehicle, but they are fixed relative to the MSs. RSs deployed in this usage model are expected to be complex as they may enter and exit the network when the vehicle enters or exits the coverage area of the network. In this model, topologies may be more than two-hops. An example of a multi-hop topology is the case where the train

travels through a tunnel and the mobile RS onboard the train connects to RSs that are deployed along the tunnel [9].

2.3 Classification of Relay

2.3.1 Amplify-Forwarding and Decode-Forwarding

RSs can be classified into *amplify-forwarding* (AF) relay and *decode-forwarding* (DF) relay.

The AF relay receives the useful signals from the transmitter with interference plus noise; then it simply amplifies the received signals and retransmits them. The receiver can selectively receive either the retransmitted signal from the RS or the signal from the BS directly; it can even combine both of the signals. Although the noise is amplified by the RS, the system performance can still be improved by the AF relay using selective receiving or combined receiving [10].

A DF relay is a RS that can decode and regenerate the received signal so that it does not retransmit the received noise, although the system time delay is longer than that with the AF scheme [11].

Other relay types exist, including the compress and forwarding (CF) relay that compresses and forwards to reduce the data to be retransmitted [11].

In this thesis the DF relay is used so that other types will not be considered further.

2.3.2 Fixed Relay and Mobile Relay

Relay also can be classified into fixed RS and mobile RS.

The position of a fixed RS is pre-determined and there is no mobility. Fixed RSs can be used to give uniform data rate coverage for all the users within the cell area as well as extending the cell coverage for high data rates in a macro-cell. The main scenario is shown in Figure 2.3 (Based on Fig. 1 from [12]).

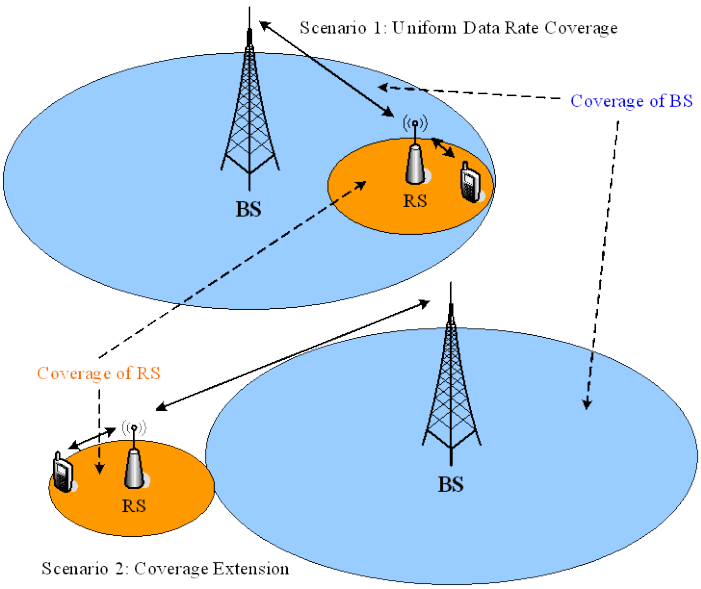

Figure 2.3 Typical applications in fixed relaying system

The mobile RS is moveable, and the topology of mobile relay based cellular networks is therefore changeable. Mobile RSs can be either a station or a mobile user that is serving as a relay for other users. There are three main scenarios for mobile RS:

Stationary RS relative to moving MS [13]: In this case the relay may be moving, in absolute terms but is stationary with respect to the terminals it is serving, such as the example of a mobile RS on a train serving the terminals in the train (that are stationary with respect to the relay).

Moving RS and moving MS: Here the RS is moving with respect to the terminals it is serving; examples might be RSs on buses to provide coverage in parks and streets.

MS acting as Mobile RS: In this scenario, the mobile terminals can act as a RS for other mobile terminals.

The deployment of fixed RS is a more common application scenario compared with the deployment of mobile RS, since the fixed RS is a more practical and easy to make deployment.

The key research points of relevant research work and standardization also focus on fixed RS scenarios. Although, the relevant research results on fixed RS can be extended to mobile RS scenarios. The algorithms proposed in this thesis can be applied to both fixed and mobile RS, albeit with some extra complexity for mobile RS. Since the deployment of fixed RS is more common, in this thesis, the performance of algorithms is only examined under the fixed RS scenario.

2.4 Relevant Research

Standards work on relay networks has been organised through The Institute of Electrical and Electronics Engineers (IEEE) 802.16's Relay Task Group, which is developing a draft under the P802.16j Project Authorization Request (PAR), which was approved by the IEEE Standards Association Standards Board on 30th March 2006. The PAR addresses "Air Interface for Fixed and Mobile Broadband Wireless Access Systems Multi-hop Relay Specification" [14].

By using multi-hop relay, the speed of 802.16e can be increased and the coverage of the cell can be expanded. The data rate is the same across the whole cell coverage area, so that users at the edge get the same achievable rates as those in the centre: this meets the targets of next generation wireless networks.

European Union (EU) projects have also been addressing relay networks, such as Winner (Wireless World Initiative New Radio) in Framework Programme 6 (FP 6) [15]. In this project, different relay concepts were introduced, such as single hop relay, fixed homogeneous multi-hop, fixed heterogeneous multi-hop, mobile multi-hop, and cooperative multi-hop.

Beside that, the document of system description of IEEE 802.16m, and proposal of 3GPP LTE-A (Long Term Evolution Advanced) have discussed the relaying technology in the cellular networks.

Using a relay can increase the throughput of the system compared with conventional single hop cellular networks; this is because the pathloss is reduced with the use of multiple hops. However, a multi-hop link may consume much more radio resource compared with the direct link, which could be a problem as radio resources are always limited. Moreover, greater interference is created, caused by the number of simultaneous transmissions in multi-hop networks. Since the resource management scheme in a relay based cellular network is more complex than in conventional cellular networks, the study of radio resource management in relay based cellular networks is necessary and important.

Radio Resource Management includes such topics as resource allocation, relay selection, access control, and load balancing and hand-over.

Radio *resource allocation*, which handles the assignment and allocation of RS, radio channels, and transmitter power, is always an important issue in wireless system design. The relay station can be seen as a new resource shared by different MSs, and the relay selection scheme is important in relay based cellular networks as it has a large influence on systems performance. The most relevant work from other areas is the routing mechanism in mobile ad-hoc networks. Although some ideas can be taken from ad hoc networks, the constraints and capabilities of relay networks are very different and so relay selection in relay networks is a subject that needs further investigation. This is more of a challenge when considering relay coordination, and even more complex when considering mobile relays [13].

The handover scheme will be different in relay networks compared with conventional cellular networks since the moving MSs can handover from RS to RS, BS to RS or RS to BS. The handover scheme will be even more complex if mobile RSs are used, but moving RSs are not within the scope of this thesis.

2.5 Orthogonal Frequency Division Multiple Access

2.5.1 Principle of OFDMA

Orthogonal Frequency-Division Multiple Access (OFDMA) is a multi-access version of the Orthogonal Frequency Division Multiplexing (OFDM) scheme. The principle of an OFDM system is to use narrow, mutually orthogonal subcarriers to carry data, and the OFDMA is achieved by assigning different subcarriers to carry data from different users.

OFDM is now thought to be the most promising technology for next generation wireless communication networks [16]. The concept of OFDM can be traced back to the 1950s when the Kineplex system [17] was proposed as a military multi-carrier high-frequency communication system. In 1966, R.W. Chang [18] described the concept of using parallel data transmission and frequency-division multiplexing (FDM). The first patent on OFDM [19] was issued in 1970 in the US, a proposal to use Inverse Discrete Fourier Transform (IDFT)/DFT to achieve multi-carrier transmission was proposed by Weinstein & Ebert [20] in 1971, and later by Hirosaki in 1981 [21]. In 1995，a digital circuit was used instead of an analogue circuit to achieve orthogonal signal modulation, thus making OFDM practical [22]. In 1980, Peled and Ruiz [23] proposed to insert a cyclic prefix (CP) into the OFDM symbol and eliminate the interference between carriers.

OFDM is multi-carrier transmission where data are divided between the different subcarriers of one transmitter. Different subcarriers are orthogonal to each other, as at the sampling instant of a single subcarrier, the other subcarriers have a zero value, as shown in Figure 2.4 [24].

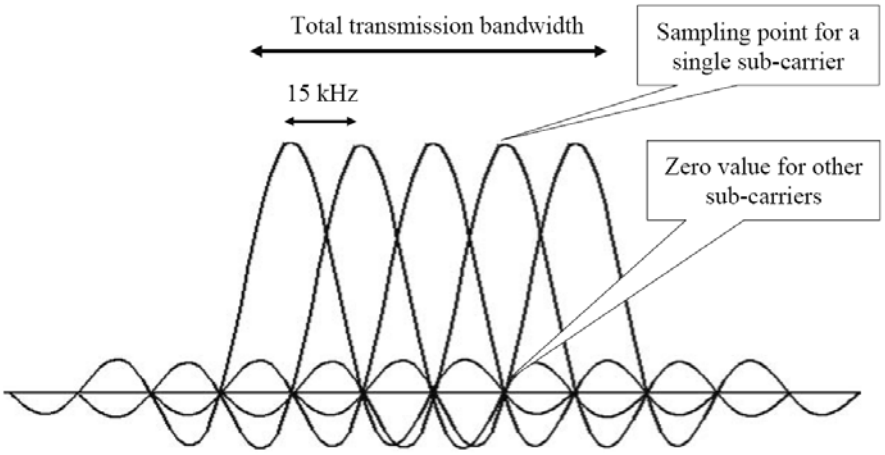

Figure 2.4 Orthogonal subcarriers

In OFDM, the orthogonal subcarriers are generated by the IFFT block. The serial stream data from the source is converted to a parallel sub-stream data, which is followed by the IFFT operation. Each input for the IFFT block corresponds to the input representing a particular subcarrier and can be modulated independently of the other subcarriers. The IFFT block is followed by adding the cyclic extension (cyclic prefix), as shown in Figure 2.5 [24].

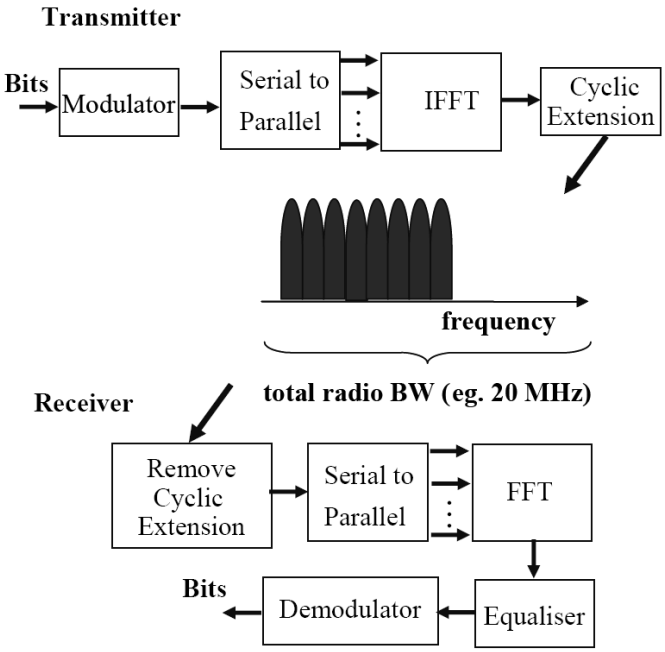

Figure 2.5 OFDM transmitter and receiver

The motivation for adding the cyclic extension is to avoid inter-symbol interference. When the transmitter adds a cyclic extension longer than the channel impulse response, the effect of the previous symbol can be avoided by ignoring (removing) the cyclic extension at the receiver.

2.5.2 OFDMA System Model

Orthogonal Frequency-Division Multiple Access (OFDMA) is a multi-access version of the OFDM modulation scheme. Since the subcarriers are orthogonal, each subcarrier can use a different modulation scheme such as: Phase Shift Keying (PSK), adaptive quadrature amplitude modulation (QAM) and it can be allocated transmission power separately. OFDMA is achieved by assigning subsets of subcarriers to individual users. Multi-user diversity allows the spectrum efficiency to be improved by allocating subchannels to those users with good channel conditions.

In the downlink of OFDM systems [25], the system bandwidth (BW) is B, the number of subcarriers is M, so the subcarrier bandwidth is $B_m = B/M$. Let $\{b_k\}$ be the set of symbols of the user k, and let $s_{k,m}$ be the transmission power allocated to the user k on the subcarrier m. Assuming channel state information (CSI) is known at both the transmitter and the receiver, $g_{k,m}$ is the channel gain between the BS and the user k on the subcarrier m, and $q_{k,m}$ is the number of bits in each data symbol of the user k on the subcarrier m.

In a single cell of an OFDMA system, the signal to noise plus interference ratio (SINR) $\gamma_{k,m}$ of the user k on the subcarrier m is:

$$\gamma_{k,m} = \frac{s_{k.m} g_{k,m}}{\sigma^2} \tag{2.1}$$

In which, σ^2 is the variance of Additive White Gaussian Noise (AWGN).

Assuming a QAM scheme is used in the OFDM system, the bit error rate (BER) of the user k on the subchannel m can be expressed as [26]:

$$BER \le \frac{1}{5}\exp\left(\frac{-1.5\gamma_{k,m}}{2^{q_{k,m}}-1}\right) \tag{2.2}$$

If $q_{k,m} \ge 2$ and $0 \le \gamma_{k,m} \le 30dB$, the expression (2.2) will be satisfied. For a certain BER, the max number of sent bits in each symbol is:

$$q_{k,m} = \log_2\left(1+\frac{\gamma_{k,m}}{\Gamma}\right) \tag{2.3}$$

in which, Γ is constant with a particular BER; this expresses the difference between the Multiple Quadrature amplitude (M-QAM) signal and Shannon channel capacity. In an Additive White Gaussian Noise (AWGN) channel, $\Gamma = -\ln(5BER)/1.5$ [26].

2.5.3 Advantages of OFDMA

High Spectral Efficiency: After the IFFT operation, subcarriers can overlap partially so the symbol transmit rate can achieve the Nyquist limitation [16]. The OFDMA system assigns different subcarriers to different users, so users are orthogonal to each other, and the interference between users is reduced substantially. Hence, OFDM technology can increase the system throughput.

Simple System Implementation: Since subcarriers are orthogonal to each other, the Discrete Fourier Transform (DFT) can be used to represent OFDM symbols. The computational complexity of DFT is very high, $o(n^2)$. However, using IFFT/Fast Fourier transform (FFT) instead of IDFT/DFT, the computational complexity of the OFDM algorithm is reduced to $o(\log_2(N))$ [16].

Anti-fading and Anti-interference: OFDMA is good against frequency-selective fading and interference. Because OFDM divides the wideband transmission into

narrowband transmission on different subcarriers, each channel (subcarrier) can be treated as a flat fading channel [16].

Flexible Resource Allocation: OFDMA can select certain subcarriers for transmission according to channel condition, so dynamic frequency allocation can be achieved; it can also fully make use of frequency diversity and multi-user diversity to get optimal system performance [16].

2.6 Deployment of Fixed Relay in OFDMA Cellular Systems

Adding relay stations (RS) between the base station (BS) and the mobile stations (MS) in OFDMA cellular systems can extend network coverage, overcome multi-path fading and increase the capacity of the system. However, there are some important parameters that affect overall system performance, such as the distance between the BS and RS, and the number of relays, the number of hops, and the frequency reuse factor.

2.6.1 Hops between BS and MS

In a relay system, traffic is transmitted over multi-hop paths. By reducing the attenuation between the transmitter and the destination, the system performance can be improved. Deploying a sufficient number of RSs in the whole cell and finding a suitable route with good links via multi-hops for packets can increase the overall capacity, and reduce the congestion happening within the cells. However, the balance between the cost of RS deployment and the performance improvement needs to be considered [12].

Using just two hops is an approach well-known for its simplicity with respect to routing and resource allocation. In addition, the two-hop scheme can provide a good tradeoff between diversity gain and repetition coding [12]. In this thesis, a two-hop structure is used between the BS and MS.

2.6.2 Definition of Terms

This thesis uses the normally accepted definitions that are found in the literature:

- **Direct link user** is the user that communicates with the BS directly.
- **Relay link user** is the user that communicates with the BS via RS using two-hops.
- **Direct link** is the link between BS and user.
- **Relay link** is the link between BS and RS (the first-hop link) and the link between RS and MS (the second-hop link).

This normal definition of links and nodes for a relay network is shown in Figure 2.6.

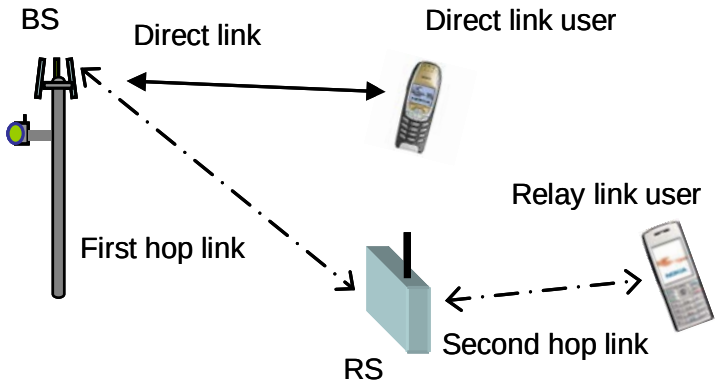

MS knows that communication is routed through the RS so the frame structure design should consider the synchronization problem of BS and RS.

The frame structure consists of downlink (DL) frame period and uplink (UL) frame period. If the system is TDD, a time guard (TG) will be inserted between the DL frame and the uplink (UL) frame.

The transparent frame structure in the downlink is shown in Figure 2.7 [27].

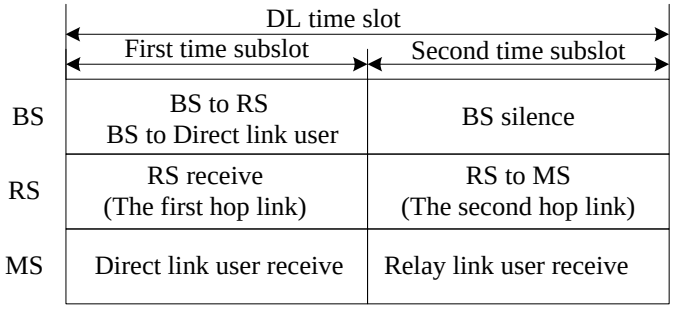

Figure 2.7 The DL transparent frame structure in relaying system

The non-transparent frame structure in the downlink is shown in Figure 2.8.

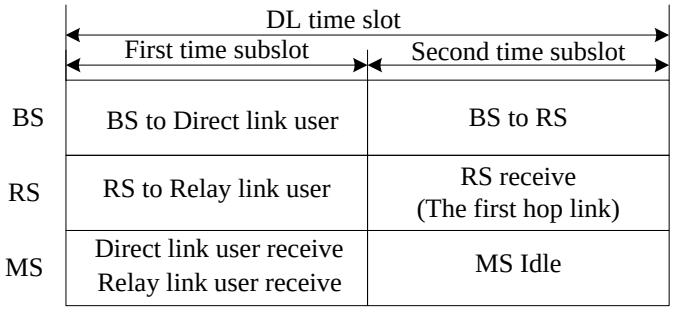

Figure 2.8 The DL non-transparent frame structure in relaying system

The transparent frame structure is used in this thesis. The BS schedules subchannels in each transmission time interval (TTI). One TTI can contain one or several time slots. In this thesis, one TTI equals one time slot, as finer scheduling interval granularity makes better use of quickly changing channel conditions. As a relay link is divided into the first hop link and the second hop link, a time slot is also divided

into the first time subslot and the second time subslot. For example, in the downlink, the subchannels in the first time subslot are allocated to the direct link users and the first hop of relay link users; the subchannels in the second time subslot are allocated to the second hop of relay link users.

2.6.4 Frequency Band

In relay based cellular networks, a transparent RS uses the same carrier frequency to communicate with nodes above and below it (BS and MS in a 2-hop network); a non-transparent RS may use the same or different frequencies [28]. A single frequency network with transparent RS is considered in this thesis, so the BS-RS link uses the same frequency band as the RS-MS link.

2.6.5 Frequency Reuse Method

There are two main frequency reuse methods [29]**.** The first method is shown in Figure 2.9a: the frequency reuse factor (FRF) of this transmission type is one. In the downlink, the BS transmits data to direct link users and RSs on same frequency band; all RSs transmit data to relay link users on the second time subslot, sharing the same frequency band as the first time subslot (TDD). Similarly, in the uplink, relay link users transmit data to RS in the first time subslot on the whole frequency band, and in the second time subslot, direct link users and RSs transmit data to BS using the same frequency band as that of the first time subslot (TDD).

The second frequency reuse method is shown in Figure 2.9b, in which the whole frequency band is divided into n sub-band for n RS and the RSs will relay data on separate frequency bands. In the downlink, the BS transmits data to all direct link users and RSs using the whole frequency band in the first time subslot, and each RS transmits data to relay link users within its coverage using independent sub-bands in the second time subslot. In the uplink, relay link users transmit data to their RS using the sub-band of this RS in the first time subslot and the direct link user and RS transmit data to the BS using the whole frequency band in the second time subslot.

There is no co-frequency intra-cell interference by using both frequency reuse method A and method B. Method B can reduce co-frequency inter-cell interference, but the spectrum efficiency of method B is lower than that of method A. In the scheduling of method A, the user can select subchannels among a wider bandwidth compared with that of the method B, so the frequency reuse gain of method A is larger than that of method B. In this thesis, frequency reuse method A is used, and a multi-cell power allocation algorithm is used in this research to reduce the co-frequency inter-cell interference.

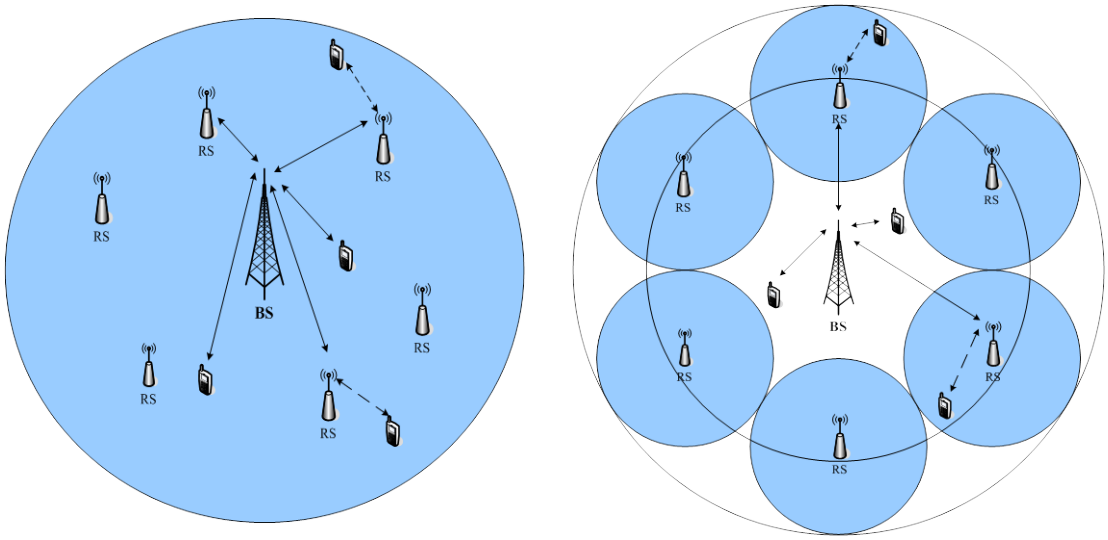

a) Frequency reuse method A b) Frequency reuse method B

Figure 2.9 Frequency reuse method

2.6.6 Distance between BS and RS

If an RS is too close to the BS, the MSs near the cell boundary cannot really take advantage of relaying, and the interference between RSs becomes high since they are close together. On the other hand, if the RS is located near the cell boundary, the coverage of each RS will be reduced since it will suffer interference from RSs in adjacent cells. Therefore, the distance between the BS and RS is an important factor to be considered and indeed some of the results in Chapter 5 show the effect of changing the position of RSs.

2.7 Summary

This chapter introduces the relevant concepts in relay networks, including the basic concept of relay, the usage model of relay, the classification of relay, and the relevant research in relay networks. Also, the basic concept of OFDMA is introduced and the network configuration in relay based OFDMA networks is discussed, including the number of hops between BS and MS, definition of terms in relay networks, frame structure, frequency band, frequency reuse method and distance between BS and MS.

Chapter 3 Simulator for OFDMA Relay Networks

3.1 Overall Design of Simulation Platform

This simulation platform was built based on an existing downlink *non-relay* OFDMA system level platform and all the modules are modified to produce a downlink relay based OFDMA system level platform by the author and to add in the specific algorithms proposed in this thesis. The simulator is designed based on IEEE 802.16j [9][27][30], and Long Term Evolution (LTE) [31][32][33]. The main simulation modules are listed below and the details of each module are given in section 3.3.

Initialize module: Creates network topology, initializes the position of BS, RS, and MS, computes large scale pathloss and shadow fading.

Multi-path fading channel module: Creates multi-path fading channel, including relay links and direct links.

CQI feedback module: Calculate the channel quality information (CQI), and feeds back the CQI to BS. The CQI information includes: CQI of BS to RS, CQI of RS to MS, and CQI of BS to MS.

Relay selection module: For each user, a certain RS should be selected to forward and transmit data. Different relay selection algorithms would result in different relay selection decisions.

Scheduling module: The subchannels in the first time subslot will be allocated to the RSs and the direct link users; the subchannels in the second time subslot will be allocated to the relay link users in terms of the scheduling algorithm according to the frame structure of relaying systems [27]. Different scheduling criteria would result in different system performance.

Power allocation module: Based on a particular power allocation algorithm, the BS allocates the power to each subchannel in the first subslot, and the RS allocates the power to each subchannel in the second subslot.

Channel capacity calculation module: Based on allocated subchannel and allocated power of each user, each user's CQI and data rate within one TTI is calculated.

System performance statistics module: Calculates the statistics of system performance, including data rate, packet loss rate and packet delay.

The simulation uses time-stepping (with the time step being equal to the TTI).

The flow within the simulator is shown in Figure 3.1.

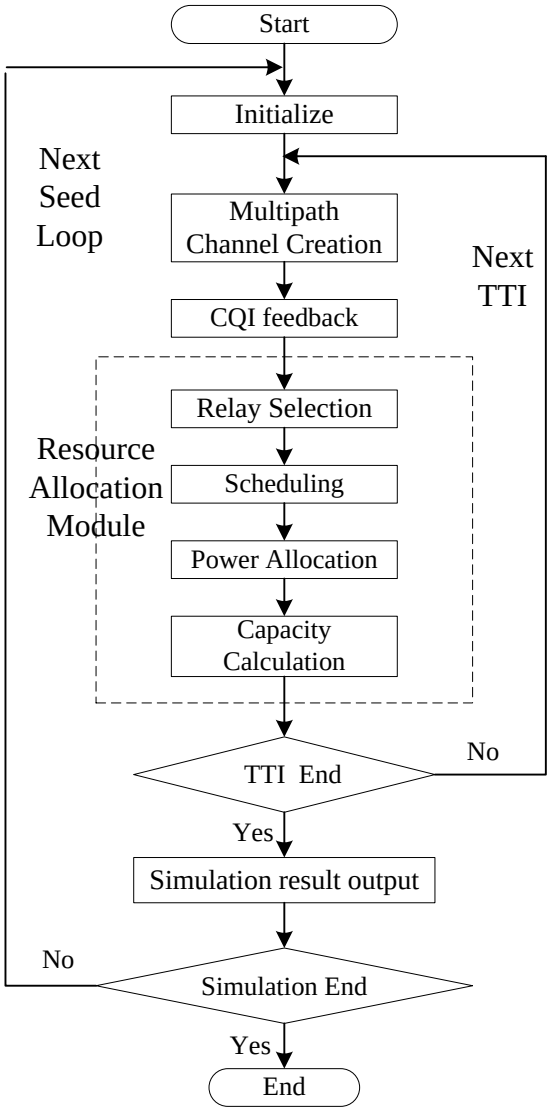

Figure 3.1 Flow chart of simulator

3.2 Simulator System Parameters

A downlink relay based OFDMA system is considered here.

In the OFDMA system, every 25 continuous subcarriers compose a subchannel, which is one frequency unit of resource allocation. One transmission timing interval (TTI) is 1 ms, and each TTI is one time unit of resource allocation. Detailed parameters of the downlink system are listed in Table 3.1 [31][32].

Table 3.1 Downlink transmission parameters

Parameter	Value
Transmission Bandwidth	10 MHz
TTI	1 ms
Subcarrier spacing	15kHz
Number of subcarriers occupied	601 [-300,300]
Number of subcarriers in use	600, subcarrier # 0 is not used
Subchannels	24
Subcarriers/subchannels	25 (consecutive)
Subchannel BW (kHz)	375

In this simulator, a typical urban macro-cell is used (defined in the 3GPP scenario Case 2 [33]), and detailed system level simulation parameters of the macro-cell reflecting typical values in an urban macro cell area are listed in Table 3.2; the transmission power of the RS is a half of that of the BS, as in [34][35][36]. The channel model refers to the IEEE 802.16j document which will be considered in Section 3.4. Note that a wrap-around model (19 cells as centre cluster) is used [33]. There are six RSs sited uniformly in each cell as is commonly used in the literature [36] and it is assumed that no additional spectrum is available and, hence, all links use the same spectrum.

The urban macro-cell scenario is chosen as that is the most likely for relay systems to increase the system capacity whereas in rural areas it is coverage that is usually the design consideration. However, the approach taken is generic and could be applied in principle to any type of cell layout, including rural and suburban.

Table 3.2 System level simulation parameter of Macro-cell

Parameter	Value
Cellular Layout	Hexagonal grid, 19 cell sites
Inter-site distance	500 m
Central Frequency/Bandwidth	2.0 GHz/10MHz
Total BS TX power	20 W
Total RS TX power	10 W
MS power class	250 mW
Minimum distance between MS and BS	>= 35 meters
Thermal noise density	-174 dBm/Hz
Penetration Losses	20 dB
Target BER	10^{-3}
Number of simulation drops	20
Simulation time per drop	1000 TTI

3.3 Module Functions and Implementation

The functions of main modules of the simulation platform are briefly explained below.

3.3.1 Initialisation Module

Function description: This module initializes the parameters of the system, and sets up the basic settings of the system, including the deployment of BSs, RSs and MSs, the measurement of antenna gain, the determination of pathloss and shadow fading.

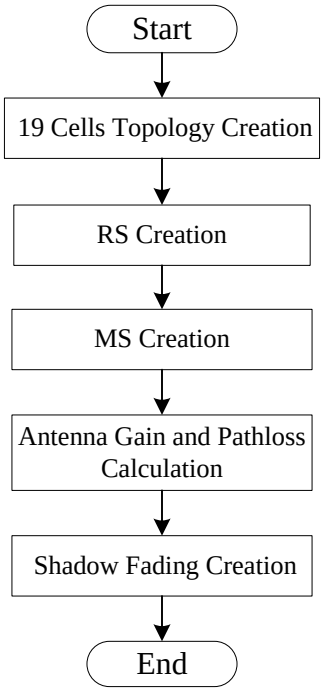

Figure 3.2 Flow chart of initial module

3.3.2 CQI Feedback Module

Function description: SINR of users on all subchannels can be calculated using (i) the BS sending power, (ii) the user's large scale fading, (iii) small scale (multi-path) fading (iv) co-channel interference from other cells and (v) AWGN.

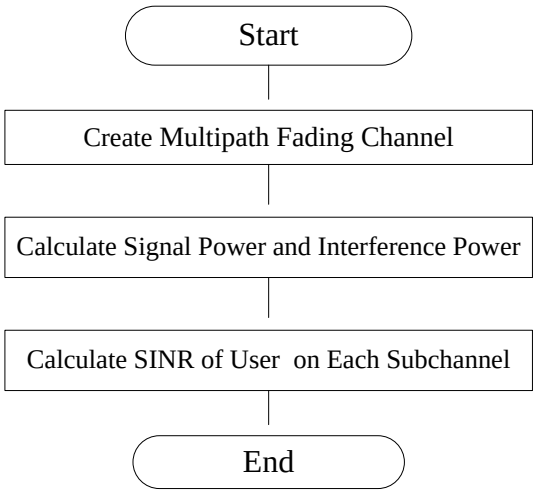

Figure 3.3 Flow chart of CQI feedback module

3.3.3 Resource Allocation Module

Function description: Based on the channel quality indicator (CQI) report from the previous TTI, resource is allocated to users according to the resource allocation algorithm. The resource here includes the choice of RS, subchannel and transmission power.

In the downlink, BS chooses to transmit data via relay link or direct link. If it transmits via relay, the BS needs to decide which relay will be used (the relay selection). There are two time subslots in one TTI. In the first time subslot, under equal power allocation, the BS allocates subchannels for relay link users and RSs; in the second time subslot, the BS allocates subchannels for relay link users. After the subchannels are allocated, the transmission power can be adjusted on each subchannel. The transmission bit rate on each channel can then be calculated using the Shannon formula.

This is the core module for the work reported in this thesis and the flow chart is shown in Figure 3.4.

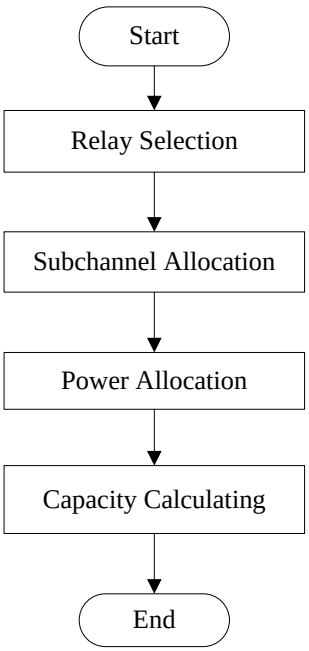

Figure 3.4 Flow chart of resource scheduling module

3.4 Channel Module

In a wireless communication system, the channel state plays an important role in determining the system performance, and it greatly affects the quality of communication. In order to rapidly and accurately simulate channel states, a large-scale fading (pathloss and shadowing) model, and small scale fading (multi-path fading) model are considered in this channel module. There are three kinds of links in relay based cellular networks: (i) the direct link (the link between BS and MS), (ii) the first hop link (the link between BS and RS) and (iii) the second hop link (the link between RS and MS). An urban macro-cell scenario is used in this paper, assuming BS and RSs are all sited above roof top (ART), and users are sited below roof top (BRT).The small-scale fading model used here is essentially that in [30].

3.4.1 Pathloss Model

The channel model of urban macro-cell scenario uses the Type H above roof top (ART) to ART model in [30] to simulate the fixed relay scenario.

3.4.1.1 Pathloss between BS and RS

The pathloss scenario of BS-RS link is shown in Figure 3.5 (Figure 2 from [29]), where node antennas have line-of-sight (LOS) between them.

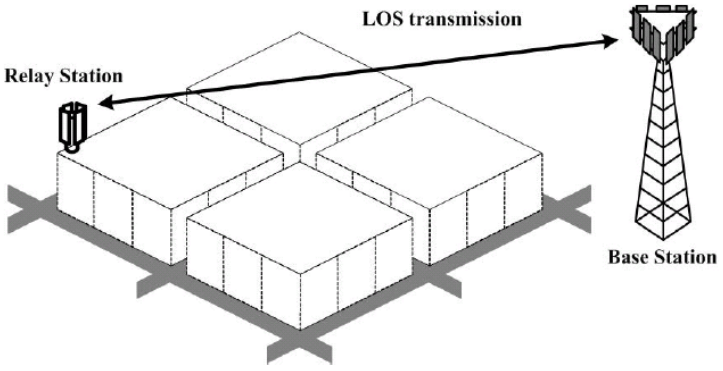

Figure 3.5 BS-RS link with LOS

The pathloss is determined using the COST 231 model (Appendix A in [37]) (but excluding the rooftop-to-MS diffraction loss because the link between BS and RS is LOS), and consists of the free-space pathloss plus the multiscreen diffraction loss L_{msd}.

The free space pathloss model is shown below (*log* denotes *log* to base 10)

$$L_f = 32.44 + 20\log(f_c / MHz) + 20\log(d / km)\,(\text{dB}) \tag{3.1}$$

where d is distance between BS and RS, and f_c is the carrier frequency.

The multiscreen diffraction loss L_{msd} is

$$L_{msd} = L_{bsh} + k_a + k_d \log(d / km) + k_f \log(f_c / MHz) - 9\log(b / metre) \tag{3.2}$$

where b is the distance between two buildings (in metres). Furthermore,

$$L_{bsh} = -18\log(1 + \Delta h_b) \tag{3.3}$$

where $\Delta h_b = h_b - h_{roof}$ is the difference between the height of the BS, h_b, and that of the building roof, h_{roof}.

From [30], values used are: $k_a = 54$, $h_b = 30\,\text{m}$, $h_{roof} = 15\,\text{m}, b = 30$.

The dependence of the pathloss on the distance and frequency is given by parameters k_d and k_f; here values are chosen as $k_d = 18$ and $k_f = -4 + 1.5(f_c / 925 - 1)$ for a metropolitan area according to the specifications of COST 259 [29].

The total pathloss L between BS to RS on the first hop link is

$$L = L_f + L_{msd} = 51.4317 + 38 \times 1og_{10}(d) + (14.5 + 1.5/925 \times f_c) + \log_{10}(f_c) \quad (3.4)$$

3.4.1.2 Pathloss between BS and MS

BS and RS are sited above the rooftops (ART) and MSs are below the rooftops (BRT), so there is non-line-of-sight (NLOS) between them. The pathloss is determined using the COST 231 model [37] which consists of the free-space pathloss L_f , the multiscreen diffraction loss L_{msd} and the rooftop-to-street diffraction loss L_{rts} . The free-space pathloss model L_f and the multiscreen diffraction loss L_{msd} expression are the same as (3.1) and (3.2) respectively.

The rooftop-to-street diffraction loss is

$$L_{rts} = -16.9 - 10\log_{10} w + 10\log_{10} f_c + 20\log_{10}(\Delta h_m) + L_0 \quad (3.5)$$

where w is the width of street (here $w = 12$ m), and Δh_m is the height difference between the building and the MS, the height of the user terminal is taken to be 1.6m, so $\Delta h_m = 15 - 1.6 = 13.4$ m. Also from COST 231, L_0 is a function of the street orientation, which here is chosen to be 90°, so that $L_0 = 4 - 0.114(90^\circ - 35^\circ)$ using the work in that reference [30].

The total pathloss L between BS to MS on the direct link is

$$\begin{aligned} L &= L_f + L_{msd} + L_{rts} \\ &= 44.0120 + 38\log_{10}(d/km) + (24.5 + 1.5/925 \times f_c) \times \log_{10}(f_c/MHz) \end{aligned} \quad (3.6)$$

3.4.1.3 Pathloss between RS and MS

The pathloss between RS and MS is determined by the Cost 231 Walfisch-Ikegami model (Appendix A in [37]) including the free-space pathloss L_f (3.1), the

multiscreen diffraction loss L_{msd} (3.2), and the rooftop-to-street diffraction loss L_{rts} (3.5).

The parameters are defined as follows:

$h_{rs} = 20\,\text{m}$, $h_{roof} = 15\,\text{m}$, the height between RS and roof is $\Delta h = 20 - 15 = 5\,\text{m}$.

The total pathloss between RS to MS is

$$\begin{aligned} L &= L_f + L_{ms} + L_{rts} \\ &= 51.6795 + 38 \times \log_{10}(d/km) + (24.5 + 1.5/925 \times f_c) \times \log_{10}(f_c/MHz) \end{aligned} \tag{3.7}$$

3.4.2 Shadow Fading Model

The level of shadow fading is usually simulated by using a log-normal distributed random variable [30], this refers to typical log-normal shadow fading model [30] is used here. To simplify the shadow fading, correlation of shadowing fading is not considered in this thesis. There is no shadow fading between BS to RS which are both located on the rooftop, but has to be considered between BS to MS and RS to MS, in which the standard deviation value is 8 dB under NLOS transmission [30].

3.4.3 Multi-path Fading Model

OFDM has the ability to resist multi-path effects produced by fast fading but since this work focuses on the adaptive resource allocation scheme a fast fading channel model should be considered in the OFDM system simulation platform.

The triple-path SUI channel model [30] is used in the simulation here. The link between BS and RS is the SUI-3 model [30], and both the BS to MS link and RS to MS link is the SUI-4 model [30]. The parameters used in SUI-3 and SUI-4 are given in Table 3.3 and Table 3.4.

The code published in [37] is modified in the simulation here.

Table 3.3 SUI-3 Model

	Tap 1	Tap 2	Tap 3	Unit
Delay	0	0.4	0.9	Ms
Power	0	-5	-10	dB
K factor	1	0	0	——
Doppler	0.4	0.3	0.5	Hz

Table 3.4 SUI-4 Model

	Tap 1	Tap 2	Tap 3	Unit
Delay	0	1.5	4.0	Ms
Power	0	-4	-8	dB
K factor	0	0	0	——
Doppler	0.2	0.15	0.25	Hz

3.5 Verification and Validation

As the credibility of simulation model is important groundwork of this thesis, the simulation code has been debugged line by line with the help of breakpoints.

3.5.1 Verification of Relay Location and MS Distribution

The relay based multi-cell scenario is shown in Figure 3.6. Nineteen cells with wrap around technology are used in this thesis, which meets the system design requirement. In each cell, six RSs (blue stars) are located on the lines that connect the cell centre to one of the six cell vertices. MSs are uniformly distributed among all the cells. In each cell, the distribution of the MSs is different, which satisfies the user random distribution characteristic.

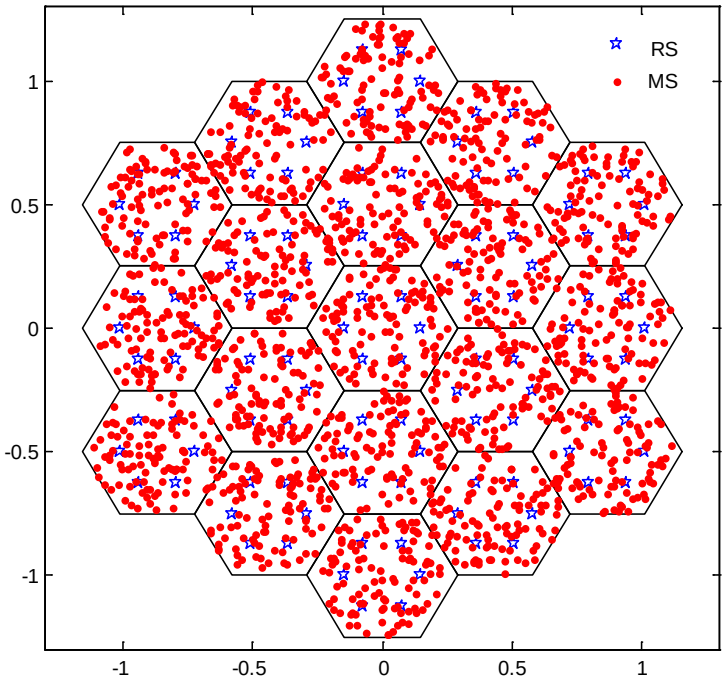

Figure 3.6 Distribution of MSs and RSs in multi-cell system

3.5.2 Verification of Channel States

A verification result for a large-scale channel is shown in Figure 3.7. Taking large-scale channel fading from BS to MS for example, Figure 3.7 is the cumulative distribution function (CDF) curve of large scale fading value (in dB). In Figure 3.7, the channel fading value is range from -160 dB to -100dB, and it is -97 dB when the probability value is 0.5. This result complies with the evaluation result of [38], which can verify the large scale fading channel design.

In [38], the Figure 5 is the results of Macro urban scenario, in which, the BS transmission power is 40 W, BS max antenna gain is 17 dB, BS sector antenna gain is 20 dB. In this thesis, the BS transmission power is 20 W, BS antenna gain is 0 dB, BS sector antenna gain 0 dB (omni antenna pattern). So the large scale fading in this thesis is 40dB less than that of [38].

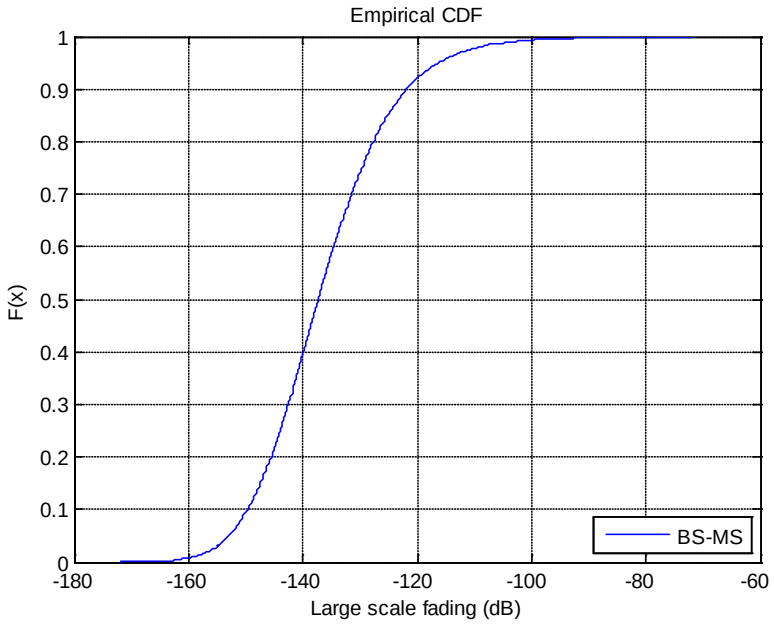

Figure 3.7 Verification of large scale channel fading between BS and MS

Verification of multipath fading channel is shown in Figure 3.8. The each tap of the envelope of the multipath fading is a Rayleigh-distributed with mean $\sqrt{\frac{\pi}{2}}\sigma$ and variance $\frac{4-\pi}{2}\sigma^2$ (the normalised transmission power is used in multipath fading, so $2\sigma^2 = 1$ [Andrea Goldsmith, WIRELESS COMMUNICATIONS]). In Figure 3.8, the CDF curve of the envelope of multipath fading (one tap) is shown, with mean 0.8786 and variance 0.2124 by statistic. This means that the result of the multipath fading simulation complies with the Rayleigh-distributed.

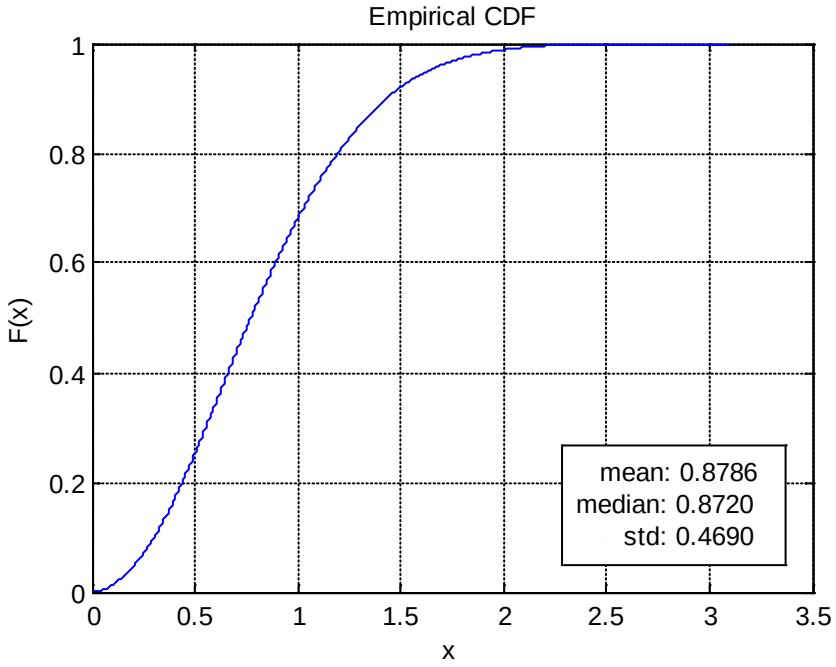

Figure 3.8 Verification of fast fading channel

3.5.3 Verification of Number of Drops

In the simulation, a random "drop" is the term used to describe the random placing of users in the scenario – not the disconnection of call in progress.

For each drop, the distribution of users obeys the specified distribution (here uniform distribution), but the actual location of MSs will change drop to drop. From a theoretical view, the bigger the number of drops, the more accurately the user distribution will approach the ergodic uniform distribution. From the simulation point of view, the bigger the number of drops, the longer the simulation time will be. Therefore, a reasonable number of drops need to be chosen. In Figure 3.9, system throughput is compared with different number of drops. In the simulation, there are 20 users within each cell, and the system parameters are as listed in Table 3.1 and Table 3.2; the subchannel allocation algorithm used here is the *partial proportional fairness scheduling algorithm* (PPF) in [36] and the relay selection algorithm is the *large-scale relay selection algorithm* in [40]. In Figure 3.9, the blue histogram shows the average system throughput when the number of drops is 100, and the red histogram

shows the average system throughput when the number of drops is 20. Simulation results show that the percentage difference of system throughput is within 5%. Moreover, the simulation results are more concerned about comparison between different algorithms and less on the absolute value of algorithm performance. Therefore, 20 drops is taken as a reasonable tradeoff between accuracy and simulation time and is used throughout this thesis.

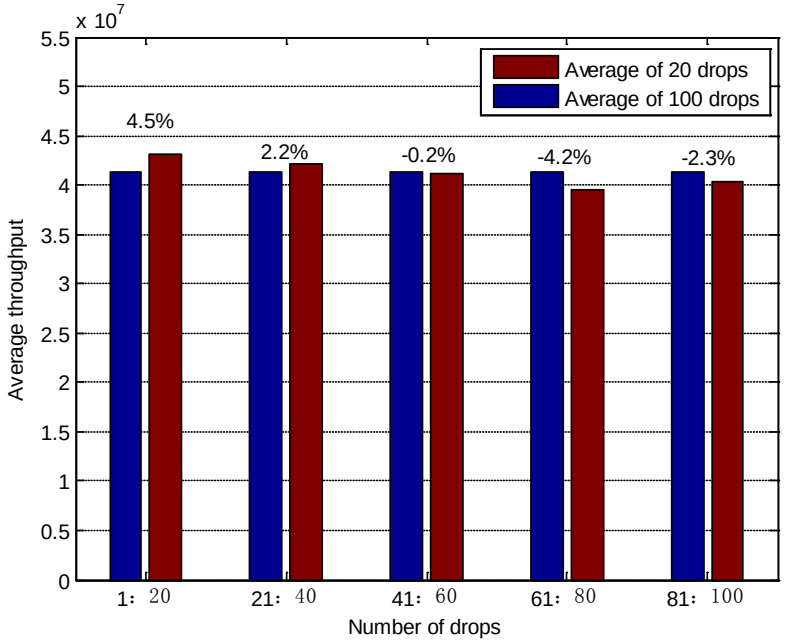

Figure 3.9 System throughput *vs.* number of drops

The simulation result is compared with the results of other relevant studies in [36] which are accurate to the same order of magnitude. In [36], the central frequency is 5 GHz and system bandwidth is 1 MHz; when the number of users is 10, the spectral efficiency of the PPF algorithm proposed in [36] is about 4.5 bps/Hz. The PPF algorithm is implemented in the simulator here for verification. In this thesis, the central frequency is 2 GHz and system bandwidth is 10 MHz and when the number of users is 10, the spectral efficiency of the PPF algorithm proposed in [36] is about 4.4 bps/Hz (can be calculated from Figure 3.10). It can be concluded that the simulation results are of the same order of magnitude.

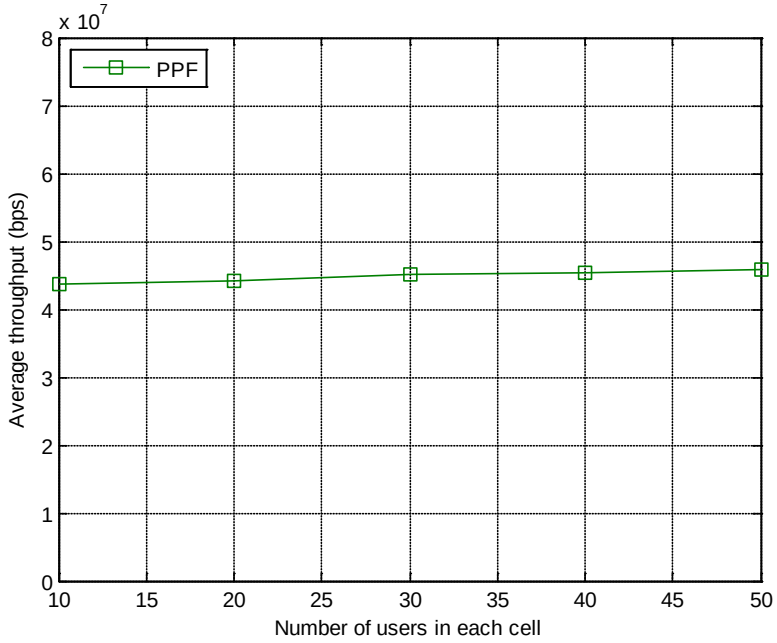

Figure 3.10 System throughput *vs.* number of users

3.6 Summary

A description of the overall design of the simulation platform and system parameters is given in the first part of this chapter, together with the system parameters. This is followed by a more detailed explanation of the most important modules. The channel model is introduced in the end of this chapter including pathloss model, shadow fading model and fast fading model.

Chapter 4 Radio Resource Allocation in OFDMA Relay Networks

4.1 Introduction to Radio Resource Management

The radio resource in wireless networks includes: transmission power, time-domain resource, frequency-domain resource and spatial-domain resource. The object of radio resource management is i) to improve system validity and reliability given the finite radio resource available, ii) to satisfy different quality of service (QoS) requirements for different types of application from users, and iii) to maximize the radio resource efficiency. The basic idea of radio resource management is that, as the channel state varies with the changing of channel fading and interference, the radio resource in the wireless system can be allocated flexibly and adjusted dynamically to meet the QoS requirements of users, and the system throughput and spectrum efficiency can be improved.

Radio resource management can be classified into three main parts: radio resource allocation, mobility management and spectrum management. Radio resource allocation focuses on allocating the radio resource to different users. When a user is moving, mobility management too becomes necessary. Spectrum management is about how best to divide up the available bandwidth from the whole system point of view.

Radio resource allocation is important for increasing wireless network capacity. There are three main issues which need to be solved in wireless resource allocation: *the first,* which wireless access point will be connected for wireless terminal; *the second*, how the system allocates subchannels to users; *the third*, what power level should be used in the transmitter.

The first issue is solved by access control and load control. Access control decides whether to accept the new access request and which access point provides the

wireless connection. Traffic load control can avoid the system load being too heavy, so causing the channel condition to deteriorate and changing the service characteristics.

A good channel allocation mechanism can solve the second issue in wireless resource allocation, improving the system throughput and user performance by allocating channel resources in the best possible way. In TDMA systems, the channel resource is a time slot; in FDMA systems, it is a frequency subchannel; in CDMA systems it is a code; and in OFDMA systems, the channel resource is a time-frequency two-dimensional block, which is defined as subchannel [41].

Packet scheduling determines the output order of the packets in the traffic buffer. For single-carrier systems, the channel is allocated to users if the packets of that user are being scheduled, i.e. scheduling has the same function as channel allocation in single carrier channel systems. For multi-carrier systems (OFDMA systems), during one scheduling interval, the packets can be transmitted in more than one subchannel. So, after packet scheduling, the subchannel needs to be allocated. Currently, most algorithms consider the packet scheduling and subchannel allocation jointly.

Power control (or power allocation) is used to solve the third issue. In wireless networks, transmission power is not only relevant to the performance of the target receiver, but also affects the performance of other receivers using the same subchannel. In 3G systems, power control is used to reduce the co-frequency interference within the cell, and to mitigate far-near effect [42].

In OFDMA systems, power control can be used to compensate propagation loss and shadow fading [43]. Moreover, power allocation should be considered to compensate the fast fading. So, compared with power control, the power allocation interval is short and the granularity of power allocation is finer. To guarantee both the performance requirement for a particular user as well as for the whole system, power allocation and subchannel allocation are usually considered jointly in each subchannel in every scheduling interval [44]. Besides, since the frequency reuse

factor is one in OFDMA systems, power allocation is one of the important methods to minimize the effect of inter-cell interference [45][46].

As mentioned in Section 2.4, resource management is a key factor in relay based cellular systems and different aspects have been researched. The resource allocation scheme devised by the author and presented in Section 5.3 captures relay selection and channel allocation tasks. However, before considering that novel work, it is necessary to discuss previous research on relay selection, channel allocation and power allocation.

4.2 Relay Selection

As discussed in Section 2.6.1, two-hop relaying is a good design choice for the tradeoff between performance gain and system complexity. In this case the routing problem is simplified into a relay selection problem, which can simplify the protocol design and minimize the communication overhead significantly compared with more complex structures (such as mesh network).

Relay selection aims at improving the data rate transmitted from the source to the destination by forwarding traffic via a suitable RS with spare capacity that is experiencing a more favourable channel condition. While it might appear at first sight that relay selection (routing) is similar to that in ad hoc networks, there are significant differences [12]:

- Small number of hops compared with a full scale ad-hoc network.
- Central processing: in multi-hop cellular networks, there is an infrastructure unlike ad-hoc networks; also the location information and flow direction in both uplink and downlink are available, especially for the case where fixed-relays are used.
- Fewer energy constraints: in contrast with the case of ad-hoc networks, especially where fixed relays are used, the power constraints and energy efficiency are not so critical in relay networks.

Various selection schemes for the relay and relay channel, from random to smart selection, with and without power control, are considered in [40]. It is observed that with the proper selection of relay, relay channel, and relay power, a significant enhancement in high-data-rate coverage can be attained through two-hop mobile relaying.

In an infrastructure-based network with fixed relays, the selection of relays is more or less predefined. The relay selection approaches based on centrally controlled methods can be used for selecting the RS for every MS in each cell, and various selection criteria can be used for designing the relay selection method. Distance based relay selection algorithms [40][47] and pathloss based relay selection algorithms [40][48] have been proposed; a transmission power-based relay selection algorithm is proposed in [49] and a congestion-based relay selection algorithm is studied in [50].

[51] considers the relay selection problem in a basic amplify-forwarding relay scenario that has one source and two destinations, so the problem is required to decide which node will be used as RS. The proposed schemes in [51] are the (i) classical round robin and (ii) a channel-based scheduling policy that requires a partial feedback from the channel. This scheme is implemented in a centralized and a distributed version. With a centralized strategy, routing is performed in a central controller, which normally possesses powerful processing capabilities so that sophisticated routing algorithms may be used. While this may optimize the system performance, it does require a lot of information to be obtained from the distributed network nodes and passed to the central controller; this leads to a significant message-passing overhead. With the distributed version, all network nodes from the source to the destination jointly perform route determination. This approach can be used without a central controller but the performance is normally limited by the knowledge of the network status within the distributed nodes [51].

In [52], relay selection is investigated in relay systems in which user terminals act as relays. Relay selection with mobile relays is more complicated than fixed relays as the topology of mobile relays is not fixed. However, this thesis considers only fixed relays so mobile relays are not considered further.

4.3 Channel Allocation

In [53], a distributed scheduling algorithm is proposed for a downlink relay network, in which MSs act as mobile relays. The authors use a scalable factor-graph-based soft information-passing algorithm to schedule simultaneous data transmissions in a distributed way. Not only dynamic routing paths for data packets are obtained, but also direct data collisions among simultaneously transmitted data packets are avoided.

The scheduling problem in a cooperative relay system is considered in [54], in which the system diversity gain is achieved by amplify and forwarding cooperative relays and the multi-user gain is obtained from adaptive channel scheduling.

The authors in [55] propose a radio resource allocation in fixed relay systems in which the optimization objective is maximizing system throughput. It is proved that this optimization problem is a NP-hard problem, so a heuristic algorithm is proposed in [55], which is called *combined resource allocation*, including routing, scheduling and relay load balancing. The scheduling scheme can adaptively handle different transmission modes (direct link mode or multi-hop link mode).

Traditionally, the channel variation in wireless networks is considered as a negative factor for reliable communication, and methods such as time interleaving, power control and multiple antennas are used to reduce its impact. On the other hand, opportunistic scheduling is designed to exploit the variation in channel conditions to improve spectrum efficiency by adding an additional degree of freedom to the system: time domain diversity, also called multi-user diversity. It improves spectrum efficiency, especially for delay-tolerant data transmissions [56].

In an opportunistic scheduling scheme, the user that has a good channel gain will have a greater opportunity to occupy this channel, so the resource can be used efficiently and the system performance improved. The proportional fairness (PF) scheduling algorithm used in CDMA High Data Rate (HDR) system is an opportunistic scheduling scheme [57]. The PF algorithm not only considers the instantaneous achievable data rate in each TTI, but also considers the average data rate of a user, which gives a good tradoff between system throughput and user fairness.

In [58] traffic-aided smooth admission control and relay aided opportunistic scheduling (RAOS) are proposed in TDMA relay systems. First, the transmission mode of the user (direct-link or two-hop link) is decided, and then the priority of each user in each time subslot is calculated. The scheduler chooses the user k with the highest priority. If the user is using a two-hop link, the BS sends data to the user k via the selected relay station $r(k)$, otherwise it sends data directly.

A partial proportional fairness scheduling (PPF) scheme is proposed in [36] for relay based OFDMA/TDD cellular systems, the traditional proportional fairness algorithm being used for the resource allocation in the second time subslot. Both direct link users and two-hop relay link users have the opportunity to be allocated in the second time subslot. In the first time subslot, RS has a priority to choose the first hop subchannels. The priority of each RS is decided by the ratio of second-hop link achieved throughput and first-hop link achieved throughput. The RS with highest priority chooses the subchannel which has the biggest gain among all the subchannels as the first-hop channel. The resource allocation to the first-hop link via each fixed RS will end when the first-hop data rates and the aggregate second-hop data rates reach a balance. The left-over resource units of the first-hop link will be assigned to direct link users on the basis of the proportional fairness principle.

[59] aims to maximise the system capacity; the optimal source/relay/subchannel allocation problem is formulated as a binary integer programming problem. The

problem is then tackled using a graph theoretical approach by transforming it into a linear optimal distribution problem in a directed graph. However, the complexity of this algorithm is very high and so is not suitable for real-time multi-hop systems. In [60], the resource allocation between the BS and RSs in OFDMA relay systems is not considered by assuming that the BS and RSs can communicate reliably through dedicated frequency bands; instead a fast heuristic algorithm is studied as a joint optimization algorithm of relay selection and subchannel allocation. In that paper, the first step is to sort a set of subchannel gains in descending order and assign subchannels to each user according to the sorted subchannel order. If a user receives a certain number of subchannels, subchannel allocation to that user is stopped and then the remaining subchannels are assigned to the user who has the best channel gain for those subchannels.

4.4 Power Allocation

Power allocation in a relay system can be classified into two kinds of problem in terms of constraint conditions. One is joint power constraint on BS and RS [61][62][63][64] (i.e. the sum of the power constraint of BS and RS is a constant) and the other is BS and RS having separate power constraints **Error! Reference source not found.**.

In [61], an optimal power allocation method to minimize the outage probability of a Rayleigh fading channel is presented. Optimal power allocation to maximize the system capacity is proposed for regenerative and non-regenerative relaying schemes in [62] respectively. However, in [61][62][63] the system considered is not OFDM so the first hop link and the second hop link use the same channel.

The problem of power allocation in OFDM relay systems is studied in [64][65]. In [64] cooperative non-regenerative relays are considered; the authors give an equivalent channel gain model for those cooperative subcarrier pairs and the optimal power allocation problem is divided into two parts, one considers the total power allocation on the cooperative subcarrier pairs and the other considers the power allocation

between the selected cooperative subcarrier pairs using the power water-filling approach.

In [65], power allocation over the frequency subchannels of one source/destination pair and one non-regenerative relay is studied to maximize the instantaneous data rate of the link. It is assumed that source and relay have their own separate transmission power constraints and the second hop link uses the same subcarrier as the first hop link. Optimal power allocation algorithm at the relay (or source) is used with an equal source (or relay) power allocation. Then, alternating iterative optimization of relay and source power allocation is proposed, where the output of the previous optimization (relay or source) is the input of the other (source or relay).

The studies of power allocation in [64] are based on the assumptions that one subcarrier on the first hop link and one subcarrier on the second hop link make up a subcarrier pair, i.e. the subcarriers of the two hop links correspond to each other, but this situation only exists in non-regenerative OFDM relay channels: with a regenerative relay channel, these kinds of subcarrier pairs do not exist.

4.5 Summary

The radio resource allocation in relay networks is introduced in this chapter. The basic concept and content of resource management is introduced first, and then the relevant work of relay selection, channel allocation and power allocation is considered.

Chapter 5 Fair Subchannel Allocation and Relay Selection

5.1 Introduction

The problem of fair resource allocation is more challenging in relay based cellular systems, for there are two kinds of users: direct link users and relay link users. Fairness issues include those (i) between relay link user and direct link user, (ii) among relay link users and (iii) among direct link users. To solve this problem, a two-hop proportional fairness algorithm is proposed which can give a tradeoff between system throughput and user fairness.

The conventional algorithms [40][47] are only based on the pathloss or distance conditions of individual users, do not consider the load of the RS, and cannot tackle the fairness problem in terms of RS load condition, especially when users are not distributed uniformly. So in this chapter a load based relay selection algorithm is proposed, which takes into account the traffic load condition (bandwidth requirement) of relay link users and direct link users, and improves the fairness of resource allocation for OFDMA based relay systems.

5.2 System Model

5.2.1 System Parameters

In relay based OFDMA systems, the system bandwidth is B, the number of subcarriers is C, and the access method is OFDMA. The number of RSs is R. As explained earlier, to balance system complexity and system performance, the number of hops is two. In practical OFDMA systems, a group of consecutive subcarriers with similar fast fading can make up a subchannel and each subchannel can be used as a resource scheduling unit instead of using subcarriers [16]. In this way, the control signal overhead can be reduced, and the algorithm complexity is decreased, but the system performance is unaffected. In the system model here, S consecutive

subcarriers are grouped together as a subchannel, the number of subchannels M is C/S and the bandwidth of each subchannel is B/M .

In each cell, the BS chooses one communication mode (direct link or relay link) for each MS. If the communication mode is relay link, the BS chooses one RS for each relay link user. k is the index of a MS in each cell. The direct link user is k_d and the set of direct link users is K_D. The relay link user k served by the RS r is denoted as k_r, the set of relay link users is K_R, and the set of users served by the RS r is expressed as K_{R_r}. The RS serving the user k is r_k.

5.2.2 Channel Capacity

The term $a_m^{k_d}$ is used to denote whether the subchannel m is allocated to the direct link user k_d; $a_m^{k_d}=1$ indicates it is allocated and $a_m^{k_d}=0$ shows that it is not. In a similar way a_m^r represents the allocation of the subchannel m to the RS r. Similarly, for the second hop link $b_m^{k_r}$ denotes whether the subchannel m is allocated to the user k via the RS r , in which k_r is the user k served by the RS r.

According to the Shannon formula, the capacity of the direct link user k_d on the subchannel m in the first time subslot is:

$$c_{m,1}^{k_d} = B_m \log_2\left(1+\frac{g_{m,1}^{k_d} p_{m,1}^{k_d}}{\Gamma\sigma^2}\right) \tag{5.1}$$

The capacity of the RS r on the subchannel m in the first time subslot is:

$$c_{m,1}^{r} = B_m \log_2\left(1+\frac{g_{m,1}^{r} p_{m,1}^{r}}{\Gamma\sigma^2}\right) \tag{5.2}$$

The capacity of the user k_r on the subchannel m in the second time subslot is:

$$c_{m,2}^{k_r} = B_m \log_2\left(1+\frac{g_{m,2}^{k_r} p_{m,2}^{k_r}}{\Gamma\sigma^2}\right) \tag{5.3}$$

B_m is the bandwidth of each subchannel; $p_{m,1}^{k_d}$ and $p_{m,1}^{r}$ are the transmission power of the BS on the subchannel m to the MS k_d and the RS r respectively; $p_{m,2}^{k_r}$ is the transmission power of RS r on the subchannel m to MS k; $g_{m,1}^{k_d}$ ($g_{m,1}^{r}$) is the subchannel gain between the BS and the MS k_d (RS r) on subchannel m; $g_{m,2}^{k_r}$ is the subchannel gain between the RS r and the MS k on the subchannel m; $\Gamma = -\ln(5\cdot BER)/1.5$ is a parameter related to the target BER [26]; σ^2 is the variance of AWGN.

For the direct link user k_d, the achieved data rate in the first time subslot is:

$$c^{k_d} = \sum_{m=1}^{M} a_m^{k_d} c_{m,1}^{k_d} \tag{5.4}$$

The achieved data rate of the relay link user k_r in the second time subslot is:

$$c_2^{k_r} = \sum_{m=1}^{M} b_m^{k_r} c_{m,2}^{k_r} \tag{5.5}$$

The data rate of the RS r in the first time subslot is shared by all the relay link users served by this RS, so the achieved data rate of the relay link user in the first time subslot is:

$$c_1^{k_r} = c_1^r \frac{c_2^{k_r}}{\sum_{K_{R_r}} c_2^{k_r}} \tag{5.6}$$

where c_1^r is the data rate of the RS r in the first time subslot:

$$c_1^r = \sum_{m=1}^{M} a_m^r c_{m,1}^r \tag{5.7}$$

The available data rate of the relay link user k_r is determined by the minimum capacity of the first time subslot and that of the second time subslot, which can be expressed as:

$$c^{k_r} = \min\left\{c_1^{k_r}, c_2^{k_r}\right\} \tag{5.8}$$

5.2.3 Optimization Problem

In order to consider proportional fairness across two hop links, the optimization problem is formulated as:

$$\max \sum_{k=1}^{K} c^k$$
$$s.t. \begin{cases} 1) c^i = c^j, \forall i, j \in \{1,2,...K\} \\ 2) \sum_{m=1}^{M}\sum_{k=1}^{K} a_m^{k_d} p_{m,1}^{k_d} + \sum_{m=1}^{M}\sum_{k=1}^{K} a_m^r p_{m,1}^r \le P_{BS} \\ 3) \sum_{m=1}^{M}\sum_{k=1}^{K} b_m^{k_r} p_{m,2}^{k_r} \le P_{RS} \\ 4) \sum_{k\in K_D} a_m^{k_r} + \sum_{r=1}^{R} a_m^r = 1 \\ 5) \sum_{r=1}^{R}\sum_{k\in K_{R_r}} b_m^{k_r} = 1 \end{cases} \tag{5.9}$$

There are five constraint conditions of the optimal target above:

1) is the requirement of data rate fairness between users, i.e. all the users achieve the same data rate in each scheduling interval;

2) shows the constraint on the total power of the BS;

3) shows the constraint on the total power of the RS;

4) expresses that one subchannel can only be allocated to one station (RS or direct link user) in the first time subslot;

5) expresses that one subchannel can only be allocated to one relay link user in the second time subslot.

This problem cannot be solved to yield an optimal solution directly, since it is not a convex optimization problem, so a heuristic method to get a suboptimal solution is used. To simplify this problem, the first constraint condition is relaxed. Long-term fairness is pursued as a constraint condition instead of aiming for short term fairness in each scheduling interval.

5.3 Two-Hop Proportional Fairness Algorithm

In a conventional OFDMA wireless system (no relay), the PF algorithm [6] achieves the best tradeoff between system throughput and user fairness. However, the PF algorithm cannot be applied directly in two-hop relaying systems since the direct link and relay link are present simultaneously: a fair allocation problem in both the two time subslots needs to be considered.

In this thesis, a new algorithm, called "two-hop proportional fairness" (THPF) scheduling algorithm, is proposed to allocate the subchannels in both time subslots with a fair subchannel allocation, in which subchannels are allocated to relay link users fairly in the second time subslot and subchannels are allocated fairly to RSs and direct link users in the first time subslot as well. The average data rate of the RS is defined as the average data rate of all relay link users served by this RS, and a match factor is proposed considering the capacity match issue between the first link and the second link for each RS.

5.3.1 Algorithm Description

The subchannel allocation in the second time subslot is considered first. The priority of the relay link user k_r on the subchannel m in the second time subslot is defined as the ratio of the instantaneous data rate of the user k_r in the current TTI to the average data rate of the user k_r achieved in the previous TTIs. The priority of the relay link user k_r on the subchannel m is expressed as:

$$q_{m,2}^{k_r} = \frac{c_{m,2}^{k_r}}{\overline{c}^{k_r}} \tag{5.10}$$

where $\overline{c}^{k_r}$ is the time average data rate of the user k_r.

Each subchannel is allocated to the relay link user who has the highest priority on this subchannel, i.e.

$$k_r^*(m) = \arg\max_{k_r \in K_R} q_{m,2}^{k_r} \tag{5.11}$$

The subchannel m which is allocated to the user k_r can be represented as m_{k_r} and $b_m^{k_r^*}$ will be set to one.

After the subchannels have been allocated in the second time subslot, the instantaneous data rate of the RS r on the second time subslot is:

$$c_2^r = \sum_{k_r \in K_{R_r}} c_2^{k_r} \tag{5.12}$$

Next, the BS allocates subchannels to either RSs or to the direct link users in the first time subslot as described in the following steps. The priority of a direct link user can be expressed as:

$$q_{m,1}^{k_d} = \frac{c_{m,1}^{k_d}}{\overline{c}^{k_d}} \tag{5.13}$$

Since the RS forwards the data received from the BS to the relay link users, the average data rate of the RS r is represented by the mean of all time average data rate of all the relay link users served by the RS r:

$$\overline{c}^r = \frac{1}{\left|K_{R_r}\right|} \sum_{k_r \in K_{R_r}} \overline{c}^{k_r} \tag{5.14}$$

in which, $\left|K_{R_r}\right|$ stands the number of relay link users in the set of K_{R_r}.

Meanwhile, in order to fully exploit the channel capacity in the second time subslot, the matching problem between achieved data rate in the two time subslots of each RS needs to be considered, a match factor β^r being defined to modify the priority function of proportional fairness.

$$\beta^r = c_2^r / c_1^r \tag{5.15}$$

The priority function of the RS r on the subchannel m can be formulated as:

$$q_{m,1}^r = \beta^r \frac{c_{m,1}^r}{\bar{c}^r} \tag{5.16}$$

The priority of direct link user and each RS on each subchannel is calculated by (5.13) and (5.16), and each subchannel is assigned to the node (RS or direct link user) which has the highest priority. For example, for the subchannel m, let $q_{m,1}^{\hat{k}_d} = \max q_{m,1}^{k_d}$, $q_{m,1}^{\hat{r}} = \max q_{m,1}^{r}$. If $q_{m,1}^{\hat{k}_d} > q_{m,1}^{\hat{r}}$, then the subchannel m is assigned to the direct link user $\hat{k}_d$, i.e., $a_m^{\hat{k}_d} = 1$. If $q_{m,1}^{\hat{k}_d} \le q_{m,1}^{\hat{r}}$, the subchannel m is assigned to the RS $\hat{r}$, $a_m^{\hat{r}} = 1$, and $c_1^{\hat{r}}$ is updated according to (5.7).

If $\beta^{\hat{r}} \le 1$, the RS $\hat{r}$ would be excluded from the candidate RSs for the subchannels allocation.

The achieved data rate of direct link users and relay link users during this scheduling interval (TTI) will be updated according to (5.4) to (5.8) respectively. Lastly, the average data rate of each user will be calculated by the exponential weighed average data rate function [36][57]:

$$\bar{c}^k(t) = (1-\rho)\cdot \bar{c}^k(t-1) + \rho \cdot c^k(t) \tag{5.17}$$

where ρ is the exponential weighed factor of the average data rate function.

5.3.2 Algorithm Procedure

The THPF algorithm procedure is as follows:

Step1: Initialization at the beginning of each scheduling interval:

$$a_m^{k_d}=0,\ a_m^r=0,\ b_m^{k_r}=0,\ c^r=0, c^{k_d}=0,\ c_1^{k_r}=0,\ c_2^{k_r}=0, \forall k,r,m$$

Step2: Subchannel allocation in the second time subslot:

For $m=1: M$

$$k_r^*(m)=\arg\max_{k_r\in K_R} q_{m,2}^{k_r} \text{ and } b_m^{k_r^*}=1$$

End

Step3: Calculate $c_1^{k_r}$, $c_2^{k_r}$, β^r, $q_{m,1}^{k_d}$, $q_{m,1}^r$.

Step 4: Subchannel allocation in the first time subslot:

For $m=1: M$

$$q_{m,1}^{\hat{k}_d}=\max q_{m,1}^{k_d},\ q_{m,1}^{\hat{r}}=\max q_{m,1}^r$$

If $q_{m,1}^{\hat{k}_d} > q_{m,1}^{\hat{r}}$

$a_m^{\hat{k}_d}=1$

Else $a_m^{\hat{r}}=1$

End

Update $c_1^{\hat{r}}$, β^r, $q_{m,1}^{\hat{r}}$

If $\beta^{\hat{r}} \le 1$, the RS $\hat{r}$ can't compete for the remains of the subchannels

End

End

Step 5: Update c^k, $\bar{c}^k$.

5.3.3 Performance Simulation and Analysis

A single-cell relay OFDMA cellular scenario is considered with six RSs uniformly located on the line that connects the cell centre to one of the six cell vertices, as shown in Figure 5.1. In the cell, MSs are distributed uniformly. A MS can either connect to the BS directly, or via an RS. The relay selection scheme depends on the pathloss [40] in this section.

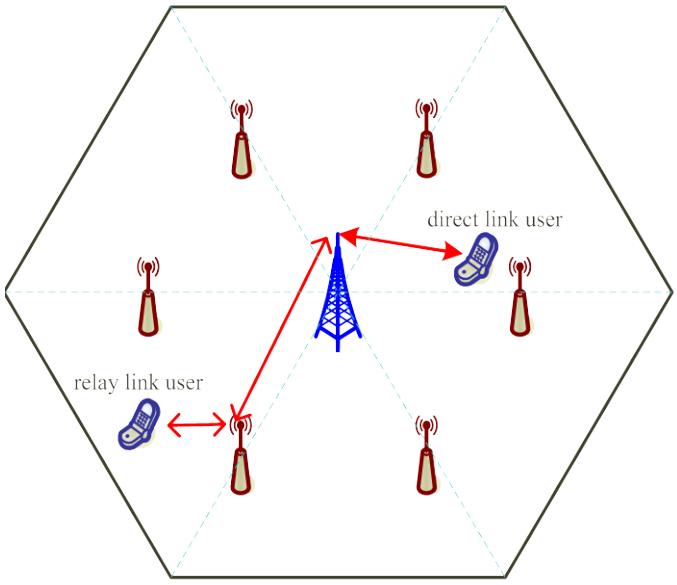

Figure 5.1 Layout of single cell relay based OFDMA network

The simulation parameters of the DF relay based OFDMA network shown previously in Table 3.1, Table 3.2 are used. It is assumed that the buffer of each RS is sufficiently large so that in each time slot, all the data received from the BS in the first time subslot, can be forwarded directly to the MS by the RS without considering any data buffer size restriction.

Max Carrier to Interference Ratio (Max C/I) [36] and Round-Robin (RR) [36] are the traditional scheduling algorithms in wireless systems. These two algorithms are

modified by the author to make them suitable for OFDMA relay systems and to allow them to be compared with THPF.

Max C/I is an opportunistic algorithm that always allocates the subchannels to users who have a good channel state. For OFDMA relay systems, in the first time subslot, each subchannel is allocated to the node (the direct link user or the RS) with the maximum SINR; in the second time subslot, each subchannel is allocated to the relay link user with the maximum SINR. In this way, a high system throughput will be obtained by Max C/I scheduling and the system resources are fully utilized. However, those users with bad channel conditions will suffer unfairness.

RR algorithm is fair and simple when the channel conditions remain approximately constant. However, in a fast fading channel, the RR algorithm has a low spectral efficiency since users are scheduled in order without considering the channel condition. In OFDMA relay systems, the RR can be modified to schedule users over two time subslots. In the second time subslot, each subchannel is allocated to the relay link users one by one until all the subchannels are allocated. In the first time subslot, each subchannel is allocated to the RSs first and then the rest of the subchannels are allocated to the direct link users in order.

In [36], a Partial Proportional Fairness (PPF) algorithm which adopts the PF algorithm for the subchannel allocation in the second time subslot was proposed. However, the PPF gives an absolute priority to the RS when assigning the first time subslot subchannels, considering neither the fairness between RSs nor the fairness between RSs and direct link users. Since the PPF algorithm is also a fair scheduling algorithm for relay based OFDMA systems, PPF is used for comparison with the THPF algorithm for further performance analysis. Note that in the PPF algorithm described in [36], direct link users can be allocated subchannels in the second time subslot; however, for better comparison with the THPF with the same frame structure, the original PPF algorithm was modified by the author of this thesis so that

direct link users can only use the first time subslot for matching the frame structure shown in Figure 2.7.

The transmission power on BS or RS is assumed to be allocated on subcarriers uniformly; this is called equal power allocation.

In this part of the research on scheduling algorithms, the system throughput and the user fairness are examined under equal power allocation, comparing the RR, Max C/I, PPF and THPF approaches.

The system average throughput is the sum of average throughput across all users. The Raj Jain fairness index [60] is adopted in this paper to measure the fairness among users.

The Raj Jain fairness index is defined as

$$F = \frac{\left(\sum_{k=1}^{K} \tilde{C}_k\right)^2}{K\sum_{k=1}^{K}\left(\tilde{C}_k\right)^2} \tag{5.18}$$

The most fair scheduling scheme is when the average data rate of each user is equal to others, where $F = 1$ represents the maximum fairness – lower values are less fair. K is the total number of users. $\tilde{C}_k$ is the time average throughput of the user k during the simulation time.

The position of the RSs will affect the transmission mode selection and RS selection of each user, so it is necessary to compare the system performance between Max C/I, RR, PPF, and THPF with different RS positions (defined in terms of D, the radius of the cell, $0.5D$, for example, meaning that the RS is $0.5D$ away from the BS).

Figure 5.2 and Figure 5.3 show the system throughput and user fairness between Max C/I, RR, PPF, and THPF against different RS normalized distance, which is defined as the ratio of the distance between the RS and the BS to cell radius D.

From the simulation result of Figure 5.2 and Figure 5.3, a good system throughput and fairness performance for these scheduling algorithms is achieved when the RS is between $0.5D$ and $0.6D$ away from the BS. Thus, in the following simulation the performance of these three algorithms is compared when the RS is located at $0.5D$ away from the BS.

From Figure 5.2, the maximum system average throughput is obtained by Max C/I while RR has the minimum system average throughput. However, Max C/I has the lowest fairness index while the THPF algorithm has the highest fairness index as shown in Figure 5.3. From these figures it can be seen that the THPF algorithm offers a good tradeoff between system throughput and fairness.

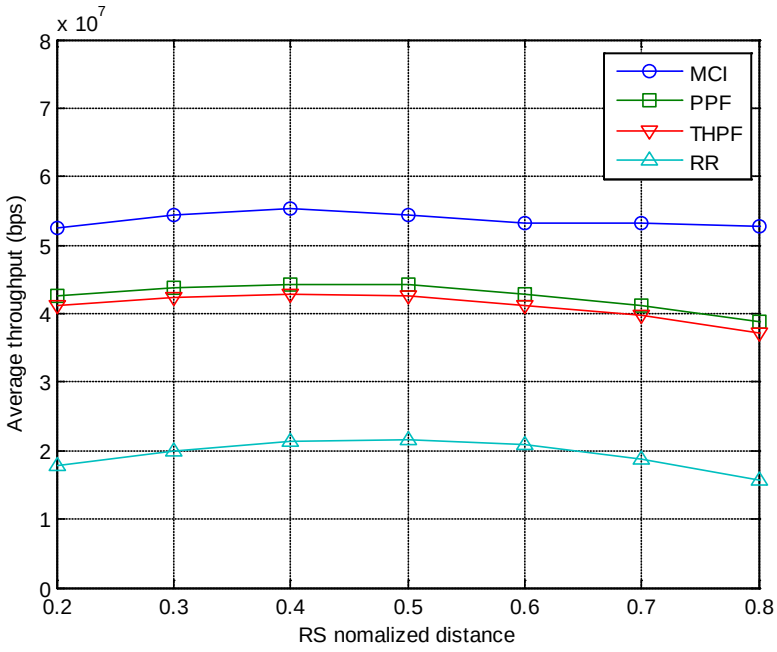

Figure 5.2 System throughput *vs.* RS normalized distance

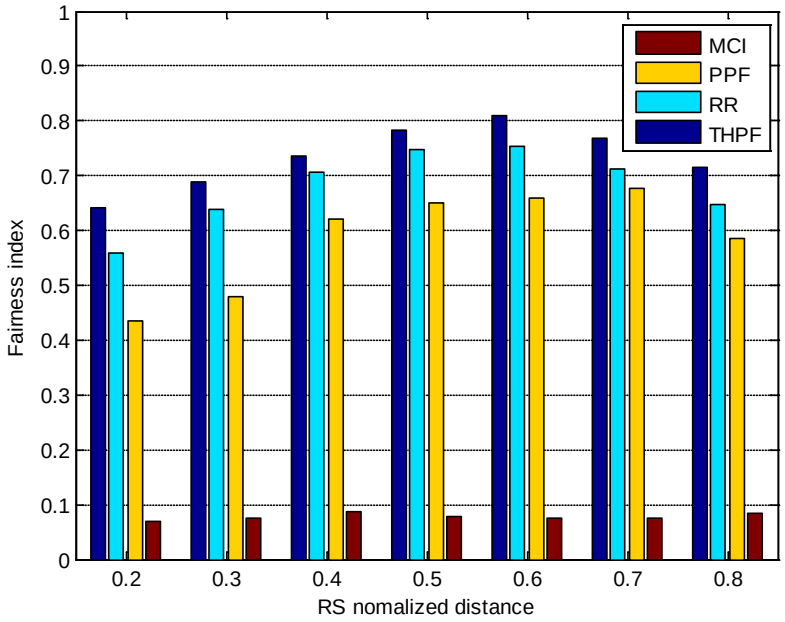

Figure 5.3 Fairness index *vs.* RS normalized distance

Figure 5.4 and Figure 5.5 show the system throughput and user fairness comparison with different numbers of users.

From the simulation results Figure 5.2-Figure 5.5, it can be seen that compared with PPF, the THPF achieves greater fairness in user data rate allocation in spite of having only a slightly lower throughput. For example, if the RS is located at $0.5D$ away from the BS, the throughput of THPF is only 4% lower than that of PPF. However, the fairness of THPF is 20% higher than that of PPF.

For the Max C/I and THPF algorithms, it can be concluded that system throughput improves as the number of users increases, as shown in Figure 5.4. The reason is that Max C/I algorithm only considers the channel conditions of users to gain maximum multi-user diversity; therefore, as the number of users increases, the system throughput increases but the fairness decreases (as in Figure 5.5). The THPF algorithm and the PPF algorithm consider both system throughput and fairness so the throughput also increases with the number of users. For the RR algorithm, the system throughput does not change with the number of users. When the number of

users is small, the fairness of RR is the best of all (because there is then enough capacity to divide fairly between the few users), but then deteriorates as the number of users increases.

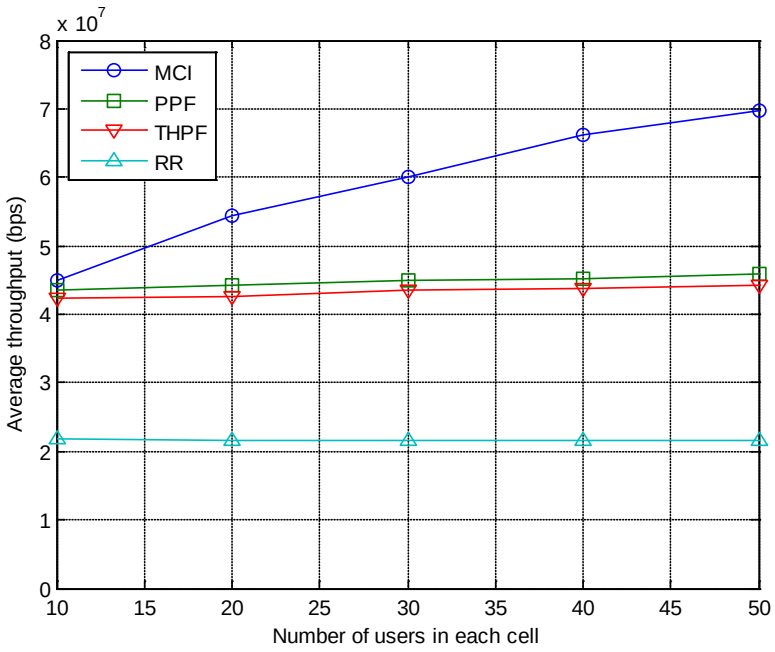

Figure 5.4 System throughput *vs.* number of users

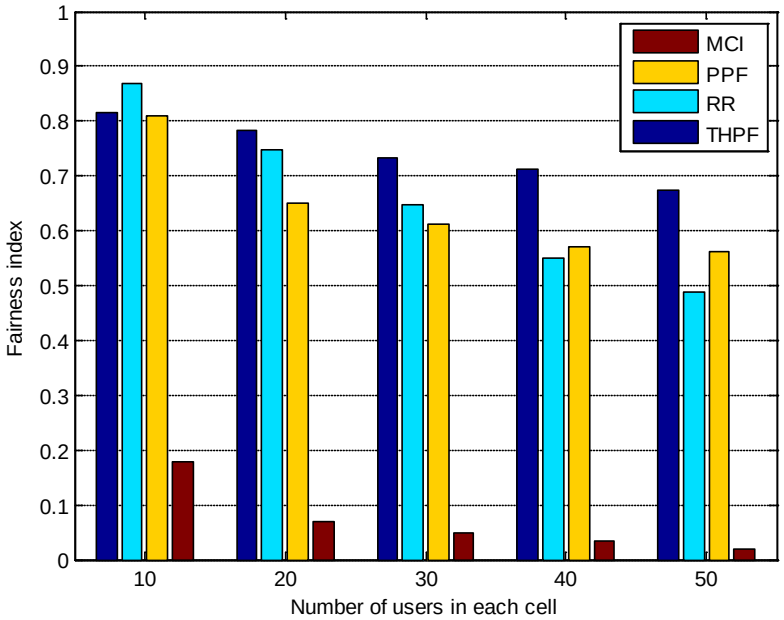

Figure 5.5 Fairness index *vs.* number of users

The average throughput of PPF is higher than THPF because the PPF algorithm only aims to make full use of the system spectral diversity gain but does not consider fairness in the first time subslot. However, the average throughput of THPF is almost 96% of that achieved by PPF and the fairness of THPF is much better than PPF, as shown in Figure 5.4 and Figure 5.5.

In Figure 5.2-Figure 5.5, the performance of the Round Robin, Max C/I, PPF and THPF algorithms are compared with different RS position and different number of users. From the simulation results, it can be seen that THPF can achieve a good tradeoff between system throughput and fairness.

5.4 Load Based Relay Selection Algorithm

The existing relay selection algorithms (such as: distance based relay selection and pathloss based relay selection) have the advantage of being very simple for relay based OFDMA systems. However, these algorithms decide which transmission mode (direct link mode or relay link mode) will be used and which RS is to be chosen only based on the pathloss or distance conditions of an individual user. For example, in a hotspot area many users are assigned to transmit through one RS (as they are near this RS or have a good channel condition) [40]; as a result the resource allocation may not be fair because some of the users may not be scheduled in the long term as there are insufficient relaying channels. In this situation, some users' transmission mode should be changed so they transmit directly to the BS, even though the instantaneous channel conditions of the relay link are better than that of the direct link.

So, these conventional algorithms do not consider the influence of the bandwidth requirements (system traffic load) of direct link users and relay link users in terms of fairness in the resource allocation. This will affect user fairness especially when users are not distributed uniformly. As RSs are usually located in some hotspot area, or are used in some emergency area, it is important that this problem is considered in the

relay selection algorithm. Unfortunately, there is little literature that focuses on this problem.

Therefore, a load based relay selection (LBRS) scheme is proposed that considers the traffic load condition of the system. With LBRS, the transmission mode of users (direct link mode or relay link mode) can be adjusted dynamically depending on the user average data rate. As adaptive scheduling and subchannel allocation can be used for fair resource allocation, the user fairness problem can be solved by the load based relay selection algorithm together with the two-hop proportional fairness scheduling algorithm proposed in the section 5.3.

5.4.1 Algorithm Description

Long-term resource allocation needs to be considered in the relay selection process so that a load-based relay selection algorithm is proposed, which considered the traffic load of BS and RS, to make the average data rate between relay link users and direct link users equal in the long-term. The relay selection is initialized by the pathloss based relay selection algorithm [40], and then the user terminal will adjust the transmission mode based on the long-term average data rate.

Examine the average data rate on the subchannel m in the second time subslot first. Assuming the probability for the subchannel m being allocated to the relay link user k_r is φ_{k_r}, the average data rate of the second hop link of the relay link users on the m^{th} subchannel in the second time subslot is:

$$C_{m,2}^{k_r} = \sum_{K_R} \varphi_{k_r} c_{m,2}^{k_r} \tag{5.19}$$

The cardinality of the set K_R is represented by $|K_R|$. Assuming the probability of occupying the m^{th} subchannel for each relay link user is $\varphi_{k_r} = \frac{1}{|K_R|}$ [66], (5.19) can be converted as follows:

$$C_{m,2}^{k_r} = \frac{\sum_{K_R} c_{m,2}^{k_r}}{|K_R|} \tag{5.20}$$

The total average data rate of the second hop link of the relay link users on all the M subchannels in the second time subslot is:

$$\tilde{C}_2^{k_r} = M \cdot C_{m,2}^{k_r} \tag{5.21}$$

Assume probability of each RS using the m^{th} subchannel is equal to that of any other RS (this will be satisfied in the long term), and the relay links users are served by the RSs, so the total average data rate of the first hop link of the relay on the m^{th} subchannel in the first time subslot is:

$$C_{m,1}^{r} = \frac{1}{|R|} \sum_{R} c_{m,1}^{r} \tag{5.22}$$

Assuming the number of subchannels allocated to all the RSs in the first hop link is x, the number of subchannels allocated to direct link users in the first hop link is $(M - x)$.

The total average data rate of the first hop link for all the relay link users on the x subchannels in the first time subslot is:

$$\tilde{C}_1^{k_r} = x \cdot C_{m,1}^{r} \tag{5.23}$$

Similarly to relay link users, the average data rate of all the direct link users on the m^{th} subchannel in the first time subslot is:

$$C_m^{k_d} = \frac{1}{|K_D|} \sum_{K_D} c_{m,1}^{k_d} \tag{5.24}$$

So the total average data rate on $(M-x)$ subchannels achieved by all the direct link users is:

$$\tilde{C}^{k_d} = (M-x)\cdot C_m^{k_d} \tag{5.25}$$

Next, calculate the average data rate of each user.

From (5.25), the average data rate of each direct link user is:

$$C^{k_d} = \frac{\tilde{C}^{k_d}}{|K_D|} = \frac{(M-x)\cdot C_m^{k_d}}{|K_D|} \tag{5.26}$$

For the DF relay, the data rate of relay link users is determined by the minimum data rate between the first hop data rate and the second hop data rate, so the average data rate of each relay link user is:

$$C^{k_r} = \frac{\min\{\tilde{C}_1^{k_r}, \tilde{C}_2^{k_r}\}}{|K_R|} = \frac{\min\{x\cdot C_{m,1}^{r}, M\cdot C_{m,2}^{k_r}\}}{|K_R|} \tag{5.27}$$

In order to make full use of the radio resource, the data rate between the two hop links should match each other, i.e. $\tilde{C}_1^{k_r} = \tilde{C}_2^{k_r}$ from long-term statistics; this can be expressed as:

$$x\cdot C_{m,1}^{r} = M\cdot C_{m,2}^{k_r} \tag{5.28}$$

If $C^{k_r} < C^{k_d}$, it means that the number of relay link users is relatively large or the total average data rate of relay link users $\tilde{C}_2^{k_r}$ is relatively small. So, from (5.27), either it is necessary to increase $C_{m,2}^{k_r}$ or decrease $|K_R|$.

Choose the relay link user who has the minimum SINR on the second hop link, i.e., $\hat{k}_r = \arg\min_{k_r}\{\gamma_{k_r}\}$; let it transmit in direct link mode and become a direct link user,

then the average data rate of the relay link user on the second hop link in the subchannel m^{th} in the second time subslot will become:

$$C'^{k_r}_{m,2} = \frac{\sum_{K_r} c^{k_r}_{m,2} - c^{\hat{k}_r}_{m,2}}{|K_R| - 1} \tag{5.29}$$

Proposition 1: Choosing the relay link user which has the minimum large scale SINR on the second hop link to be the direct link user would increase $C^{k_r}_{m,2}$.

Proof:

$$\frac{C'^{k_r}_{m,2}}{C^{k_r}_{m,2}} = \frac{\sum_{K_R} c^{k_r}_{m,2} - c^{\hat{k}_r}_{m,2}}{|K_R| - 1} \cdot \frac{|K_R|}{\sum_{K_R} c^{k_r}_{m,2}}$$

$$= \frac{|K_R| \sum_{K_R} c^{k_r}_{m,2} - |K_R| c^{\hat{k}_r}_{m,2}}{|K_R| \sum_{K_R} c^{k_r}_{m,2} - \sum_{K_R} c^{k_r}_{m,2}}$$

Since $\hat{k}_r = \arg\min_{k_r} \{\gamma_{k_r}\}$, $\sum_{K_R} c^{k_r}_{m,2} \geq |K_R| c^{\hat{k}_r}_{m,2}$, so that $C'^{k_r}_{m,2} / C^{k_r}_{m,2} > 1$, i.e. the average data rate of the second hop link of relay link users will increase.

From (5.27) it can be seen that the average data rate of relay link users C^{k_r} will increase since $C^{k_r}_{m,2}$ increases and $|K_R|$ decreases. Changing the user $\hat{k}_r$ into a direct link user not only improves the utilization of the second time subslot, it also increases the scheduling opportunity of the user $\hat{k}_r$.

On the other hand, $C^{k_r} > C^{k_d}$ means the number of direct link users is relatively large or the total average data rate of direct link users $\tilde{C}^{k_d}$ is relatively small. In

order to increase the average data rate of direct link user, according to (5.26), $|K_D|$ should be decreased or the $\tilde{C}^{k_d}$ should be increased.

Assume $\hat{k}_d$ is changed to be a relay link user. In direct transmit mode, the data rate of this user is $c_{m,1}^{\hat{k}_d}$, while in relay transmit mode, the data rate of this user is $c_{m,2}^{\hat{k}_r}$.

The sufficient condition of increasing $(M-x)\cdot C_m^{k_d}$ can be calculated from the following.

From (5.20), (5.24), (5.26), and (5.28):

$$\tilde{C}^{k_d} = (M-x)\cdot C_m^{k_d} = \left(M - M\frac{\sum_{K_R} c_{m,2}^{k_r}}{C_{m,1}^{k_r}\cdot |K_R|} \right) \frac{\sum_{K_D} c_{m,1}^{k_d}}{K_D} \tag{5.30}$$

If $\hat{k}_d$ changes the transmission mode from direct link user into relay link user, then:

$$\begin{aligned} \tilde{C}'^{k_d} &= (M-x')\cdot C_m'^{k_d} \\ &= \left(M - M\frac{\sum_{K_R} c_{m,2}^{k_r} + c_{m,2}^{\hat{k}_r}}{C_{m,1}^{k_r}\cdot (|K_R|+1)} \right) \frac{\sum_{K_D} c_{m,1}^{k_d} - c_{m,1}^{\hat{k}_d}}{|K_D|-1} \end{aligned} \tag{5.31}$$

From (5.30) (5.31):

$$\frac{(M-x)\cdot C_m^{k_d}}{(M-x')\cdot C_m'^{k_d}} = \frac{\left(C_{m,1}^{k_r}\cdot|K_R| - \sum_{K_R} C_{m,2}^{k_r}\right)\cdot\sum_{K_D} c_{m,1}^{k_d}\cdot\left(|K_R|+1\right)\cdot\left(|K_D|-1\right)}{\left(C_{m,1}^{k_r}\cdot\left(|K_R|+1\right) - \sum_{K_R} c_{m,2}^{k_r} - c_{m,2}^{\hat{k}_r}\right)\cdot\left(\sum_{K_D} c_{m,1}^{k_d} - c_{m,1}^{\hat{k}_d}\right)\cdot|K_R|\cdot|K_D|} = \frac{\left(C_{m,1}^{k_r}\cdot\left(|K_R|\right)^2 + |K_R|\cdot C_{m,1}^{k_r} - |K_R|\cdot\sum_{K_R} c_{m,2}^{k_r} - \sum_{K_R} c_{m,2}^{k_r}\right)\cdot\left(|K_D|\sum_{K_D} c_{m,1}^{k_d} - \sum_{K_D} c_{m,1}^{k_d}\right)}{\left(C_{m,1}^{k_r}\cdot\left(|K_R|\right)^2 + |K_R|\cdot C_{m,1}^{k_r} - |K_R|\cdot\sum_{K_R} c_{m,2}^{k_r} - |K_R|\cdot c_{m,2}^{\hat{k}_r}\right)\cdot\left(|K_D|\sum_{K_D} c_{m,1}^{k_d} - |K_D|\cdot c_{m,1}^{\hat{k}_d}\right)} \quad (5.32)$$

From (5.32) it can be seen that if:

$$\sum_{K_R} c_{m,2}^{k_r} \geq |K_R|\cdot c_{m,2}^{\hat{k}_r} \text{ and } \sum_{K_D} c_{m,1}^{k_d} \geq |K_D|\cdot c_{m,1}^{\hat{k}_d} \quad (5.33)$$

then (5.32) is smaller than 1 and $(M-x)\cdot C_m^{k_d}$ will increase. In fact, (5.33) is a sufficient condition but not a necessary one, but it is simple to be satisfied and easy to implement.

Choosing the direct link user $\hat{k}_d$ who has the smallest large scale SINR, and if (5.33) is satisfied changing $\hat{k}_d$ into a relay link user, will increase the average data rate of direct link users. If this condition is not satisfied, select the second smallest SINR direct link user, check if that fulfils the above condition to be a relay link user, and so on.

5.4.2 Algorithm Procedure

Define the time interval T, called the algorithm execution interval which is longer than one TTI. The LBRS algorithm will operate in each T as follows:

Step 1: Initialise the transmission mode and select the RS by the pathloss based relay selection algorithm.

Step 2: If $C^{k_r} < C^{k_d}$, go to step 3, else go to step 4.

Step 3: Choose the relay link user with the minimum large scale SINR on the second hop link to be a direct link user. Update C^{k_r} and C^{k_d}, then go to step 2.

Step 4: Choose the direct link user with the smallest large scale SINR, to be a relay link user provided it satisfies equation (5.33). If it does not, the same procedure is carried on the direct link user with the next smallest SINR until equation (5.33) is satisfied. Repeat this step until $C^{k_r} < C^{k_d}$.

Step 5: Schedule the subchannel for each user and transmit data in each TTI.

Step 6: Repeat step 1-5 for the next T.

It should be noted that the length of the algorithm execution interval T will be determined by the speed of the traffic load change. If the load of the cell changes quickly, T will be shorter.

5.4.3 Performance Simulation and Analysis

The performance (system average throughput and average fairness of users) of the proposed LBRS is compared with a traditional relay selection algorithm, and the pathloss based relay selection algorithm (PBRS) [40]. THPF scheduling [67] is used in each TTI. The average system throughput is the sum of average user throughput and again the Raj Jain fairness index is used to measure the fairness among users. In order to show the advantage of the LBRS algorithm, two typical traffic load distribution scenarios (uniform distributed scenario and hotspot scenario) are simulated. In the simulation, it is assumed that all the users have the same traffic requirement, so the user distribution is the same as traffic load distribution.

With uniform distribution of users in the target area, using polar coordinates to express the location of user (ρ,θ), it can be deduced that $\rho^2 \sim U(0,R^2)$, and $\theta \sim U(0,2\pi)$ [31]. A random drop of user location example is shown in Figure 5.6.

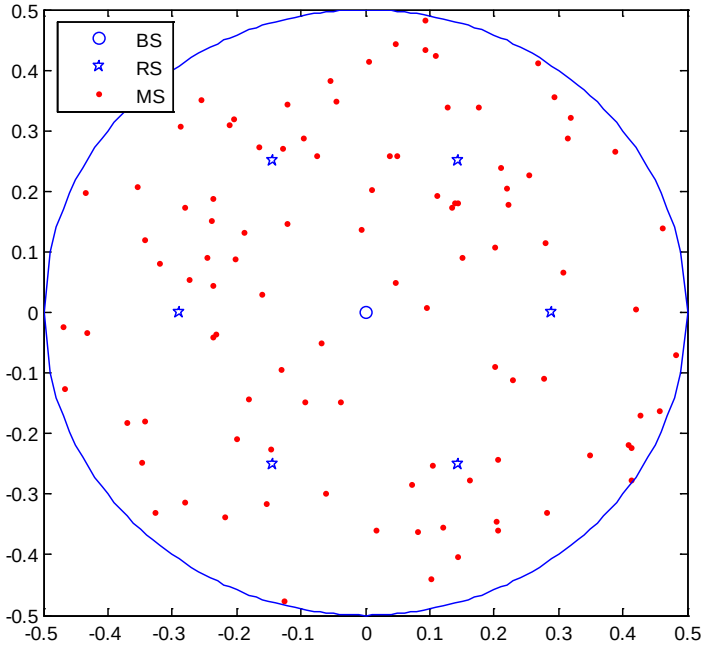

Figure 5.6 Traffic load of uniform distribution

Figure 5.7 and Figure 5.8 show the performance comparison of these two algorithms with different user numbers under uniform distribution. As the number of users increases, the system average throughput increases and the fairness index decreases in the long-term view. The PBRS gives a slightly better average throughput compared with LBRS, but LBRS shows better fairness – this is especially true for a larger number of users where there is little difference in throughput but the improvement in fairness is maintained. For example, when there are 20 users in the cell, the average throughput of LBRS is about 4.6% worse than that of PBRS but the fairness index of LBRS is 8% more than that of LBRS; when the number of users increased to 50, the average throughput of LBRS is about 4.8% worse than that of PBRS but the fairness index of LBRS is 12% more than that of LBRS.

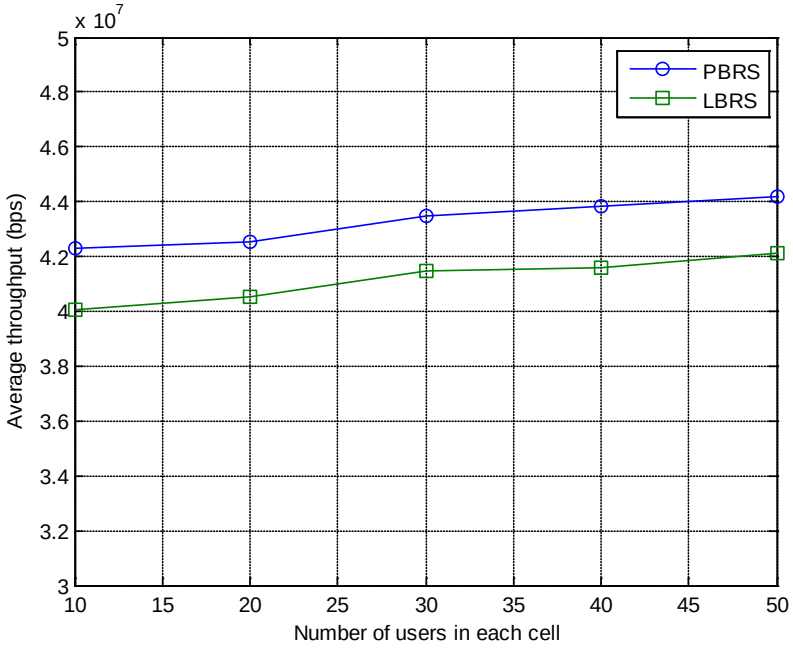

Figure 5.7 System throughput comparison in uniform distribution

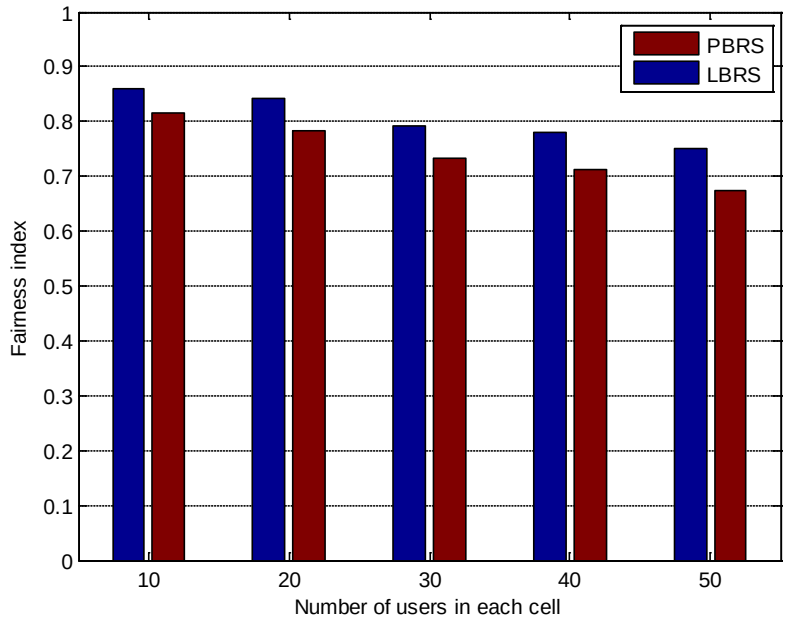

Figure 5.8 User fairness comparison in uniform distribution

Then consider the hotspot scenario for comparison of the PBRS and LBRS algorithms. In the hotspot scenario, $\rho^4 \sim U(0, R^4)$ and $\theta \sim U(0,2\pi)$. An example of this load

distribution is shown in Figure 5.9, where most of the users are distributed at the edge of the cell.

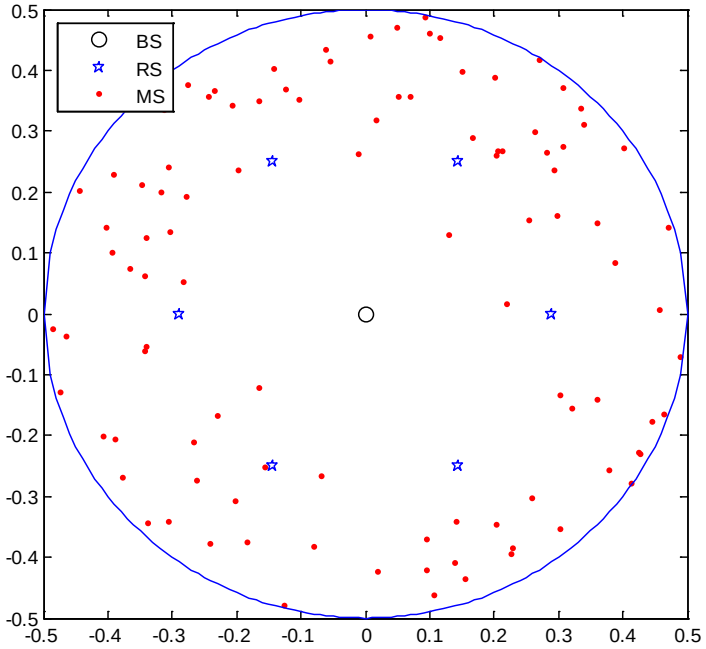

Figure 5.9 Traffic load of hotspot scenario

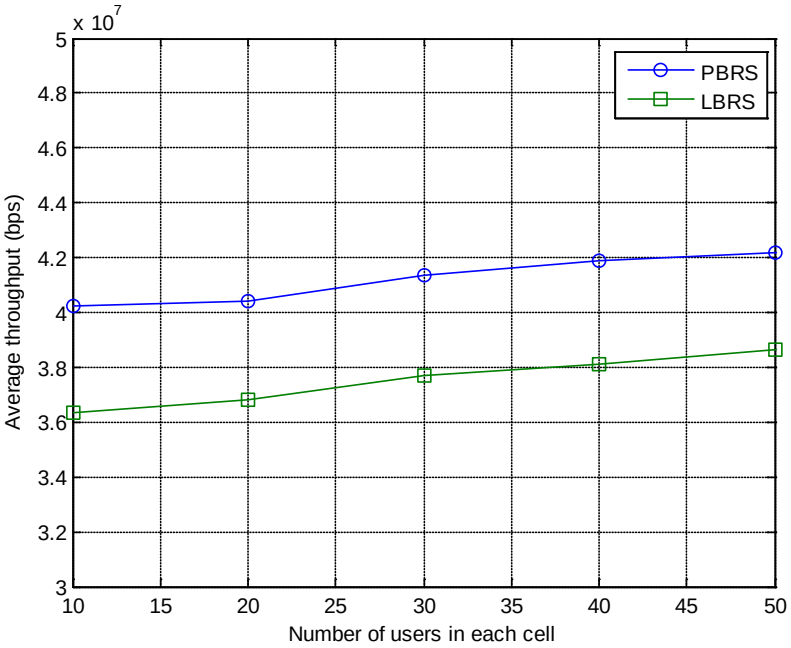

Figure 5.10 System throughput comparison in hotspot scenario

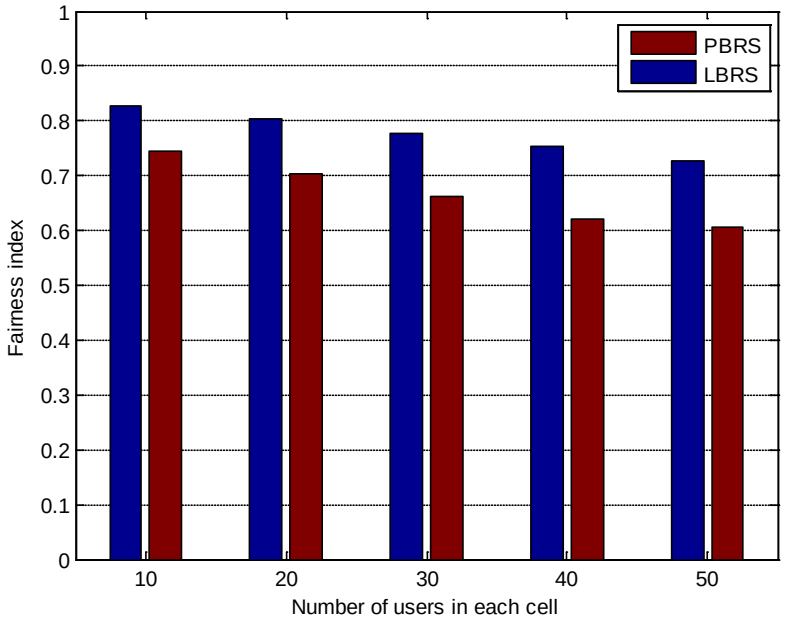

Figure 5.11 Fairness index comparison in hotspot scenario

Figure 5.10 and Figure 5.11 show the performance comparison of the LBRS and PBRS in the hotspot scenario. It can be seen that when the number of users increases, the user fairness gain of LBRS will be enhanced, which is the same as the conclusions drawn from Figure 5.7 and Figure 5.8. From the simulation results, it also can be seen that the LBRS algorithm achieves better fairness gain in the hotspot scenario than that with uniform distribution. When there are 50 users in the cell, the average throughput with LBRS is about 8% less that of PBRS but the fairness index of LBRS is 20% better than that of PBRS.

These simulation results show that the LBRS algorithm can achieve better fairness than the traditional relay selection algorithm in both typical traffic load distribution scenarios.

5.5 Summary

This chapter studied the fairness radio resource allocation issue. A two-hop proportional fairness algorithm which improves system throughput while

guaranteeing user data rate is proposed. In addition, a load based relay selection algorithm which considered the fairness issue between direct link user and relay link user is proposed.

This work was done without considering the power efficiency problem, and equal power allocation is used in relay selection and subchannel allocation. Work on a suitable power allocation scheme is given in the next chapter.

Chapter 6 Energy Efficient Power Allocation

The work in this chapter is new and entirely that of the author.

6.1 Introduction

In relay based cellular networks, under equal power allocation for BS and RS, the subchannel capacity of the first hop link of an RS is not coupled with that of the second hop link. In order to keep the data rate of the two hop links balanced, a two-hop power allocation (THPA) algorithm is proposed to adjust the transmission power of the BS and the RS dynamically according to the difference in data rates between these two hop links. The aim of this algorithm is power efficiency at the transmission node.

In a multi-cell OFDMA scenario, because the interference is *inter-cell* interference, the performance of users at the cell edge is affected most. Therefore, a multi-cell power allocation considering inter-cell interference has also been studied by the author and, based on a multi-cell non-cooperative game model, a distributed multi-cell power allocation algorithm has been implemented. Different utility functions are defined for different optimisation objectives (system throughput and user fairness respectively) and the existence and uniqueness of the Nash equilibrium as a solution of the non-cooperative power allocation game is proved mathematically. The performance of this algorithm has been investigated by simulation.

6.2 Power Allocation between Two-Hops

6.2.1 Existing problem

In a relay system, the data rate of each RS depends on the minimum of the first hop link data rate (achieved data rate in the first time subslot) and the second hop link data rate (achieved data rate in the second time subslot). The data rate of the two hop links is usually different with equal power allocation. This is illustrated in Figure 6.1 where the transmission data rate for the two hop links at different TTI is compared.

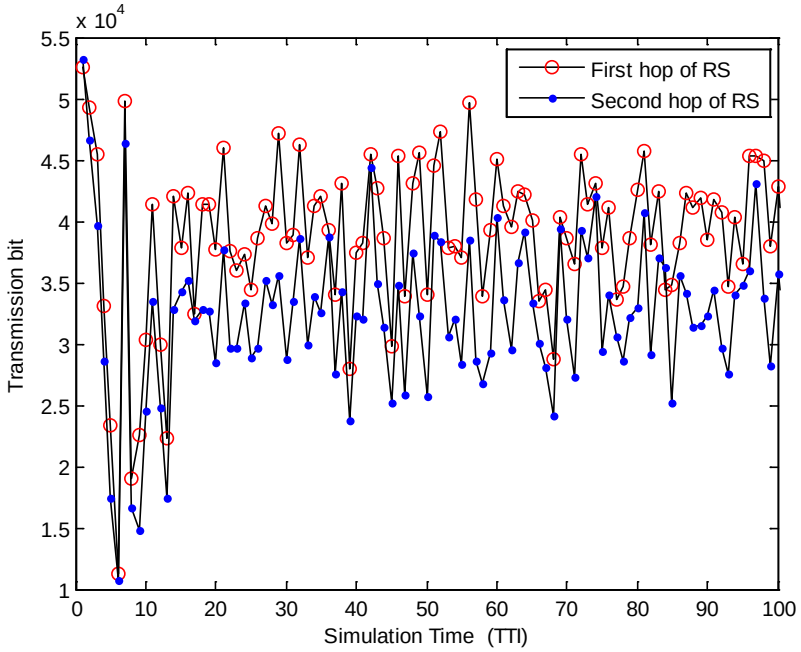

Figure 6.1 Two-hop throughput of RS with equal power allocation

For two-hop link data rate balance, the transmission power of BS and RS can be adjusted adaptively to make the data rate of the first hop link and the second hop link matched to each other. If the data rate of the first hop link is smaller than that of the second hop link, increasing the transmission power of the BS can increase the data rate of the first hop link to the same value as the data rate of the second hop link, and system throughput will be increased; on the other hand, decreasing the transmission power of the RS can decrease the data rate of the second hop link to the same value as the data rate of the first hop link, and transmission power will be saved. If the data rate of the first hop link is larger than that of the second hop link, the situation is similar, but the other way round.

In the two-hop power allocation (THPA) algorithm, the optimization target is power efficiency in which the transmission power of the BS and RS is optimised to minimize the total transmission power.

6.2.2 Two-Hop Power Allocation

For RS r, M_1^r is the set of allocated subchannels on the first time subslot and M_2^r is the set of allocated subchannels on the second time subslot, and M_{k_r} is the set of subchannels allocated to the user k_r.

The available data rate of the RS r is determined by the minimum transmission data rate of the first hop link and the second hop link, which can be expressed as:

$$c^r = \min\left\{c_1^r, c_2^r\right\} \tag{6.1}$$

For the RS r, the data rate difference between the second hop link and the first hop link is：

$$\Delta c^r = c_2^r - c_1^r \tag{6.2}$$

If $\Delta c^r < 0$, the data rate of the second hop link is smaller than the data rate of the first hop link. While maintaining the system throughput, the transmission power of the BS can be reduced so that the data rate of the second hop link matches that of the first hop for each RS.

Let $\hat{p}_{m,1}^r$ be the transmission power from the BS to the RS r on the subchannel m $\left(m \in M_1^r\right)$ after THPA. Define $p_{m,1}^r$ as the transmission power from the BS to the RS r on the subchannel m $\left(m \in M_1^r\right)$ with equal power allocation. The adjusted power value can be calculated according to Δc^r.

From (5.2) (5.7), the Δc^r is:

$$\Delta c^r = \sum_{m \in M_1^r} B_m \log_2\left(1 + \frac{g_{m,1}^r \hat{p}_{m,1}^r}{\Gamma \sigma^2}\right) - \sum_{m \in M_1^r} B_m \log_2\left(1 + \frac{g_{m,1}^r p_{m,1}^r}{\Gamma \sigma^2}\right) \tag{6.3}$$

Let $\Delta c_{m,1}^{r}$ be the decreased data rate on the subchannel m $\left(m \in M_1^r\right)$ of the first hop link of the RS r:

$$\Delta c_{m,1}^{r} = B_m \left[\log_2 \left(1 + \frac{g_{m,1}^{r} \hat{p}_{m,1}^{r}}{\Gamma \sigma^2} \right) - \log_2 \left(1 + \frac{g_{m,1}^{r} p_{m,1}^{r}}{\Gamma \sigma^2} \right) \right] \tag{6.4}$$

The total data rate change is the sum of the individual change on each subchannel, so:

$$\Delta c^{r} = \sum_{m \in M_1^r} \Delta c_{m,1}^{r} \tag{6.5}$$

For simplicity, let the reduced data rate on each allocated subchannel in the first time subslot be equal; then

$$\Delta c_{m,1}^{r} = \frac{\Delta c^{r}}{\left| M_1^r \right|} \tag{6.6}$$

From (6.3)-(6.6), the transmission power from the BS to the RS r on the subchannel m $\left(m \in M_1^r\right)$ after power allocation can be calculated as:

$$\hat{p}_{m,1}^{r} = 2^{\frac{\Delta c_{m,1}^{r}}{B_m}} \left(p_{m,1}^{r} + \frac{\Gamma \sigma^2}{g_{m,1}^{r}} \right) - \frac{\Gamma \sigma^2}{g_{m,1}^{r}} \tag{6.7}$$

If $\Delta c^{r} > 0$, the data rate of the second hop link is bigger than the data rate of the first hop link. So the data rate of the second hop link can be reduced by Δc^{r} to match the data rate of the first hop link of RS r by reducing the transmission power of RS, and the system throughput is not changed.

In order to maintain the user fairness, the reduced Δc^{r} is proportionally distributed among the MSs served by the RS r. Let the reduced data rate of the user k_r is Δc^{k_r}, so:

$$\Delta c^{k_r} = \Delta c^r \frac{c_2^{k_r}}{\sum_{k_r \in K_{R_r}} c_2^{k_r}} \tag{6.8}$$

Similar to the derivation of (6.7), the transmission power from the RS r to the user k_r on the subchannel m $\left(m \in M_{k_r}\right)$ after power allocation $\hat{p}_{m,2}^{k_r}$ becomes:

$$\hat{p}_{m,2}^{k_r} = 2^{\frac{\Delta c^{k_r}}{B_m \left| M_{k_r} \right|}} \left(p_{m,2}^{k_r} + \frac{\Gamma \sigma^2}{g_{m,2}^{k_r}} \right) - \frac{\Gamma \sigma^2}{g_{m,2}^{k_r}} \tag{6.9}$$

The adaptive two-hop power allocation algorithm will operate as follows:

Step 1: The subchannels of both the first and the second time subslots are assigned by the THPF algorithm.

Step 2: Each RS r calculates the data rate of the first hop link c_1^r and that of the second hop link c_2^r in terms of equal power allocation of BS and each RS.

Step 3: If $\Delta c^r < 0$, the transmission power of BS on the subchannel m $\left(m \in M_1^r\right)$ occupied by the RS r will be derived from (6.7), while the transmission power of the RS r on the subchannel m $\left(m \in M_2^r\right)$ will remain equivalent to the equal power allocation case.

Else, the transmission power of BS on the subchannels m $\left(m \in M_1^r\right)$ occupied by the RS r will be unchanged, and the transmission power of RS r on the subchannel m $\left(m \in M_{k_r}\right)$ will be calculated by (6.9) instead.

Step 4: Downlink data packet will be sent with the transmission power of BS and RS according to step 3.

6.2.3 Performance Simulation and Analysis

It has been pointed out that the throughput of each RS in the first hop link and that in second hop link do not match each other in every TTI with equal power allocation on every subchannel; this is shown in Figure 6.1 showing the simulation results on the throughput comparison of two hop links without THPA.

In this section, the system performance under THPA is tested. Figure 6.2 is the throughput comparison of two hop links with THPA. It can be seen that the throughput of the first hop link and that of second hop link now match each other in every TTI. The average data rate in the first hop link is 3.18×10^{7} bit/s, and of the average data rate in the second hop link is 3.18×10^{7} bit/s as well. Since the throughput is determined by the minimum of the capacity of the first hop link and the second hop link of each RS, the system performance with the THPA is *the same as* that with equal power allocation.

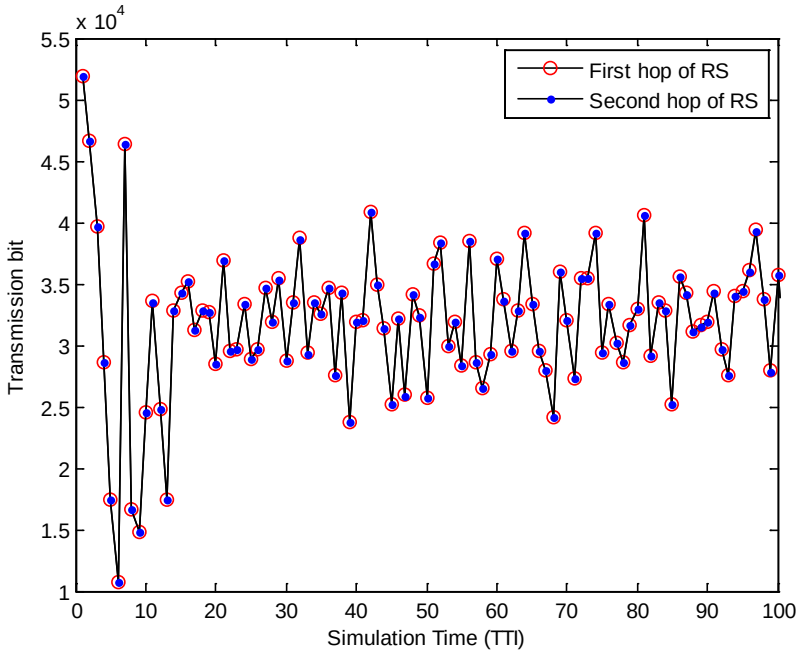

Figure 6.2 Two-hop throughput of RS with THPA

Figure 6.3 and Figure 6.4 shows that the transmission power of the BS and RSs with the THPA algorithm is significantly reduced compared with that of equal power allocation (EQPA).

In Figure 6.3, when the RSs are located at the edge of the cell, the amount of power reduction for the BS is less than that when the RSs are $0.4D$ to $0.5D$ away from BS. This is because the proposed THPA algorithm considered the power saving related to relay link users, (when the RSs are located at the cell edge, the number of relay link users is less than the number of relay link users when relay is located in the cell centre) and the channel state of the second hop link is better than that of first hop link. However, the total transmission power of RSs is greatly reduced when RSs are at the edge of the cell because the channel state of the second hop link is better than that of the first hop link, and RSs will reduce the power to balance the data rate between the two hop links.

On the other hand, when RSs are located near the BS, the channel state of the second hop link is poor so the transmission power of RSs almost remains the same as the power with equal power allocation while the transmission power of the BS is reduced.

Although power reduction of a component (BS or RS) varies with distance of the RS from the BS, Figure 6.4 shows that the total power saving is approximately constant. The total transmission power of BS plus six RSs with the THPA algorithm is reduced roughly 30% compared to that of equal power allocation.

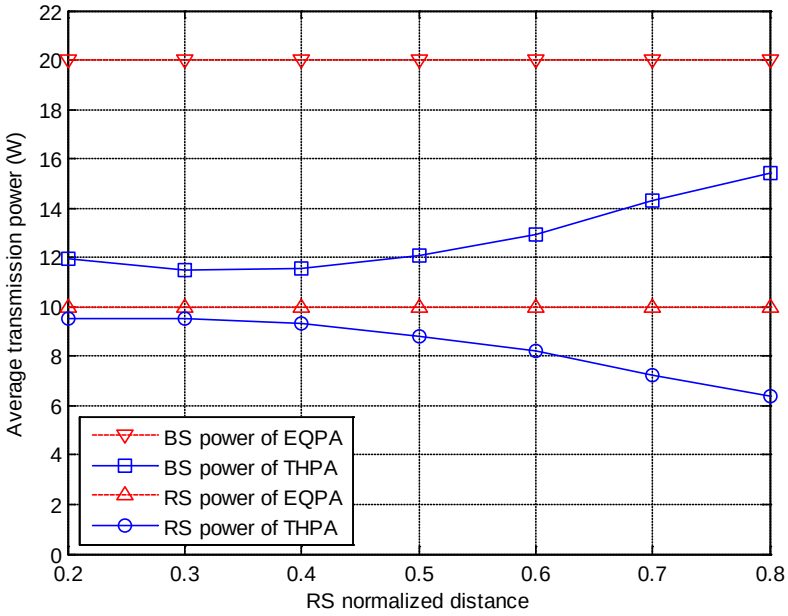

Figure 6.3 BS/RS transmission power *vs.* RS normalized distance

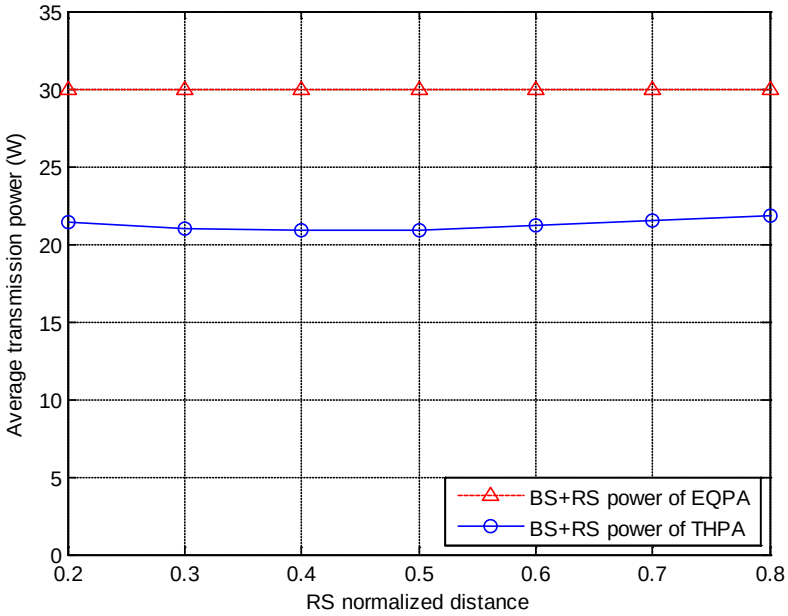

Figure 6.4 Total transmission power *vs.* RS normalized distance

From Figure 6.3 to Figure 6.4 it can be seen that, THPA can effectively reduce transmission power.

6.3 Power Allocation among Multi-Cells

THPA is only one aspect of the problem: although it balances the data rate on the two hop links to minimize the transmission power, it does not consider inter-cell interference or how to minimize the transmission power among multiple cells. Some work on power allocation in OFDMA relay systems has been given in [64][65], however, these algorithms only consider a single cell scenario and omit the co-channel interference (CCI) in multiple cells. In this section, power allocation in a multi-cell OFDMA relay system is considered and a distributed power allocation algorithm based on non-cooperative game theory is determined.

6.3.1 Background of Game Theory

Game theory is a branch of applied mathematics which attempts to mathematically capture behaviour in strategic situations in which an individual's success in making choices depends on the choices of others [68].

Game theory was originally proposed by John von Neumann and Oskar Morgenstern in 1944 in the book 'Theory of games and economic behaviour' [69]. In the following decades, game theory has been developed into a wider area and is widely recognized as an important tool in many fields.

In the communications area, game theory has been applied to analyze and solve different problems in a broad number of areas such as cryptographic protocols [70][71], peer to peer (P2P) systems [72], as well as wireless communications and mobile networking [73][74][75][76]. Later in this section there is an explanation as to how this work is different from previous use of game theory in OFDMA networks.

A game has *players* who each have a *strategy* that they use to try to achieve the optimum *utility*.

Player k has a strategy set S_k that consists of a number of individual strategies s_k so $S_k = \{s_k\}$ and the player can decide which strategy from its set it can use. The

vector $\mathbf{s} = (s_1, \ldots, s_n)$, is the strategy profile, i.e. the profile of the strategies of all the users $k = \{1,2,\cdots,n\}$.

The utility level $u_k\{\mathbf{s}\}$ is decided by the strategy profile of all the players, i.e. it not only depends on the strategy chosen by the player k, but also on the strategies chosen by all the other players.

There are two different types of games: cooperative and non-cooperative. This thesis uses non-cooperative game theory as users are competing against each other [77] to get the capacity they require, whereas in cooperative game theory users form coalitions and contracts between them.

The game aims to find an *equilibrium* that gives the maximum utility; the *equilibrium* is a set of strategies where users are unlikely to change their behaviour. Many equilibrium concepts have been developed, but the most generally used is the Nash equilibrium [77]. This uses the concept for equilibrium that, as a player knows the equilibrium strategies of the others, it will know that it cannot improve its utility by changing its own strategy if the other players keep theirs unchanged. This means that each player chooses the optimal response according to the other players' strategies and if any player changes its strategy independently, its utility will be reduced.

A strategy profile $\mathbf{s}^* = (s_1^*, \ldots s_n^*)$ is said to be a Nash Equilibrium if:

$$u_k(s_k^*, s_{-k}^*) \geq u_k(s_k', s_{-k}^*) \quad \forall s_k' \neq s_k^* \tag{6.10}$$

In setting up a non-cooperative game, the research is on how to maximize the players' utilities with given strategy sets and how to reach equilibrium.

A basic model for non-cooperative power control game in CDMA networks was first proposed by D. Goodman [78][79], in which the quality of service (QoS) of a user is

the utility, and non-cooperative game theory is used to devise a power control scheme to maximize the utilities. The interference in CDMA is mainly intra-cell interference, while the interference in OFDMA systems is generally inter-cell interference. Non-cooperative power allocation game is used for work on OFDMA systems in [80] to maximize users' utilities in a distributed way in multi-cell systems. [81] considers the non-cooperative power allocation game in multi-cell OFDMA relay networks, however, it considers power allocation only in the second time subslot and only in slow fading channel scenarios.

There has not been related work that addresses the problems considered here.

6.3.2 Multi-Cell System Model

In OFDMA cellular systems, the subchannels are orthogonal to each other, so there will be no intra-cell interference. The frequency reuse factor of OFDMA systems is generally "1" to maximise the overall spectrum efficiency. However, this means that co-channel interference (CCI) in co-frequency subchannels will be the dominant inter-cell interference between adjacent cells and cause the performance of users at the cell edge to deteriorate. Figure 6.5 shows an example of the downlink inter-cell interference between two cells in the second hop link in relay OFDMA networks.

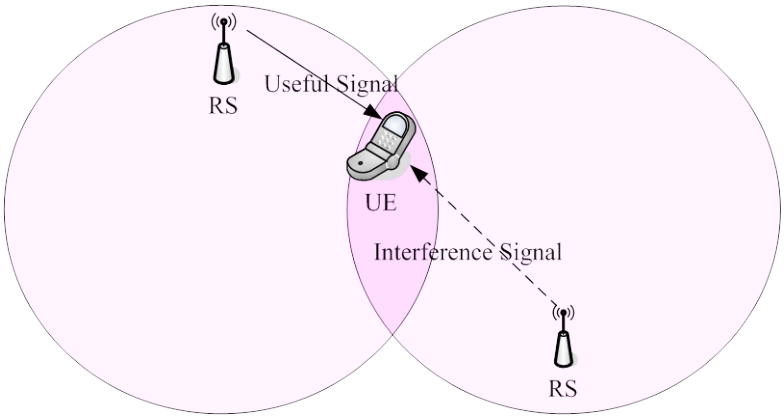

Figure 6.5 Downlink inter-cell interference in the second hop link

The layout of multiple cells as used in this research is shown in Figure 6.6.

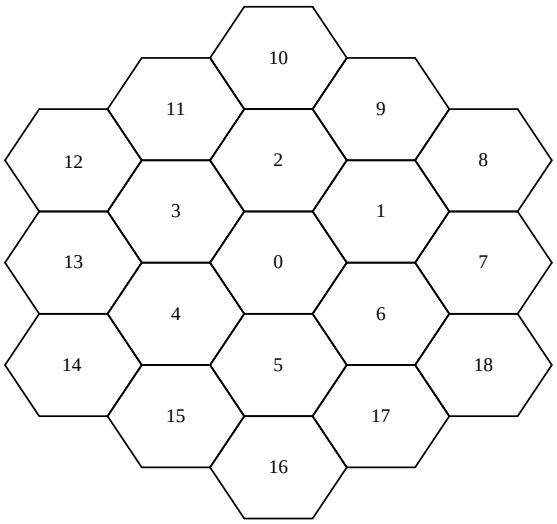

Figure 6.6 Layout of multi-cell system

Notation used here is as follows:

- ✧ total number of cells is N ;
- ✧ total bandwidth is B ;
- ✧ the number of subchannels is M , so the subchannel bandwidth is $B_m = B/M$;
- ✧ $n \in (1,2,\cdots N)$ is the index of a cell;
- ✧ s is the index of a transmitter in each cell (note that the use of s as an index should not be confused with s_i as a strategy);
- ✧ in the first time subslot the transmitter is BS ($s = 0$), and in the second time subslot the transmitter is RS ($s = r$, r is the index of RSs);
- ✧ the time subslot is $i \in (1,2)$;
- ✧ the index of subchannel is $m \in (1,2,\cdots M)$;
- ✧ k is the index of a receiver in each cell:
  - when the RS is a receiver, $k = r$
  - the direct link user is k_d
  - the relay link user served by RS r is denoted as k_r .

- ✧ $p_{n,m,i}^{(s,k)}$ is transmission power on the subchannel m in the cell n between the transmitter s and the receiver k at the i^{th} time subslot;

- ✧ $g_{n,m,i}^{(s,k)}$ is the useful signal link gain on the subchannel m in the cell n between the transmitter s and the receiver k at the i^{th} time subslot;

- ✧ $g_{n',m,i}^{(s',k)}$ is the interference link gain on the subchannel m between the transmitter s' in the cell $n'\left(n' \neq n\right)$ and the receiver k in the cell n at the i^{th} time subslot.

The interference plus noise received by the transmitter s (BS or RS) and the receiver k (RS or MS) in the n^{th} cell on the subchannel m at the i^{th} time subslot $I_{n,m,i}^{(s,k)}$ is:

$$I_{n,m,i}^{(s,k)} = \sum_{\{n',n' \neq n\}} g_{n',m,i}^{(s',k)} p_{n',m,i}^{(s',k')} + \sigma^2 \tag{6.11}$$

in which, σ^2 is the power of AWGN.

The signal to interference plus noise ratio (SINR) on the m^{th} subchannel between the transmitter s and the receiver k at the i^{th} time subslot in the n^{th} cell is:

$$\gamma_{n,m,i}^{(s,k)} = g_{n,m,i}^{(s,k)} p_{n,m,i}^{(s,k)} \Big/ I_{n,m,i}^{(s,k)} \tag{6.12}$$

The capacity of the m^{th} subchannel between s and k of the cell n in the time subslot i is:

$$c_{n,m,i}^{(s,k)} = B_m \log_2\left(1+\gamma_{n,m,i}^{(s,k)}\right) \tag{6.13}$$

The subchannels can be allocated with any scheduling algorithm. A fixed subchannel allocation is used here to cancel the effect of scheduling on system performance. In

the cell n, for a direct link user k_d, the achieved data rate is $c_n^{k_d}$ and the achieved data rates of the relay link user k_r in the first hop link and second hop link are $c_{n,1}^{k_r}$ and $c_{n,2}^{k_r}$ respectively. The available data rate of a relay link user $c_n^{k_r}$ is determined by the minimum capacity of the first hop link and the second hop link in DF relay [6], which can be expressed as:

$$c_n^{k_r} = \min\left\{c_{n,1}^{k_r}, c_{n,2}^{k_r}\right\} \tag{6.14}$$

6.3.3 Non-Cooperative Power Allocation Game

In OFDMA systems, there is no intra-cell interference, but there is inter-cell interference. So the power allocation problem of multi-cell OFDMA relay systems can be viewed as a non-cooperative game, in which the BSs (RSs) in multiple cells will compete with each other on co-frequency subchannels for channel capacity by increasing the transmission power selfishly.

6.3.3.1 Model of NPAG

In OFDMA systems, the subchannels are independent, so the utility maximization of one cell is equivalent to maximizing the utility on each subchannel in that cell. Thus, the multi-cell non-cooperative power allocation game (NPAG) can be formulated on each co-frequency subchannel. Furthermore, the BSs transmit data in the first time subslot and the RSs transmit data in the second time subslot, so the NPAG can be formulated as $G^{BS} = \left[\{n\}, \{p_{n,m}^{BS}\}, \{u_{n,m}^{BS}\}\right]$ in the first time subslot, and $G^{RS} = \left[\{n\}, \{p_{n,m}^{RS}\}, \{u_{n,m}^{RS}\}\right]$ in the second time subslot. In G^{BS}, $\{n\}$ is the set of co-channel interference cells, i.e. a set of players competing with each other; $P_{n,m}^{BS} = [p_{n,m}^{\min}, p_{n,m}^{\max}]$ is the strategy set of transmission power of the BS on the m^{th} subchannel in the n^{th} cell; $\mathbf{P}_m^{BS} = \left(p_{1,m}^{BS}, p_{2,m}^{BS}, \cdots, p_{N,m}^{BS}\right)$ is the BS transmission power vector of all the cells on the m^{th} subchannel; $\mathbf{P}_{-n,m}^{BS}$ is the BS transmission power

vector on the m^{th} subchannel of all the cells excluding the power $p_{n,m}^{BS}$ in the n^{th} cell. So, the BS transmission power vector on the m^{th} subchannel of all the cells can be expressed as $\mathbf{P}_m^{BS} = \left(p_{n,m}^{BS}, \mathbf{P}_{-n,m}^{BS}\right)$. $u_{n,m}^{BS}$ is the utility of the BS on the m^{th} subchannel in the n^{th} cell, and each cell will maximize its utility rationally. Similarly, n, $p_{n,m}^{RS}$ and $u_{n,m}^{RS}$ are defined in G^{RS}.

Since each transmitter prefers to increase its transmission power to increase its capacity, this will also increase the interference and degrade the capacity of adjacent cells in which users are using a co-frequency subchannel. Then the cells whose capacities are affected also prefer to increase their transmission power to increase their capacities. So a pricing factor is used in order to force transmitters in each cell consider not only their own capacity but also control the interference to others [79].

The utility of the BS on the subchannel m in the n^{th} cell can then be defined as:

$$u_{n,m}^{BS}\left(\mathbf{P}_m^{BS}\right) = B_m \log_2\left(1+\gamma_{n,m,1}^{(0,k)}\right) - \alpha^{BS} p_{n,m,1}^{(0,k)} \tag{6.15}$$

In the following, $p_{n,m}^{BS}$ is used to represent $p_{n,m,1}^{(0,k)}$ for simplicity and α^{BS} is the pricing factor of a BS (this is a positive scalar and can be considered to have units of bps/W). With the introduction of α^{BS}, a transmitter will not just increase the power selfishly to increase its channel capacity, but also will consider the interference to others. The larger α^{BS} is, the higher the price for increasing power is, so each cell will use attempt to use less transmission power, which causes less interference to other cells.

In order to use the channel efficiently, the match issue between the second hop link and the first hop link of the RS r should be considered. A match factor is introduced,

which is defined as the ratio of the first hop link capacity of the RS r and second hop link capacity of the RS r in the cell n:

$$\beta_n^r = \frac{\sum_{k_r \in K_{R_r}} c_{n,1}^{k_r}}{\sum_{k_r \in K_{R_r}} c_{n,2}^{k_r}} \tag{6.16}$$

As the BS transmits data for both direct link users and RSs in the first time subslot, the pricing factor for direct link users and RSs is different in the first time subslot, which is:

$$\alpha^{BS} = \begin{cases} \alpha'^{BS} & \text{for direct link user} \\ \alpha'^{BS} \cdot \beta_n^r & \text{for RS } r \text{ in the cell } n \end{cases} \tag{6.17}$$

α'^{BS} is the basic pricing factor for both direct link user and RS. From (6.17) it can be seen that the direct link users and the RSs use a different pricing factor to compete for transmission power. When $\beta_n^r > 1$, i.e., the channel capacity of the first hop link is bigger than that of the second hop link, the α^{BS} increases compared with the basic pricing factor α'^{BS}. Therefore, the BS decreases its transmission power to the RS r to match the capacity of the first hop link and that of the second hop link. The larger the difference between the data rate of two hop links is, the bigger β_n^r is; as a result, α^{BS} becomes bigger, and the transmission power is more strictly controlled. When $\beta_n^r < 1$, the BS tends to increase its transmission power to increase the first hop link capacity of RS to match that of the second hop link.

Similarly to (6.15), the utility of RS in the n^{th} cell on the m^{th} subchannel in the second time subslot can be defined as:

$$u_{n,m}^{RS}\left(\mathbf{P}_m^{RS}\right) = B_m \log_2\left(1 + \gamma_{n,m,2}^{(r,k)}\right) - \alpha^{RS} p_{n,m,2}^{(r,k)} \tag{6.18}$$

in which, α^{RS} is the basic pricing factor of the RS, which has the same function as α^{BS} and in the following parts, $p_{n,m}^{RS}$ is used to represent $p_{n,m,2}^{(r,k)}$ for simplicity.

6.3.3.2 Solution of NPAG

The widely used solution of non-cooperative game problem is the Nash equilibrium [79], the definition of which for this problem is:

$$\forall p'^{BS}_{n,m} \in P^{BS}_{n,m}, \quad u^{BS}_{n,m}\left(p^{BS}_{n,m}, \mathbf{P}^{BS}_{-n,m}\right) \geq u^{BS}_{n,m}\left(p'^{BS}_{n,m}, \mathbf{P}^{BS}_{-n,m}\right)$$

The power vector $\mathbf{P}_m^{BS}$ is the Nash equilibrium of NPAG. In the Nash equilibrium, given the power of other cells, a cell cannot improve its utility by changing its individual power. So the Nash equilibrium is a point of balance that each player who succeeds in a competition does not want to deviate from. The existence and uniqueness of the Nash equilibrium point in NPAG are illustrated in this section.

The Nash equilibrium for NPAG exists in the first time subslot when the following two conditions are satisfied [79]:

i) $\left\{p_{n,m}^{BS}\right\}$ is a nonempty, convex and compact subset of a finite Euclidean space R^N;

ii) $u_{n,m}^{BS}\left(\mathbf{P}_m^{BS}\right)$ is continuous in $\mathbf{P}_m^{BS}$ and quasi-concave in $\mathbf{P}_m^{BS}$.

A subset of Euclidean space R^N is called compact if it is closed and bounded [82]. Since the strategy $p_{n,m}^{BS}$ of every BS is identified as $p_{n,m}^{BS} \in [p_{n,m}^{\min}, p_{n,m}^{\max}]$ and $p_{n,m}^{\min} \neq p_{n,m}^{\max}$, it is a nonempty, convex [82] and compact subset of R^N. So the first condition is satisfied.

For the second condition, $u_{n,m}^{BS}\left(\mathbf{P}_m^{BS}\right)$ is obviously a continuous function in $\mathbf{P}_m^{BS}$ as defined in (6.15). Thus it is only necessary to prove the quasi-concave property of $u_{n,m}^{BS}\left(\mathbf{P}_m^{BS}\right)$.

Taking the first-order partial derivative of (6.15) with respect to $p_{n,m}^{BS}$ for any $n \in \{n\}$ yields:

$$\frac{\partial u_{n,m}^{BS}\left(\mathbf{P}_m^{BS}\right)}{\partial p_{n,m}^{BS}} = \frac{B_m}{\ln 2} \frac{g_{n,m,1}^{(0,k)}}{I_{n,m,1}^{(0,k)} + g_{n,m,1}^{(0,k)} p_{n,m,1}^{(0,k)}} - \alpha^{BS} \tag{6.19}$$

The second-order partial derivative of (6.15) with respect to $p_{n,m}^{BS}$ for any $n \in \{n\}$ is

$$\frac{\partial^2 u_{n,m}^{BS}\left(\mathbf{P}_m^{BS}\right)}{\partial^2 p_{n,m}^{BS}} = \frac{B_m}{\ln 2} \frac{-\left(g_{n,m,1}^{(0,k)}\right)^2}{\left(I_{n,m,1}^{(0,k)} + g_{n,m,1}^{(0,k)} p_{n,m,1}^{(0,k)}\right)^2} < 0 \tag{6.20}$$

From (6.20), $u_{n,m}^{BS}\left(\mathbf{P}_m^{BS}\right)$ is strictly concave in $\mathbf{P}_m^{BS}$, thus it is strictly quasi-concave in $\mathbf{P}_m^{BS}$ as well [83]. Since both conditions of the existence of Nash equilibrium are satisfied, the Nash equilibrium exists in NPAG.

The Nash equilibrium solution of NPAG is $\arg\max_{p_{n,m}^{BS} \in P_{n,m}^{BS}} u_{n,m}^{BS}\left(\mathbf{P}_{n,m}^{BS}\right)$. For a continuous function, the necessary condition for a first-order optimization is:

$$\partial u_{n,m}^{BS}\left(\mathbf{P}_m^{BS}\right) / \partial p_{n,m}^{BS} = 0 \tag{6.21}$$

From (6.19)：

$$p_{n,m}^{BS} = \frac{B_m}{\ln 2 \cdot \alpha^{BS}} - \frac{I_{n,m,1}^{(0,k)}}{g_{n,m,1}^{(0,k)}} \tag{6.22}$$

If $p_{n,m}^{BS}$ from (6.22) is within $[p_{n,m}^{\min}, p_{n,m}^{\max}]$, $p_{n,m}^{BS}$ is the Nash equilibrium solution of NPAG in the first time subslot; otherwise, $p_{n,m}^{\min}$ or $p_{n,m}^{\max}$ are Nash equilibrium solution of NPAG in the first time subslot.

Next, the uniqueness of Nash equilibrium of NPAG in the first time subslot must be considered. If (6.22) converges to a unique solution, the Nash equilibrium of NPAG

is unique as (6.22) is the Nash equilibrium of NPAG. From (6.12), (6.22) can be rewritten as:

$$p_{n,m}^{BS} = \frac{B_m}{\ln 2 \cdot \alpha^{BS}} - \frac{p_{n,m}^{BS}}{\gamma_{n,m,1}^{(0,k)}} \tag{6.23}$$

The iterative expression of $p_{n,m}^{BS}$ can be expressed as:

$$p_{n,m}^{BS}(t) = \frac{B_m}{\ln 2 \cdot \alpha^{BS}} - \frac{p_{n,m}^{BS}(t-1)}{\gamma_{n,m,1}^{(0,k)}(t-1)} \tag{6.24}$$

In order to verify whether (6.24) converges to a unique solution, it is necessary to prove the convergence of the difference between two adjacent iterations. From (6.11) and (6.23) the difference between the $(t+1)^{th}$ and the t^{th} iteration is:

$$p_{n,m}^{BS}(t+1) - p_{n,m}^{BS}(t) = \frac{\sum_{\{n',n' \neq n\}} g_{n',m,1}^{(0,k)} \left(p_{n',m,1}^{(0,k)}(t-1) - p_{n',m,1}^{(0,k)}(t) \right)}{g_{n,m,1}^{(0,k)}} \tag{6.25}$$

If there exists infinitely small ε such that $\left| p_{n,m}^{BS}(t) - p_{n,m}^{BS}(t-1) \right| \leq \varepsilon$, then:

$$\left| p_{n,m}^{BS}(t+1) - p_{n,m}^{BS}(t) \right| / \varepsilon < \sum_{\{n',n' \neq n\}} g_{n',m,1}^{(s',k)} \Big/ g_{n,m,1}^{(0,k)} \tag{6.26}$$

If $g_{n,m,1}^{(0,k)} \Big/ \sum_{\{n',n' \neq n\}} g_{n',m,1}^{(s',k)} > 1$, then (6.24) is convergent. This condition can be transferred into the request of each user's SINR and can be realized through the admission control (if the SINR of a user is higher than 1, i.e., 0 dB which can be achieved easily [84], this user will be allowed to access the system, through the access control). It means that when $g_{n,m,1}^{(0,k)} \Big/ \sum_{\{n',n' \neq n\}} g_{n',m,1}^{(s',k)} > 1$ the uniqueness of the Nash equilibrium of NPAG in the first time subslot can be satisfied.

Similarly, the existence and uniqueness of the NPAG Nash equilibrium $G^{RS} = \left[\{n\}, \{p_{n,m}^{RS}\}, \{u_{n,m}^{RS}\} \right]$ in the second time subslot can be satisfied as well, and the iterative expression of $p_{n,m}^{RS}$ can be expressed as:

$$p_{n,m}^{RS}(t) = \frac{B_m}{\ln 2 \cdot \alpha^{RS}} - \frac{p_{n,m}^{RS}(t-1)}{\gamma_{n,m,2}^{(r,k)}(t-1)} \tag{6.27}$$

6.3.3.3 Process of NPAG

The process of the NPAG algorithm is given as follows:

Step 1: On each subchannel m, initialize transmission power $\mathbf{P}_m^{BS}(0) = 0$, $\mathbf{P}_m^{RS}(0) = 0$, and set iterative convergence parameter ε to be very small so that ε tends to 0 ($\varepsilon \to +0$).

Step 2: Let $t = 0$. Execute NPAG in the second time subslot.

Step 3: Let $t = t + 1$, calculate $\mathbf{P}_m^{RS}(t)$ according to (6.27).

Step 4: If $\left|\mathbf{P}_m^{RS}(t) - \mathbf{P}_m^{RS}(t-1)\right| < \varepsilon$, the NPAG of RS is over, $\mathbf{P}_m^{RS} = \mathbf{P}_m^{RS}(t)$ is the power allocation result of RSs on the subchannel m, and go to step 5; otherwise, go to step 3.

Step 5: Calculate the second hop link data rate of relay link users according to $\mathbf{P}_m^{RS}$ in step 4, and update the match factor β_n^r of the RS r in the cell n.

Step 6: Execute NPAG in the first time subslot. Let $t = 0$.

Step 7: Let $t = t + 1$, calculate $\mathbf{P}_m^{BS}(t)$ according to (6.24).

Step 8: If, $\left|\mathbf{P}_m^{BS}(t) - \mathbf{P}_m^{BS}(t-1)\right| < \varepsilon$, the NPAG of BS is over, $\mathbf{P}_m^{BS} = \mathbf{P}_m^{BS}(t)$ is the power allocation results of BS on the subchannel m, and go to step 9; otherwise, go to step 7.

Step 9: Calculate the first hop link data rate of relay link users and that of the direct link users according to $\mathbf{P}_m^{BS}$ in step 8.

It can be seen that steps 1-9 are performed in a distributed manner by each cell and different cells only need to exchange co-channel SINR information. The complexity of this algorithm depends on the number of cells but not on the number of users within the cell.

6.3.3.4 Performance Simulation and Analysis

A multi-cell downlink OFDMA relay system is simulated. Wrap-around technology is used for multi-cell interference, and the channel model [10] includes shadow fading, large scale pathloss, and multi-path fading, as discussed in section 3.2. In each single cell, one BS positioned in the centre of cell and 6 RSs are uniformly distributed in the cell, located at 0.5 cell radius away from the BS; multiple users are uniformly distributed across the cell. Detailed simulation parameters are as shown in Table 3.1.

First, in order to examine the second hop link average data rate of relay link users with different RS basic pricing factors, the limitation of the first hop link data rate of the relay link user is omitted, and assume that the end to end data rate of relay link user is only decided by the data rate of second hop link here. Figure 6.7 shows that the second hop link data rate increases first and then decreases with increasing RS basic pricing factor. Figure 6.8 shows the simulation results of RS transmission power with varying RS basic pricing factor compared with that with equal power allocation (EQPA), in which RS transmission power decreases significantly as the RS basic pricing factor increases.

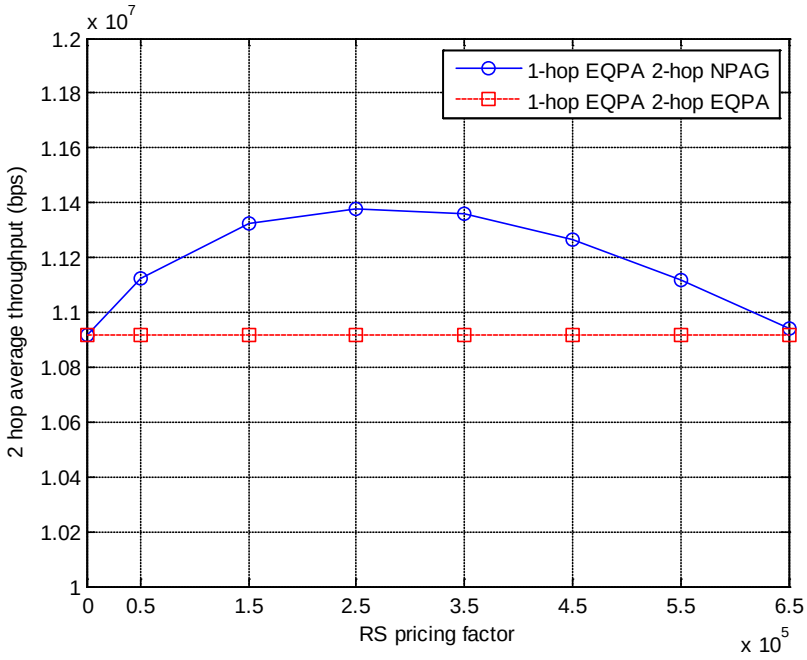

Figure 6.7 The second hop average throughput *vs.* RS basic pricing factor

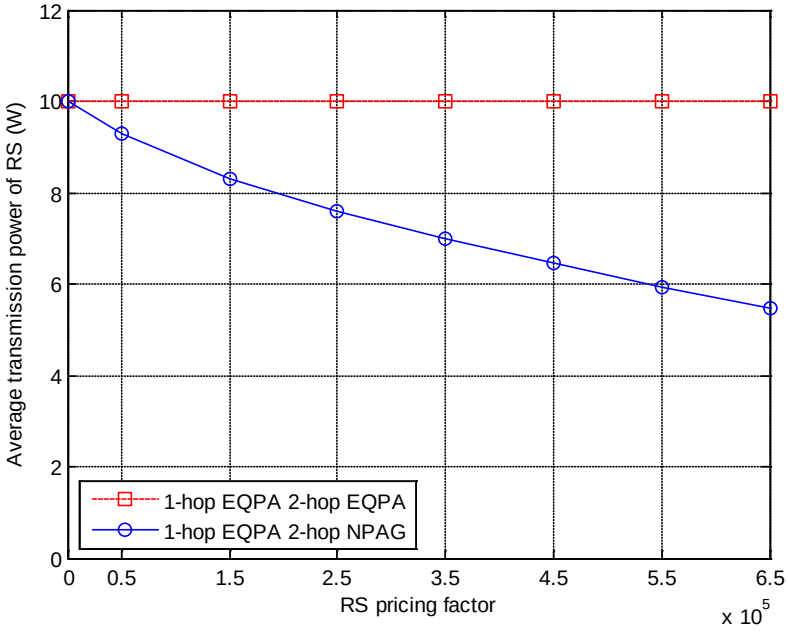

Figure 6.8 RS power *vs.* RS basic pricing factor

From Figure 6.7 and Figure 6.8, it can be seen that, when the basic pricing factor equals zero, NPAG of RS will converge to the RS equal power allocation. The

maximum second hop link data rate of NPAG is achieved when the basic price factor is about 2.5×10^5, where the data rate is increased by 4.5% compared with that of equal power allocation of RS and the average transmission power of RS is reduced by 24% compared with that of equal power allocation. The RS basic price factor can be considered as the price paid for each unit of power, i.e., the higher the RS basic pricing factor, the more expensive it is for one RS to increase its throughput by increasing transmission power. When the RS basic pricing factor exceeds a certain threshold (2.5×10^5 in the simulation), the transmission power of RS tends to converge to a smaller value, which causes the second hop link average data rate to decrease.

The effect of the BS basic pricing factor on system performance is examined in Figure 6.9 - Figure 6.11, with optimal RS pricing factor (2.5×10^5 as explained above).

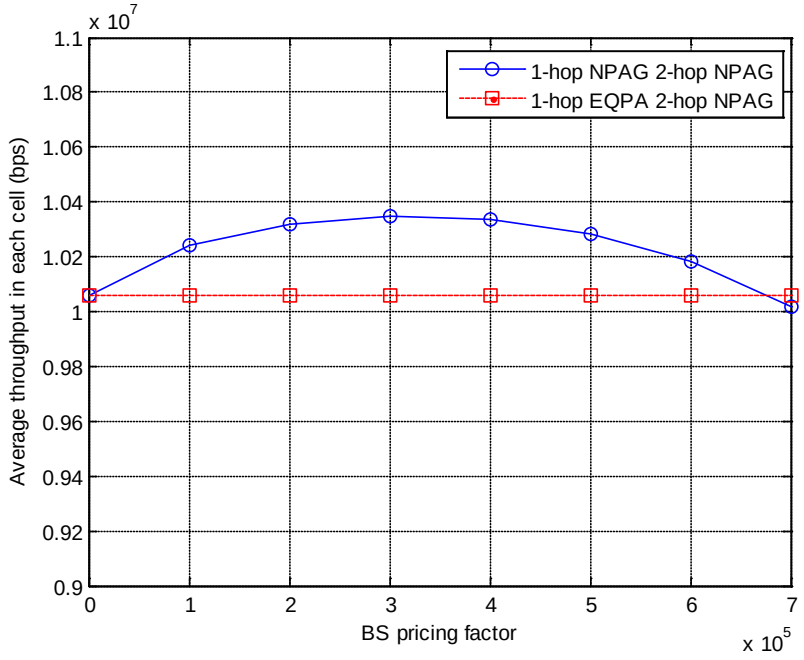

Figure 6.9 System throughput *vs.* BS basic pricing factor (fixed RS pricing factor)

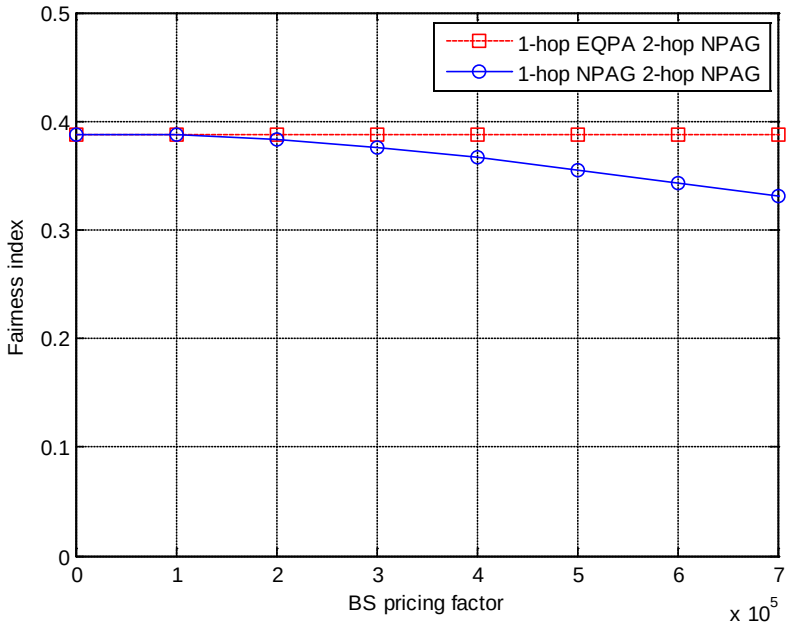

Figure 6.10 User fairness *vs.* BS basic pricing factor (fixed RS pricing factor)

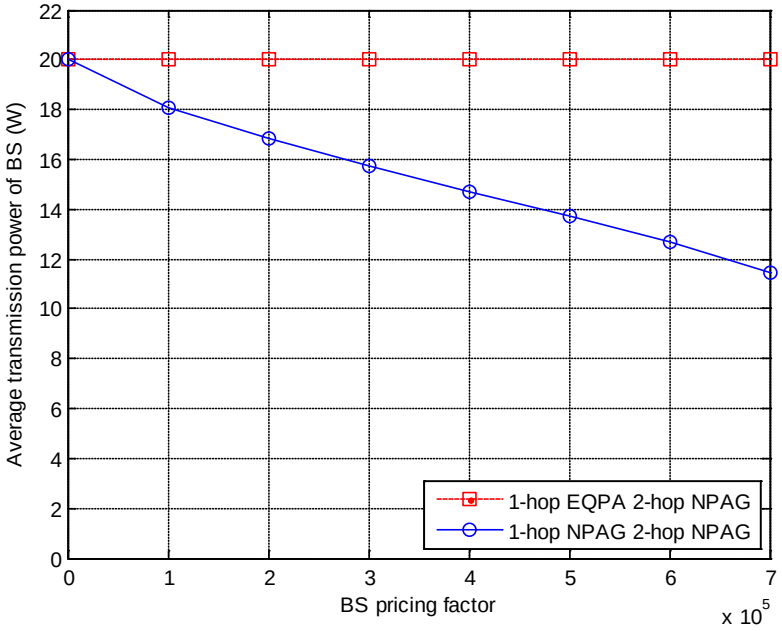

Figure 6.11 BS power *vs.* BS basic pricing factor (fixed RS pricing factor)

It can be seen from Figure 6.9 that when the BS basic pricing factor is zero, the system throughput is the same as that given by equal power allocation, and system

throughput increases first and then decreases with increasing BS pricing factor. When the BS basic pricing factor equals 3×10^5, the largest system throughput gain is obtained and increases to 3% compared with that of BS equal power allocation. The fairness index deceases with increasing BS pricing factor, as shown in Figure 6.10.

Figure 6.11 is the average BS transmission power under different BS basic pricing factor (RS basic pricing factor equals 2.5×10^5), which shows that the BS average transmission power decreases as pricing factor rises. In Figure 6.11, it can also be seen that, when BS basic pricing factor is 3×10^5 and RS basic pricing factor is 2.5×10^5, the average power of a BS will reduce by 25% compared with that of BS using equal power allocation. With a BS basic pricing factor higher than 7×10^5, the BS transmission power is so small that the system throughput gain of NPAG will decrease, and the average throughput of NPAG would be smaller even than that of equal power allocation. It is not hard to understand that with a very high price, nobody wants to spend much on power for data transmission.

In Figure 6.12 – Figure 6.14, the system performance of NPAG is compared with equal power allocation on each subchannel (EQPA) with different user numbers. In the simulation, the BS basic pricing factor is 3×10^5 and RS basic pricing factor is 2.5×10^5, the values at which maximum throughput will be obtained.

Figure 6.12 is the system throughput of each cell with different user numbers. At first, the system throughput increases directly with the number of uses, but after a certain number is reached the throughput saturates and then decreases. This is because the larger the user number, the bigger the multi-user diversity gain, but, as the Round Robin scheduling tries to keep user fairness, the system throughput will decrease as the number gets too large. It can be seen that the throughput of NPAG is nearly 4% larger than that of EQPA.

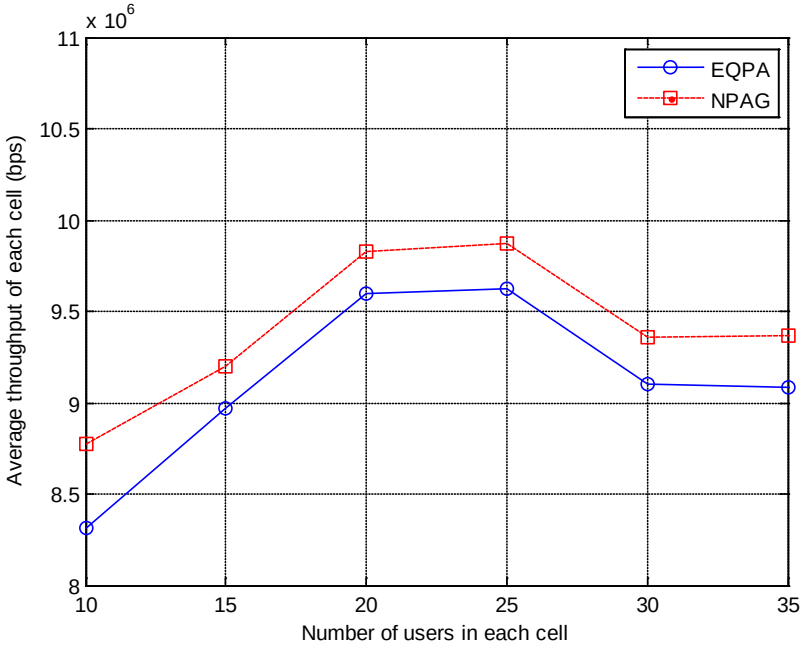

Figure 6.12 System throughput *vs.* number of users in each cell

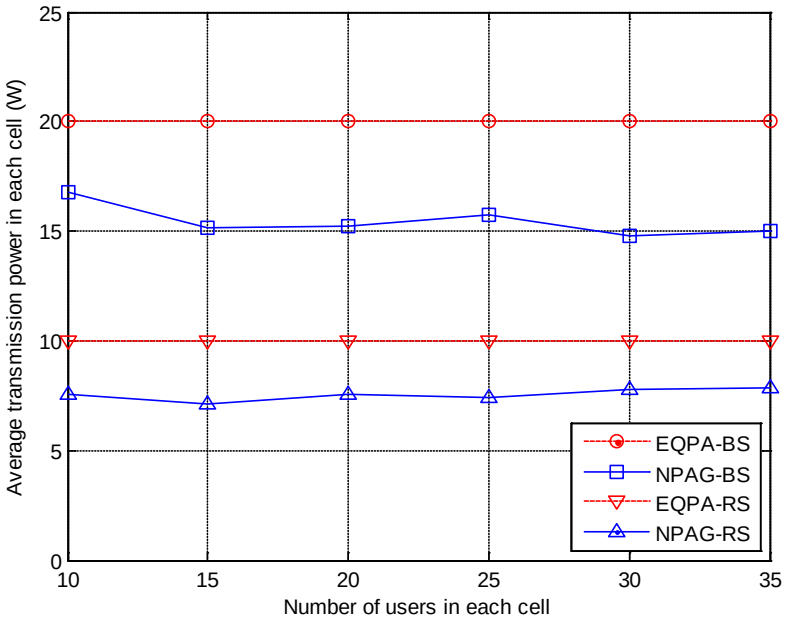

Figure 6.13 Transmission power *vs.* number of users in each cell

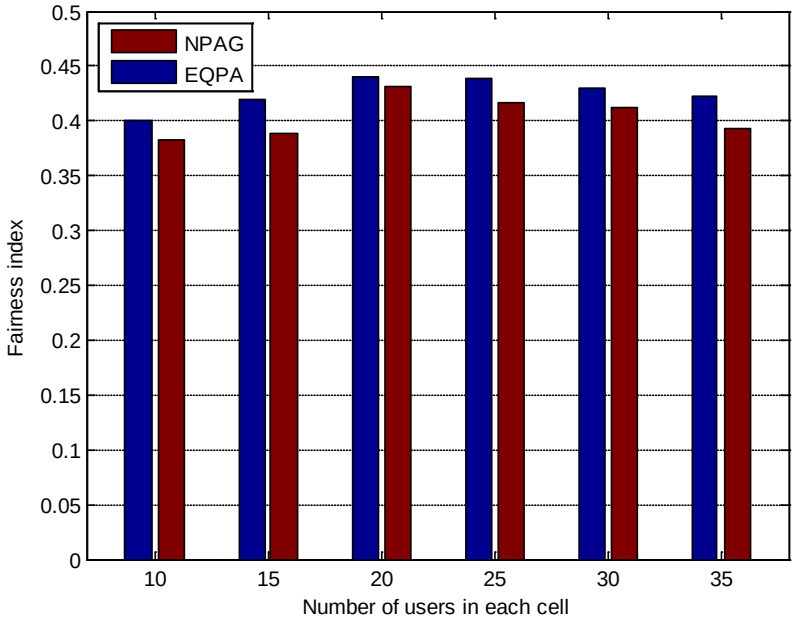

Figure 6.14 Fairness index *vs.* number of users in each cell

Figure 6.13 shows the average transmission power of BS and RS under EQPA and NPAG. Compared with EQPA, it is clear that the transmission powers of BS and RS are reduced greatly by the use of NPAG, in which, the overall power (BS power plus and RSs power) will be reduced by about 25%.

The user fairness index with different user numbers is shown in Figure 6.14. It can be seen that the NPAG will decrease the user fairness compared with EQPA, which is consistent with the result of Figure 6.10. The user fairness of NPAG is nearly 4% less than that of EQPA, but this reduction is much less than the improvement in power saving.

The simulation results show that system throughput is improved and transmission power is reduced compared with that of EQPA. This is important as while power saving is important the performance seen by the users needs to be maintained for the system to be acceptable.

6.3.4 Non-Cooperative Power Allocation Game for Fairness

In the previous section, both the power allocation game in the first time subslot and the second time subslot are defined in a fast-fading channel scenario. The multi-cell non-cooperative power allocation game can increase the system throughput and reduce power consumption but will also lead to a reduction in the data rate fairness among users. The reason is that by the utility function defined in (6.15) and (6.18), the users with good channel conditions will be allocated more transmission power. However, the cell edge users will suffer larger co-channel interference than that of cell centre users and have a worse channel condition than that of cell central users, which means that the cell edge users will suffer lower data rates, so it is unfair for the cell edge users. In this section, a novel utility function to improve the user fairness is defined.

6.3.4.1 Utility Definition for User Fairness

Based on the non-cooperative power allocation game model constructed in 6.3.3.1, the pricing factors defined for the BSs and for the RSs are modified to take into account the average data rate of receivers for fairness.

The utility of the n^{th} BS on the subchannel m can be defined as:

$$u_{n,m}^{BS}\left(\mathbf{P}_m^{BS}\right) = B_m \log_2\left(1+\gamma_{n,m,1}^{(0,k)}\right) - \alpha^{BS} R_n^{(0,k)} p_{n,m,1}^{(0,k)} \tag{6.28}$$

in the following, $p_{n,m}^{BS}$ is used to represent $p_{n,m,1}^{(0,k_m)}$ for simplicity and α^{BS} is the BS pricing factor, which is defined the same as in (6.17). $R_n^{(0,k)}$ is the normalised average data rate of the receiver k in the cell n, which is:

$$R_n^{(0,k)} = \frac{\bar{c}_n^k}{\frac{1}{K}\sum_{k=1}^{K}\bar{c}_n^k} \tag{6.29}$$

If the receiver k is a direct link user, $\overline{c}_n^k = \overline{c}_n^{k_d}$. Since the RS will receive the data from BS, retransmitting this data to a relay link user, the RS will act as a receiver in the first time subslot. So the average data rate of all the users served by the RS r is used to represent the average data rate of the RS r:

$$\overline{c}_n^r = \frac{\sum_{k_r \in K_{R_R}} \overline{c}_n^{k_r}}{\left| K_{R_r} \right|} \tag{6.30}$$

In (6.28), the $\alpha^{BS} R_n^{(0,k)}$ is called the modified pricing factor of BS. With the introduction of the normalised average data rate $R_n^{(0,k)}$ to the pricing factor α^{BS}, a transmitter will not just increase its power selfishly to increase the channel capacity, but will consider the interference to other cells; i.e. it will take a view of the whole system. The larger $\alpha^{BS} R_n^{(0,k)}$ is, the higher the price that will be incurred for increasing power; therefore the BS in each cell prefers to use less power, causing less interference to other cells. The modified pricing factor of a BS is adjusted by the normalized average data rate of the receiver k which occupies the subchannel m. If a receiver has a low average data rate, the modified pricing factor will be decreased: as a result, the algorithm will allow the transmitter to use more power to this receiver and hence obtain a higher throughput.

As a BS transmits data for both direct link users and RSs in the first time subslot, the modified pricing factor $\alpha^{BS} R_n^{(0,k)}$ for direct link users and RSs is different in the first time subslot, which is:

$$\alpha^{BS} R_n^{(0,k)} = \begin{cases} \alpha'^{BS} R_n^{(0,k)} & \text{for direct link user} \\ \alpha'^{BS} \beta_n^r R_n^{(0,k)} & \text{for RS } r \text{ in cell } n \end{cases} \tag{6.31}$$

in which, α'^{BS} is the basic pricing factor of BS, β_n^r is the match factor of the RS r in the cell n defined in (6.16). $\alpha'^{BS} R_n^{(0,k)}$ is the modified pricing factor for a direct link user, and $\alpha'^{BS} \beta_n^r R_n^{(0,k)}$ is the modified pricing factor for a RS. From (6.28) and (6.31),

it can be seen that direct link users and the RSs use different prices to compete for transmission power. When $\beta_n^r > 1$, the achieved data rate of RS r of the first hop link is bigger than that of the second hop link, the value of $\alpha'^{BS}\beta_n^r R_n^{(0,k)}$ will increase compared with $\alpha'^{BS} R_n^{(0,k)}$. Therefore, the BS can decrease its transmission power for matching the capacity of the first hop link and that of the second hop link of RS r. The larger the difference between the data rate of two hop links, the bigger is β_n^r; as a result, $\alpha'^{BS}\beta_n^r R_n^{(0,k)}$ becomes larger, and the transmission power is more strictly controlled. When $\beta_n^r < 1$, the BS tends to increase its transmission power to increase the first hop link capacity of a RS to match that of the second hop link.

Similarly to (6.28), the utility of a RS in the n^{th} cell on the m^{th} subchannel in the second time subslot can be defined as:

$$u_{n,m}^{RS}\left(\mathbf{P}_m^{RS}\right) = B_m \log_2\left(1+\gamma_{n,m,2}^{(r,k)}\right) - \alpha^{RS} R_n^{(r,k_r)} p_{n,m,2}^{(r,k)} \tag{6.32}$$

in which, α^{RS} is the basic pricing factor of RS, $R_n^{(r,k_r)}$ is the normalised average data rate of the receiver k_r in the cell n, $\alpha^{RS} R_n^{(r,k_r)}$ is the modified pricing factor of RS, and in the following, $p_{n,m}^{RS}$ is used to represent $p_{n,m,2}^{(r,k)}$ for simplicity. $R_n^{(r,k_r)}$ is defined by:

$$R_n^{(r,k_r)} = \frac{\bar{c}_n^{k_r}}{\frac{1}{K}\sum_{k=1}^{K}\bar{c}_n^{k}} \tag{6.33}$$

6.3.4.2 Solution of NPAG-F

The existence and uniqueness of the Nash equilibrium point in NPAG-F is the same as that of NPAG. The Nash equilibrium solution of NPAG in the first time subslot is $\arg\max_{p_{n,m}^{BS}\in P_{n,m}^{BS}} u_{n,m}^{BS}\left(\mathbf{P}_{n,m}^{BS}\right)$.

For a continuous function, the necessary condition for a first order optimization is:

$$\partial u_{n,m}^{BS}\left(\mathbf{P}_m^{BS}\right)/\partial p_{n,m}^{BS} = 0 \tag{6.34}$$

Taking the first-order partial derivative of (6.28) with respect to $p_{n,m}^{BS}$ for any $n \in \{n\}$ yields:

$$\frac{\partial u_{n,m}^{BS}\left(\mathbf{P}_m^{BS}\right)}{\partial p_{n,m}^{BS}} = \frac{B_m}{\ln 2}\frac{g_{n,m,1}^{(0,k)}}{I_{n,m,1}^{(0,k)} + g_{n,m,1}^{(0,k)} p_{n,m,1}^{(0,k)}} - \alpha^{BS} R_n^{(0,k)} \tag{6.35}$$

From (6.34) and (6.35):

$$p_{n,m}^{BS} = \frac{B_m}{\ln 2 \cdot \alpha^{BS} \cdot R_n^{(0,k)}} - \frac{p_{n,m}^{BS}}{\gamma_{n,m,1}^{(0,k)}} \tag{6.36}$$

Using the same method to get (6.24), then the iterative expression of $p_{n,m}^{BS}$ can be expressed as:

$$p_{n,m}^{BS}(t) = \frac{B_m}{\ln 2 \cdot \alpha^{BS} \cdot R_n^{(0,k)}(t-1)} - \frac{p_{n,m}^{BS}(t-1)}{\gamma_{n,m,1}^{(0,k)}(t-1)} \tag{6.37}$$

Similarly, the iterative expression of $p_{n,m}^{RS}$ can be expressed as:

$$p_{n,m}^{RS}(t) = \frac{B_m}{\ln 2 \cdot \alpha^{RS} \cdot R_n^{(r,k_m)}(t-1)} - \frac{p_{n,m}^{RS}(t-1)}{\gamma_{n,m,2}^{(r,k_m)}(t-1)} \tag{6.38}$$

The process of the NPAG-F is same as NPAG described in session 6.3.3.3.

6.3.4.3 Performance Simulation and Analysis

Round Robin scheduling is used for subchannel allocation. The system average throughput is the sum of average throughput achieved by each user in one cell. The Raj Jain fairness index (5.18) is used as before to measure the fairness among users. In the simulation, the BS basic pricing factor α'^{BS} and the RS basic pricing factor α^{RS} are the algorithm factors of NPAG-F. The system performance under different

pricing factors of BS and RS are compared with the equal power allocation with maximum transmission power limitation.

Figure 6.15 shows the effect of the BS basic pricing factor and RS basic pricing factor on the system throughput. Increasing the BS basic pricing factor or RS basic pricing factor will decrease the average throughput.

Figure 6.16 is the simulation result on user fairness. The user fairness increases first and decreases later with increasing BS basic pricing factor or RS basic pricing factor, but the change is quite small. The optimal user fairness point varies with different BS basic pricing factors if the RS pricing factor is fixed. When $\alpha'^{BS} = 7\times10^5$ and $\alpha^{RS} = 5\times10^5$ the user fairness index is about 0.49, and that of equal power allocation is about 0.41, an increase of more than 20%.

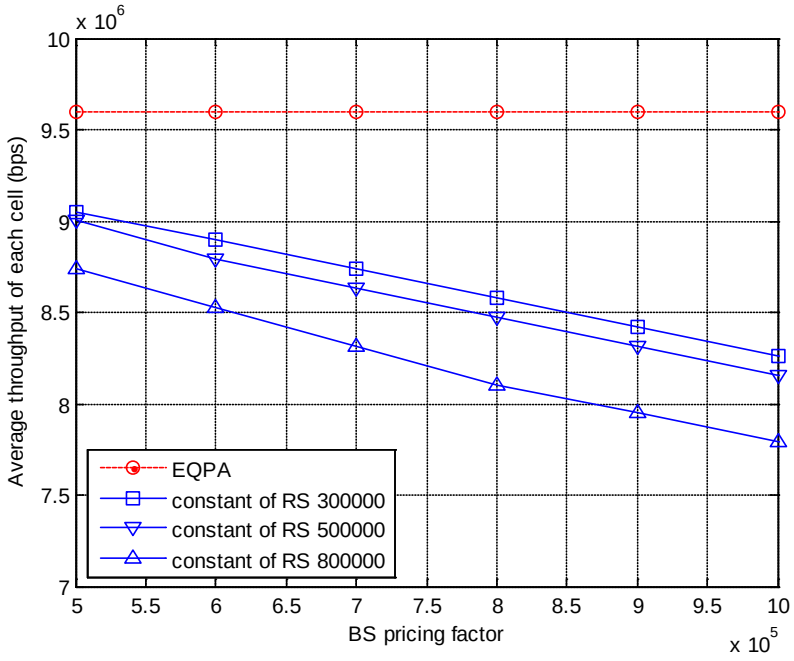

Figure 6.15 System throughput *vs.* BS basic pricing factor

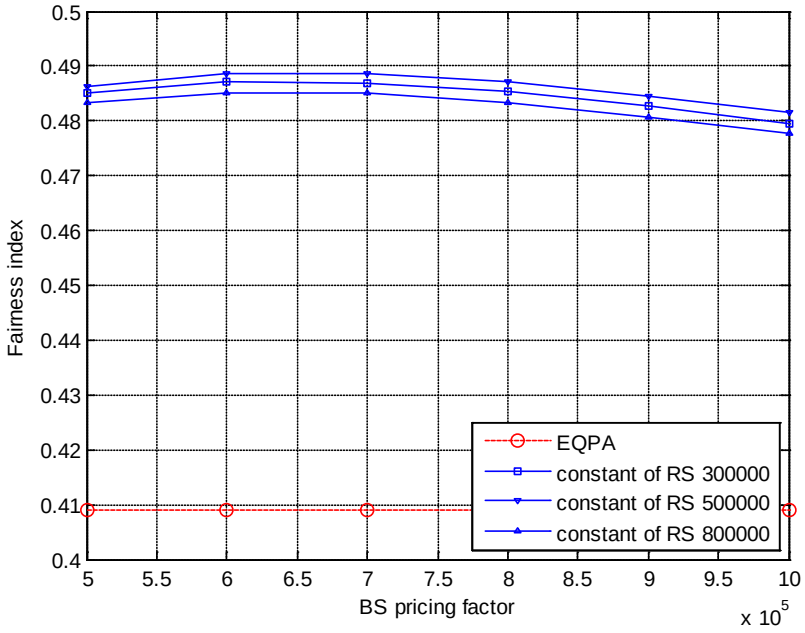

Figure 6.16 User fairness *vs.* BS basic pricing factor

Figure 6.17 and Figure 6.18 show the average transmission power of BS and RS respectively, both of which reduce with increasing respective basic pricing factor.

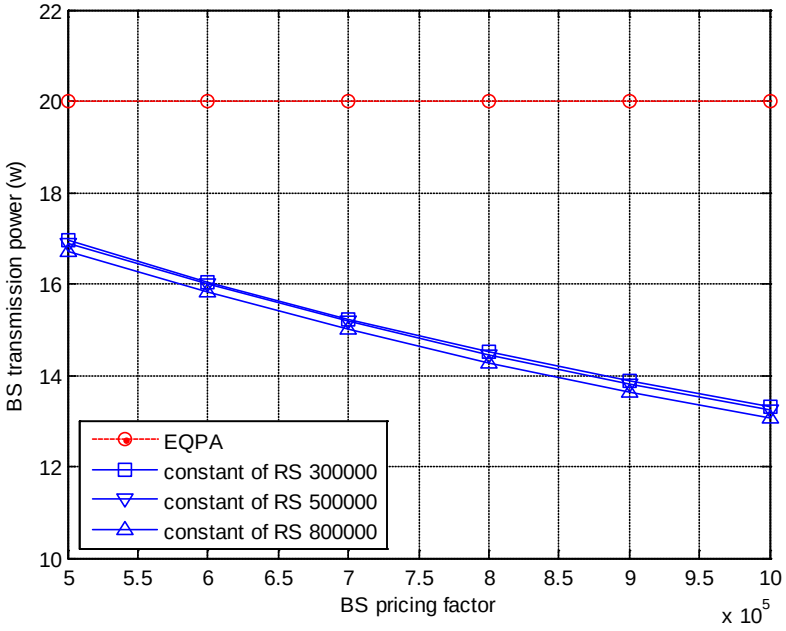

Figure 6.17 BS transmission power *vs.* BS basic pricing factor

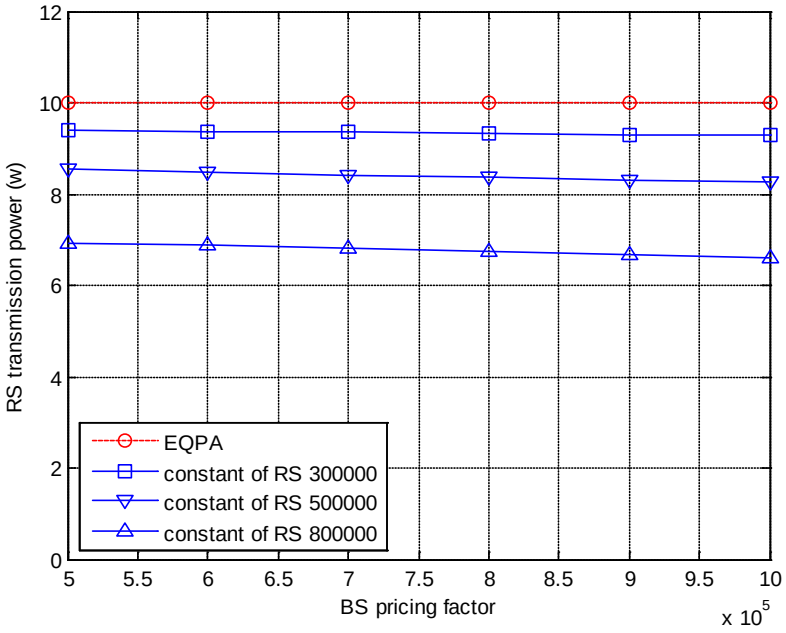

Figure 6.18 RS transmission power *vs.* BS basic pricing factor

Under equal power allocation, the transmission power of BS is 20 W and that of RS is 10 W, so the energy is reduced greatly when NPAG-F is used.

Table 6.1: RS basic pricing factor is 300,000

BS basic pricing factor α'^{BS}						
	500,000	600,000	700,000	800,000	900,000	1000,000
Fairness	+18.6%	+19.1%	+19.0%	+18.7%	+18.0%	+17.2%
Throughput	-5.7%	-7.3%	-9%	-10.6%	-12.3%	-13.9%

Table 6.2: RS basic pricing factor is 500,000

BS constant pricing factor α'^{BS}						
	500,000	600,000	700,000	800,000	900,000	1000,000
Fairness	+18.9%	+19.41%	+19.43%	+19.1%	+18.5%	+17.8%
Throughput	-6.2%	-8.4%	-10.0%	-11.7%	-13.3%	-15.0%

Table 6.3: RS basic pricing factor is 800,000

BS constant pricing factor α'^{BS}

	500,000	600,000	700,000	800,000	900,000	1000,000
Fairness	+18.2%	+18.6%	+18.6%	+18.2%	+17.5%	+16.8%
Throughput	-9%	-11.2%	-13.3%	-15.5%	-17.2%	-18.8%

From the simulation results, it can be seen that there should be an optimal point which will achieve a best tradeoff between user fairness and system throughput. From Table 6.1-Table 6.3, the optimal point is when $\alpha'^{BS} = 6\times10^5$ and $\alpha^{RS} = 3\times10^5$, in which case the user fairness is increased 19.1% and throughput is decreased 7.3%.

6.4 Joint Power Allocation of THPA and NPAG

This section gives a joint distributed multi-cell power allocation (DMPA) algorithm which is a combination of non-cooperative power allocation game (NPAG) and two-hop power allocation (THPA) for energy efficiency and throughput improvement.

6.4.1 Algorithm Procedure

The process of the DMPA algorithm is given as following:

Step 1: On each subchannel m, initialize transmission power $\mathbf{P}_m^{BS}(0) = 0$, $\mathbf{P}_m^{RS}(0) = 0$, and set iterative convergence parameter ε to be very small so that ε tends to 0 ($\varepsilon \to +0$).

Step 2: Let $t = 0$. Execute NPAG in the second time subslot.

Step 3: Let $t = t + 1$, calculate $\mathbf{P}_m^{RS}(t)$ according to (6.27).

Step 4: If $\left|\mathbf{P}_m^{RS}(t) - \mathbf{P}_m^{RS}(t-1)\right| < \varepsilon$, the NPAG of RS is over, $\mathbf{P}_m^{RS} = \mathbf{P}_m^{RS}(t)$ is the power allocation result of RSs on the subchannel m, and go to step 5; otherwise, go to step 3.

Step 5: Calculate the second hop link data rate of relay link users according to $\mathbf{P}_m^{RS}$ in the step 4, and update the match factor β_n^r of the RS r in the cell n.

Step 6: Execute NPAG in the first time subslot. Let $t = 0$.

Step 7: Let $t = t + 1$, calculate $\mathbf{P}_m^{BS}(t)$ according to (6.24).

Step 8: If, $\left|\mathbf{P}_m^{BS}(t) - \mathbf{P}_m^{BS}(t-1)\right| < \varepsilon$, the NPAG of BS is over, $\mathbf{P}_m^{BS} = \mathbf{P}_m^{BS}(t)$ is the power allocation results of BS on the subchannel m, and go to step 9; otherwise, go to step 7.

Step 9: Calculate the first hop link data rate of relay link users and that of the direct link users according to $\mathbf{P}_m^{BS}$ in step 8.

Step 10: Calculates Δc^r from (6.2) for RS r in the cell n. If $\Delta c^r < 0$ go to step 11, else go to step 12 .

Step 11: The BS transmission power will be derived from (6.7), while the RS transmission power remains as $\mathbf{P}_m^{RS}$.

Step 12: The RS transmission power will be calculated by (6.9), and the transmission power of BS is unchanged.

6.4.2 Performance Simulation and Analysis

The system throughput and transmission power of BS and RS of DMPA are compared with two schemes: one is equal power allocation on each subchannel (named EQPA), and the other is NPAG (as in section 6.3.3). Round Robin scheduling is used for subchannel allocation. In the simulation, the BS basic pricing factor is 3×10^5 and the RS basic pricing factor is 2.5×10^5 (these values give maximum throughput as shown in section 6.3.3.4).

Figure 6.19 is the average throughput of each cell with different numbers of users. The system throughput increases at first as the number of users increases and then decreases. This is because multi-user diversity gain occurs as the number of users gets bigger; however, as the Round Robin scheduling aims to keep user fairness, making the number of users too large will decrease the system throughput. It can be seen that the throughput of DMPA is nearly 4% larger than that of EQPA, and the throughput of DMPA improves almost 1% over that of NPAG.

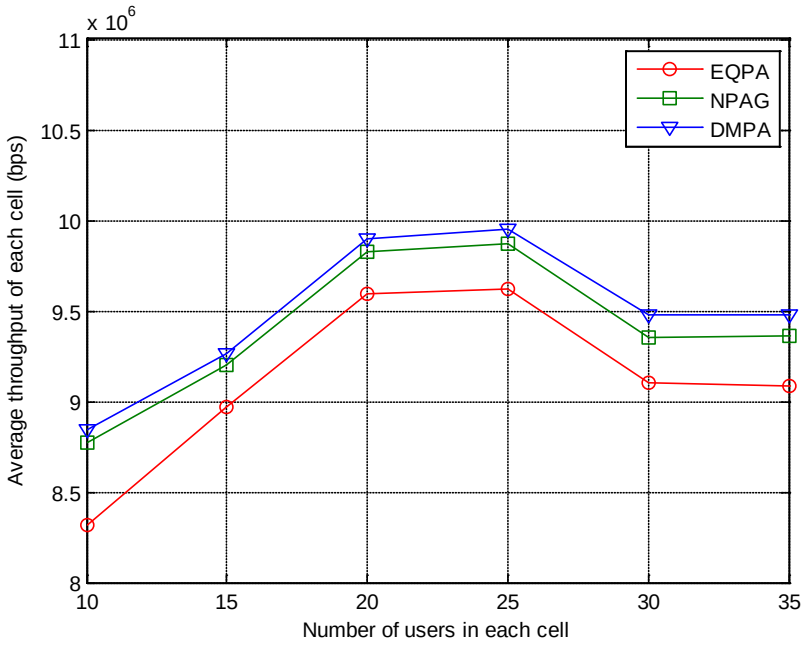

Figure 6.19 System throughput *vs.* number of users in each cell

Figure 6.20 is the comparison of performance of average power of BS with different numbers of users for the EQPA, NPAG and DMPA algorithms. Figure 6.21 is the comparison of average power of RS among EQPA, NPAG and DMPA algorithms respectively. Compared with EQPA, both the power of BS and RS of NPAG and DMPA are greatly reduced. The DMPA consumes the smallest power both on BS and on RS. From Figure 6.21, compared with EQPA, it can be seen that the RS power saving of DMPA is 40% and the RS power saving of NPAG is 25%.

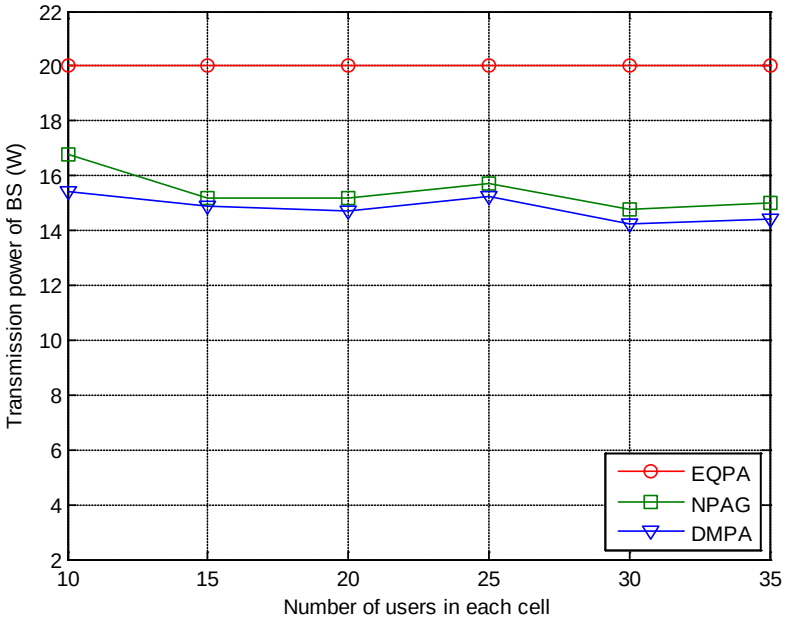

Figure 6.20 BS transmission power *vs.* number of users in each cell

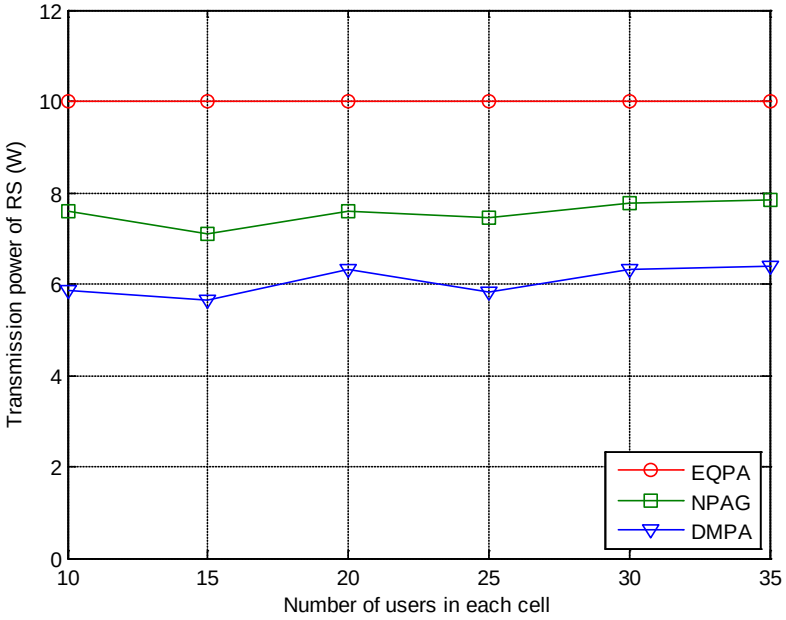

Figure 6.21 RS transmission power *vs.* number of users in each cell

Overall, the DMPA in the multi-cell scenario not only saves energy, but also improves system throughput. This is because, using THPA will decrease the

transmission power of the BS or RS to match the data rates of the two-hop links. This will not decrease the system throughput of the cell but will reduce the interference to other cells.

6.5 Summary

An adaptive power allocation algorithm called two-hop power allocation (THPA) has been proposed. The transmission power of BS and RS decreases greatly but the achieved system throughput remains the same as that with equal power allocation, which is verified by the simulation results.

Subsequently, the power allocation for multiple cells with co-channel interference in OFDMA relay networks is studied. A non-cooperative power allocation game is defined for maximizing throughput and reducing co-frequency interference.

Next, the user fairness problem is considered for multi-cell OFDMA relay systems with co-channel interference. A novel utility function is defined for user fairness. Compared with equal power allocation, the user fairness is improved greatly with only a small impact on system throughput; importantly with current concerns on energy efficiency, the transmission power of the BS and the RSs is reduced greatly.

Besides, the joint power allocation algorithm which considers power allocation between multi-cell and power allocation between two-hop is given, in which THPA and NPAG is combined. From the simulation analysis, the joint power allocation algorithm can reduced the transmission power efficiently and increase the system throughput. This is considered further in the next chapter where a more systematic study of combining the techniques researched in this thesis is presented.

Chapter 7 Joint Radio Resource Allocation Algorithm

In the earlier chapters, different individual techniques for increasing system throughput, improving user fairness and energy efficiency are proposed: in Chapter 5, a novel relay selection algorithm (LBRS), and a subchannel allocation algorithm (THPF) are given to improve user fairness; the emphasis in Chapter 6 is on energy efficient power allocation with a two-hop power allocation algorithm (THPA) and a multi-cell power allocation algorithm (NPAG or NPAG-F), plus an initial investigation of combining NPAG and THPA. In this chapter, the proposed radio resource allocation algorithms are combined with different algorithms and the system performance (throughput, user fairness, and energy efficiency) is investigated.

The optimization target of NPAG is increasing the system throughput and that of NPAG-F is improving the user fairness. By using different subchannel allocation, a different power allocation result will be obtained after carrying out the NPAG (or NPAG-F) algorithm. In this chapter, different combinations of relay selection, subchannel allocation, power allocation between hops and power allocation between cells are considered (as shown in Table 7.1).

Table 7.1 Joint Algorithms Used for Comparison

Joint algorithm name	Relay selection	Subchannel allocation	Power allocation between hops	Power allocation between cells
LRTN	LBRS	RR	THPA	NPAG
LTTN	LBRS	THPF	THPA	NPAG
PRNG	PBRS	RR	EQPA	NPAG
PTNG	PBRS	THPF	EQPA	NPAG
LRTN-F	LBRS	RR	THPA	NPAG-F
LTTN-F	LBRS	THPF	THPA	NPAG-F
PRNG-F	PBRS	RR	EQPA	NPAG-F
PTNG-F	PBRS	THPF	EQPA	NPAG-F
PREQ	PBRS	RR	EQPA	EQPA
PTEQ	PBRS	THPF	EQPA	EQPA

The comparisons shown in this chapter are:

1) LRTN, PRNG and PREQ

2) LTTN, PTNG and PTEQ

3) LRTN and LTTN

4) LRTN-F, PRNG-F and PREQ

5) LTTN-F, PTNG-F and PTEQ

6) LRTN-F, LTTN-F

7) LTTN and LTTN-F

In (1), the scheduling algorithm is the RR algorithm, and different relay selection algorithms are combined with the NPAG algorithm. PREQ, which is composed of traditional algorithms (RR, PBRS and equal power allocation), is compared with the proposed algorithms. In (2), the THPF algorithm is used instead of RR algorithm in (1). In (3) different scheduling algorithms (RR and THPF) are combined with NPAG, LBRS and THPA respectively. Similarly, in (4)-(6), the NPAG-F algorithm is used instead of NPAG in (1)-(3) to allow the target of improved fairness. In (7), LTTN and LTTN-F are compared; these both contain all the new algorithms proposed in this thesis.

For these comparisons, a multi-cell simulation scenario is used with the detailed parameters being the same as in section 6.3.3.4.

7.1 Performance Comparison using the NPAG variants

7.1.1 Performance Comparison between LRTN, PRNG and PREQ

The simulation results of the LRTN algorithm are compared with those of the PRNG algorithm and the PREQ algorithm in Figure 7.1 - Figure 7.6. In the simulation, the

PRNG algorithm uses the optimal BS basic pricing factor 3×10^5 and the RS basic pricing factor 2.5×10^5 for maximal system throughput as shown in Chapter 6 (since PRNG in this Chapter is NPAG in the previous Chapter).

In Figure 7.1, the system throughput is plotted against BS basic pricing factor for different RS basic pricing factors. The throughput of LRTN algorithm clearly peaks with optimal BS and RS basic pricing factor of $\alpha'^{BS} = 3\times10^5$ and $\alpha^{RS} = 3\times10^5$ respectively, at 1.1185×10^7 bps. The optimal system throughput of LRTN algorithm is 8.2% higher than that of the PRNG algorithm (1.034×10^7 bps in the simulation). Compared with the system throughput of the PREQ algorithm (1.003×10^7 bps in the simulation), the system throughput of LRTN algorithm is 11.5% higher.

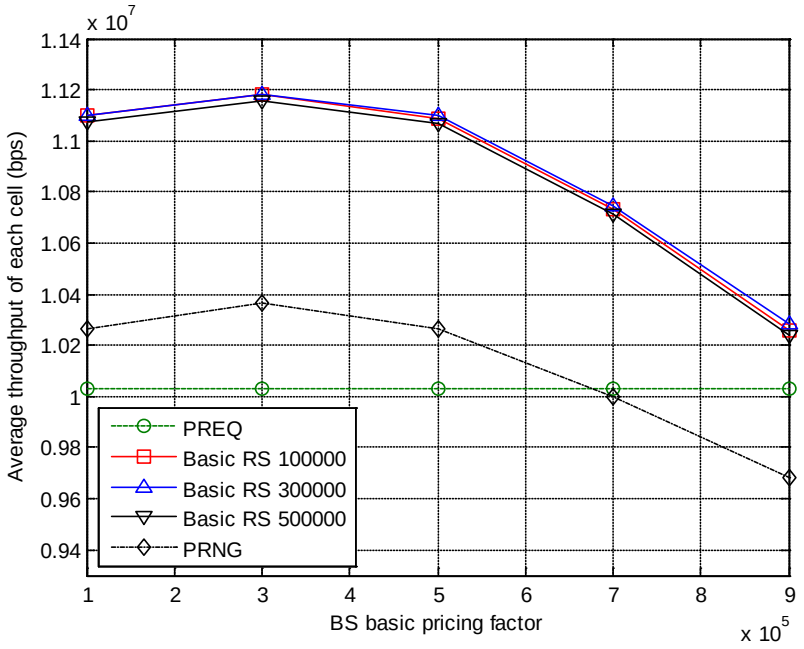

Figure 7.1 System throughput *vs.* BS basic pricing factor

Figure 7.2 shows the comparison result of user fairness with different BS basic pricing factors and different RS basic pricing factors. For LRTN and PRNG, user fairness decreases as the BS basic pricing factor or the RS basic pricing factor increase. The fairness index of the PREQ algorithm is 0.3881, and with the optimal basic

pricing factor $\alpha'^{BS} = 3\times10^5$ and $\alpha^{RS} = 3\times10^5$ where the peak throughput is obtained, the fairness index of the LRTN algorithm is 0.3699. So the LRTN achieves 95.3% of the fairness index of that of PREQ. The fairness of the PRNG is decreased with the increasing of BS basic pricing factor, and the LRTN achieves 98.7% of the fairness index of that of PRNG (0.3747 in the simulation).

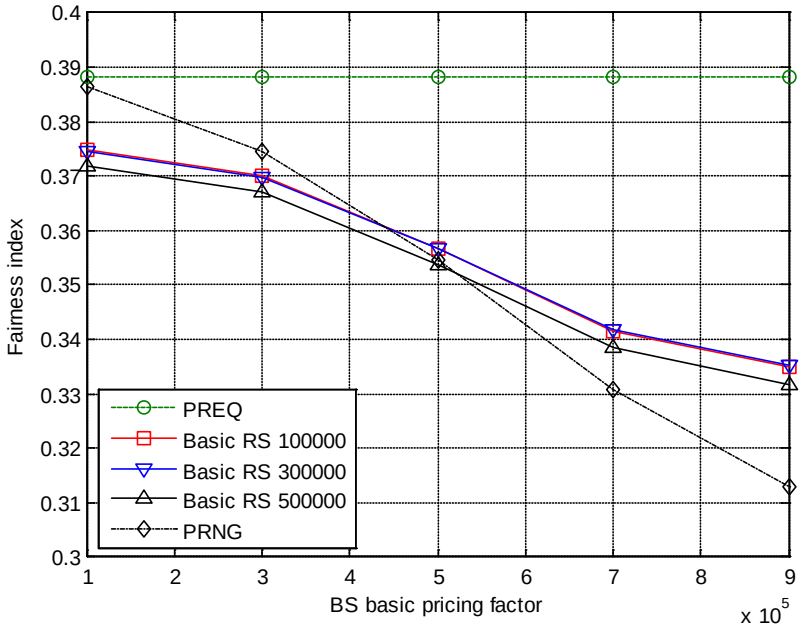

Figure 7.2 User fairness *vs.* BS basic pricing factor

In Figure 7.3, Figure 7.4 and Figure 7.5, the BS transmission power consumption and RS transmission power consumption is examined. Compared with PREQ, the transmission power of LRTN is reduced significantly.

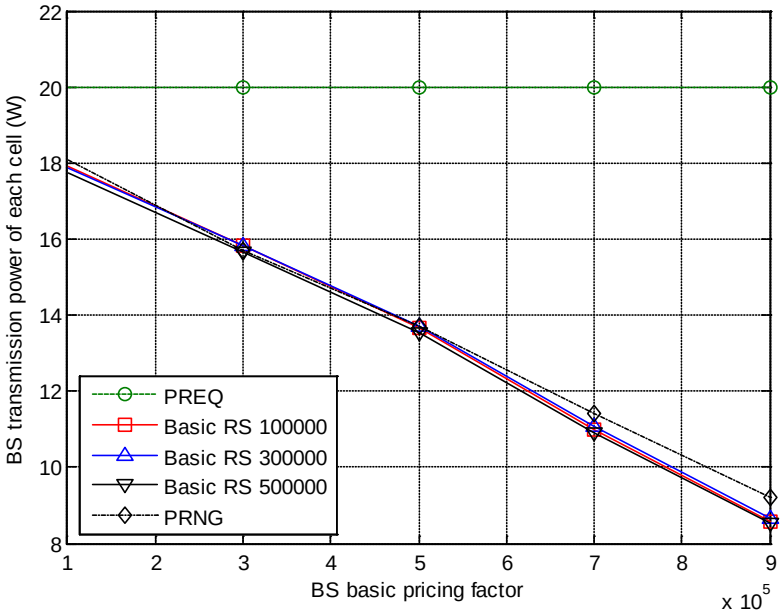

Figure 7.3 BS transmission power *vs.* BS basic pricing factor

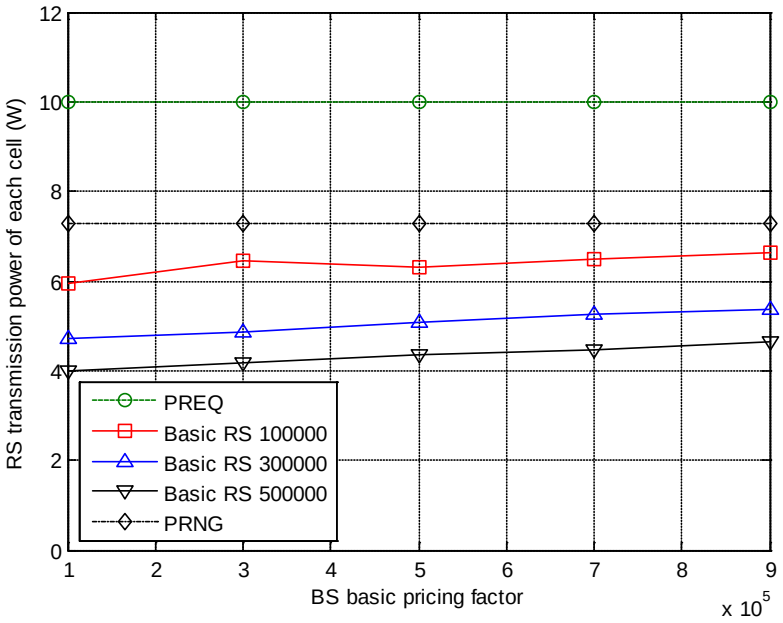

Figure 7.4 RS transmission power (all 6 RS) *vs.* BS basic pricing factor

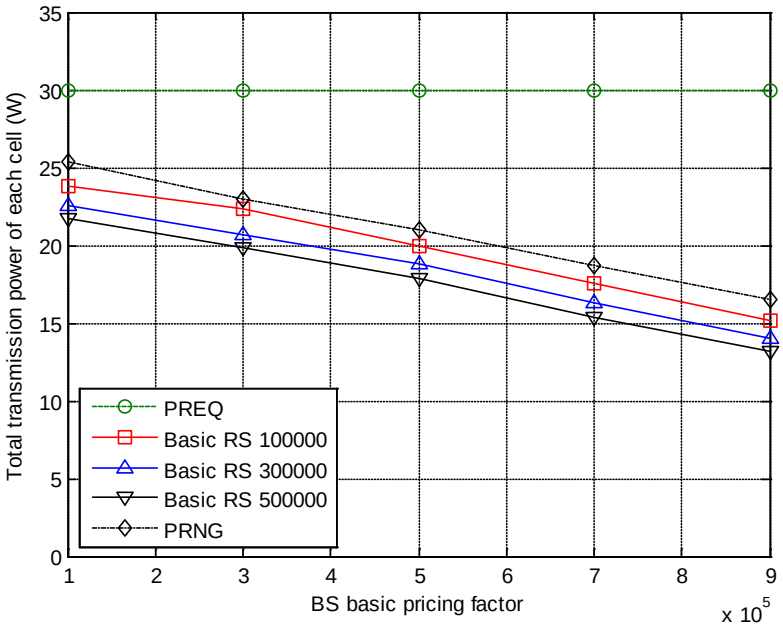

Figure 7.5 Total transmission power *vs.* BS basic pricing factor

The BS transmission power of LRTN and PRNG varies significantly with α'^{BS}, but the RS transmission power is more or less unaffected by α'^{BS}, but does decrease with increasing α^{RS}. These conclusions are similar to those drawn for Figure 6.17 and Figure 6.18.

At the optimum (for throughput) value for α'^{BS} of 3×10^5 and α^{RS} of 3×10^5, the BS transmission power of LRTN is reduced from 20W to 15.8W and the RS power (for all 6 RSs) is reduced from 10W to around 4.8W – i.e. the total power is reduced from 30W to 20.6W - a saving of nearly 32%. At the optimum (for throughput) value, compared with PRNG, the LRTN can save 5% total transmission power.

However, that calculation optimises the throughput – if power saving is the most significant requirement then a α'^{BS} can be used and the throughput kept more or less the same as PREQ. As an example, if α'^{BS} is changed to 9×10^5, the BS power of

LRTN is reduced to 8.5W and the overall power is 14.2W and the saving is 53%, without any loss of throughput from PREQ, but with reduced fairness.

Table 7.2 Performance of LRTN relative to PREQ

		Performance relative to PREQ		
Optimization target	α^{BS} ($\times 10^5$)	Throughput	Fairness	Power
Max throughput	3	+11.5%	-4.7%	-32%
Power saving	9	+2%	-14%	-53%

Summarising the performance in Table 7.2 shows that there is a tradeoff the designer can use between power, fairness and throughput. This is also shown in Figure 7.6 where the performance gain in power saving and the reduction in fairness are plotted against the improvement in throughput.

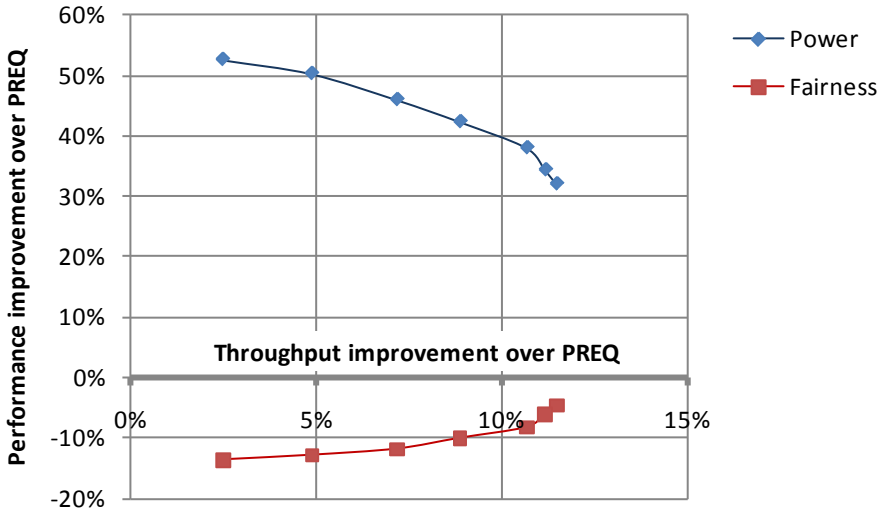

Figure 7.6 Performance change of LRTN relative to PREQ

7.1.2 Performance Comparison between LTTN, PTNG and PTEQ

In this section the LTTN algorithm is compared with the PTNG, PTEQ algorithm using a similar methodology as in the previous section.

Notice that, when both the BS and RS basic pricing factors equal zero, the system throughput of the LTTN algorithm is still higher than in PTEQ. This is because in LTTN, THPA is used for controlling the transmission power of the BS and RS, so reducing co-frequency interference and hence increasing the total system throughput.

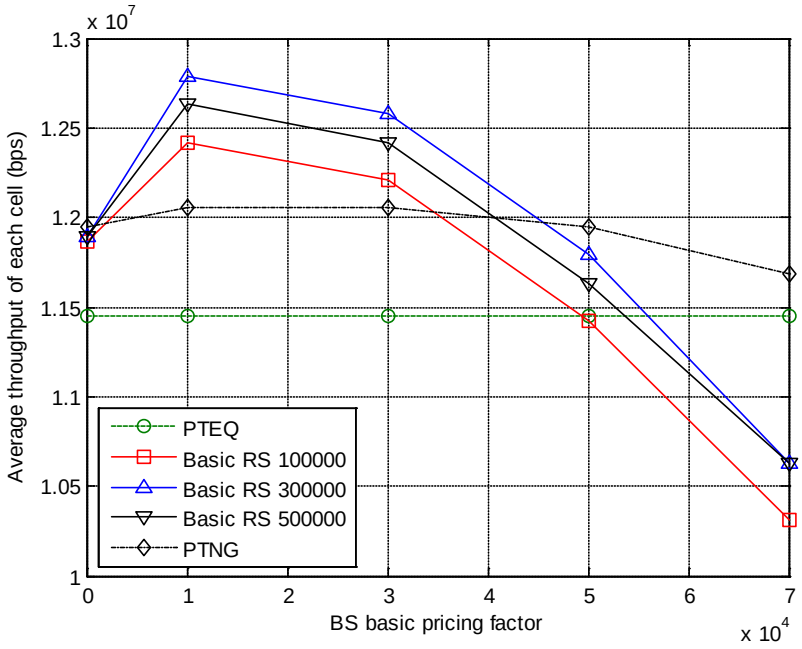

Figure 7.7 Average throughput *vs.* BS basic pricing factor

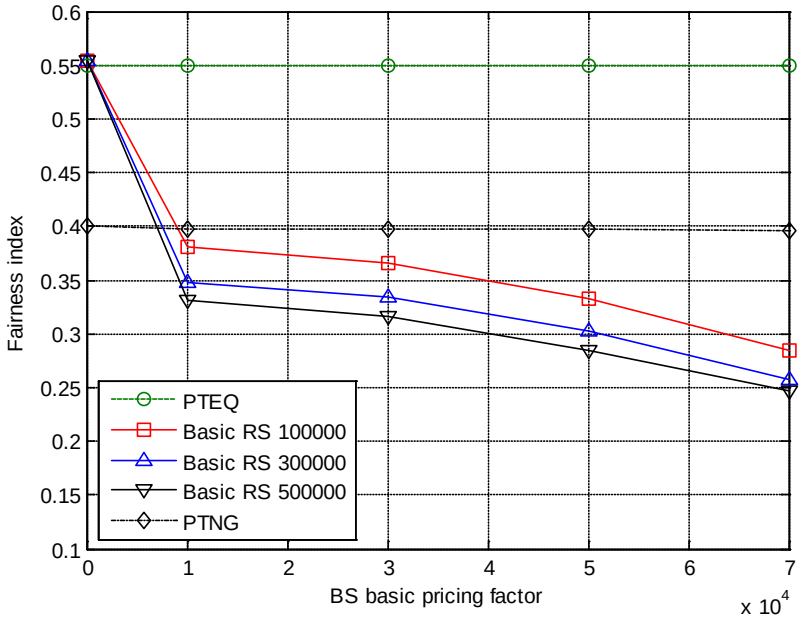

Figure 7.8 User fairness *vs.* BS basic pricing factor

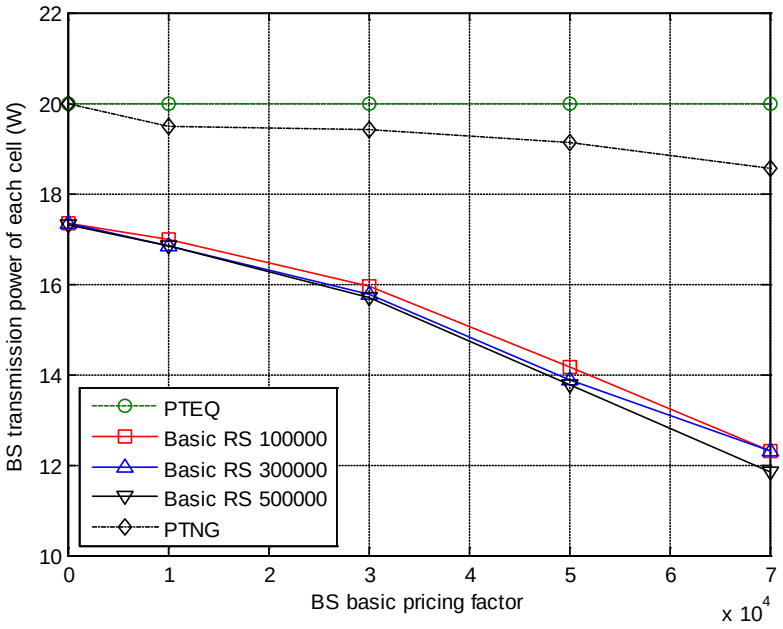

Figure 7.9 BS transmission power *vs.* BS basic pricing factor

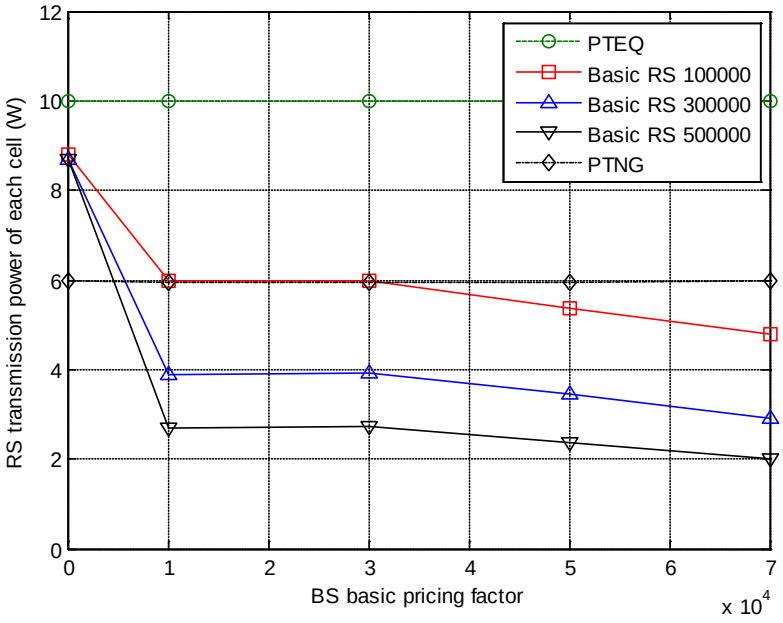

Figure 7.10 RS transmission power *vs.* BS basic pricing factor

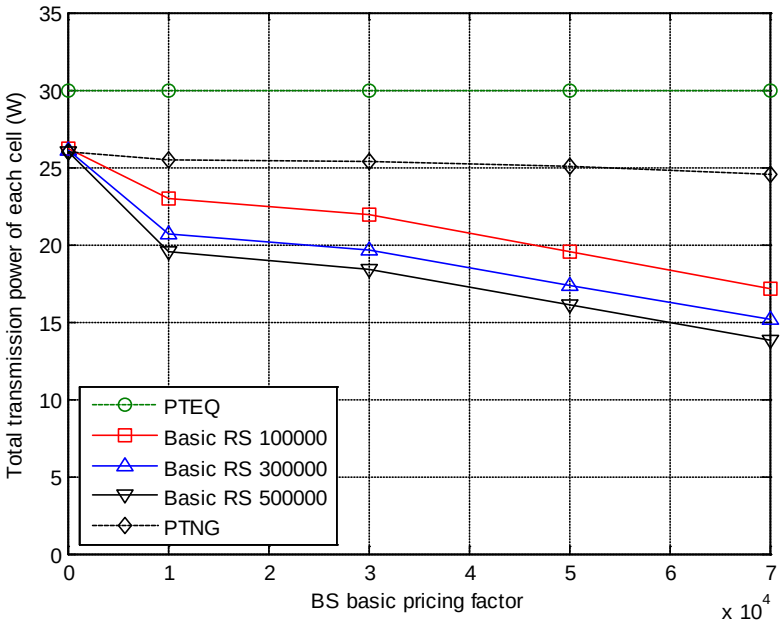

Figure 7.11 Total transmission power *vs.* BS basic pricing factor

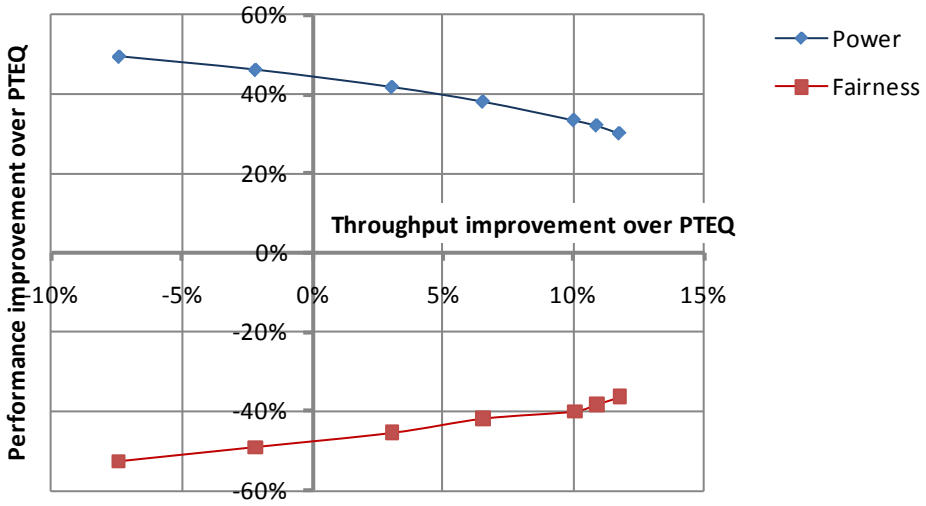

Figure 7.12 Performance improvement of LTTN over PTEQ

Figure 7.12 shows the performance improvement of LTTN over PTEQ in the same way that Figure 7.6 compared LRTN with PREQ. In this case with pricing values of $\alpha'^{BS} = 1\times10^{4}$ and $\alpha^{RS} = 3\times10^{5}$ (corresponding to the biggest system throughput).

7.1.3 Performance Comparison between LRTN and LTTN

LRTN and LTTN are different in that the channel allocation algorithm is different: using RR and THPF respectively. Since THPF is designed to improve user fairness it might be thought that RR might be a better solution when other factors are important.

Figure 7.13 compares the two approaches using throughput (absolute, not relative to PREQ or PTEQ) as a common factor. It can be clearly seen that LTTN uses less power to achieve the same throughput, or with the same fairness LTTN achieves better throughput than LRTN. As explained earlier, this is likely to be because LTTN uses THPF, which achieves a better tradeoff between throughput and fairness than RR.

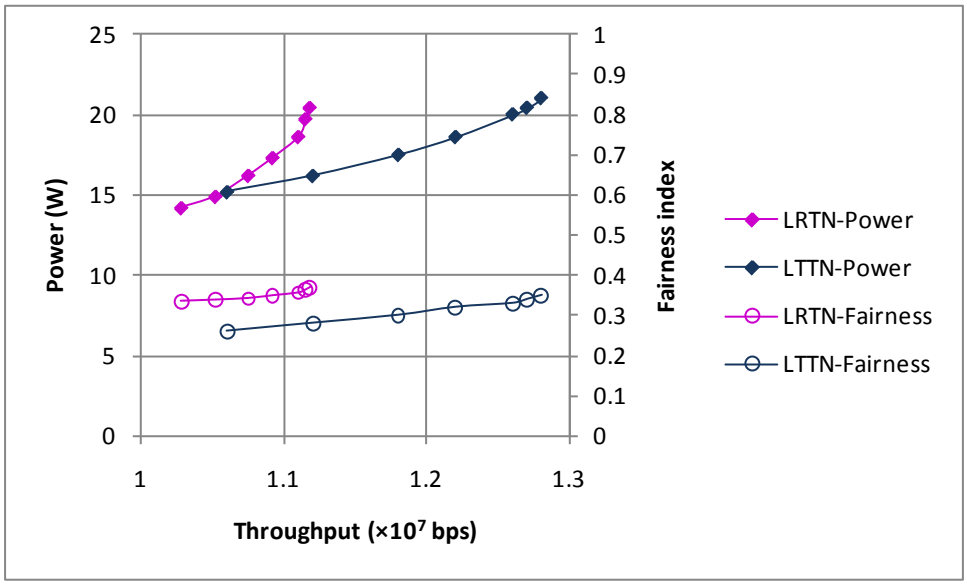

Figure 7.13 Comparison between LRTN and LTTN based on same throughput

7.2 Performance Comparison using the NPAG-F variants

In this section the NPAG-F variants are used for the comparison using exactly the same approach as in the previous section. For that reason detailed analysis for comparisons of every attribute for every combination are not considered, but simply the summary results show how, for a given throughput, each variant offers different power saving and different fairness index. This overall comparison is shown in Figure 7.16.

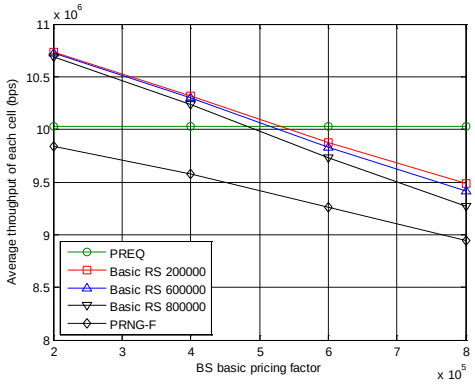

a) Throughput of each cell

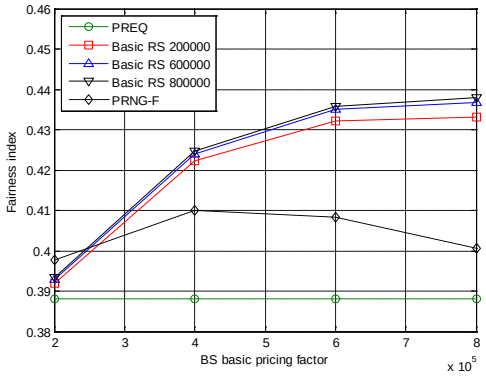

b) Fairness index of each cell

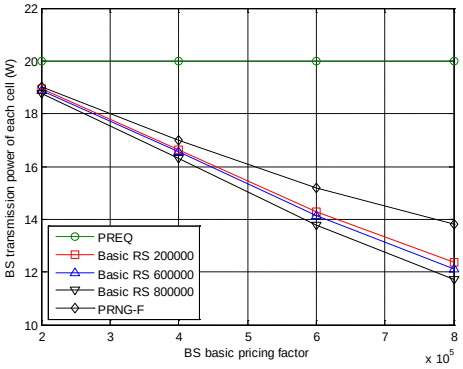

c) BS transmission power of each cell

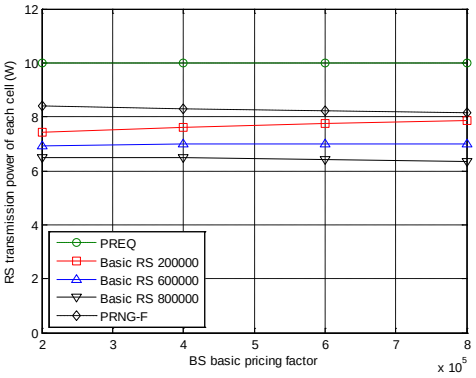

d) RS transmission power of each cell

Figure 7.14 Comparison between LRTN-F, PRNG-F and PREQ

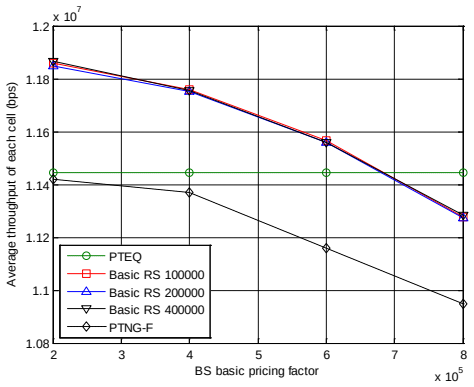

a) Throughput of each cell

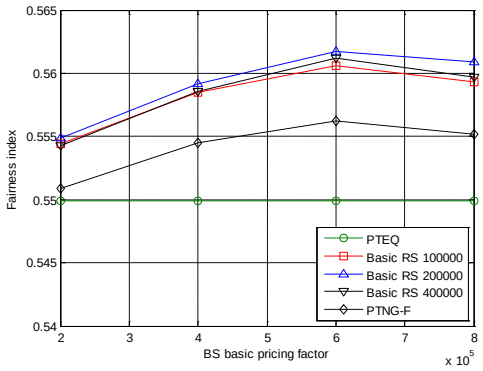

b) Fairness index of each cell

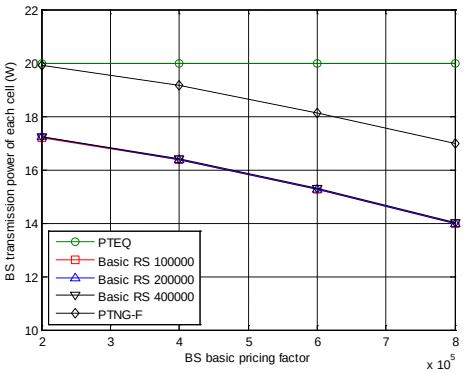

c) BS transmission power of each cell

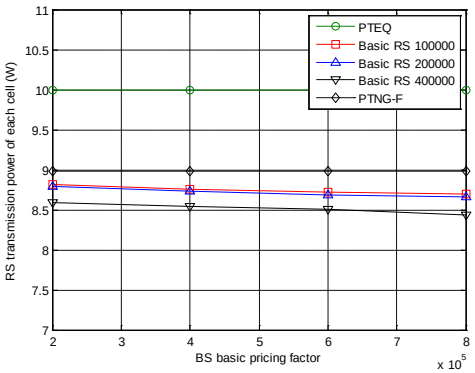

d) RS transmission power of each cell

Figure 7.15 Comparison between LTTN-F, PTNG-F and PTEQ

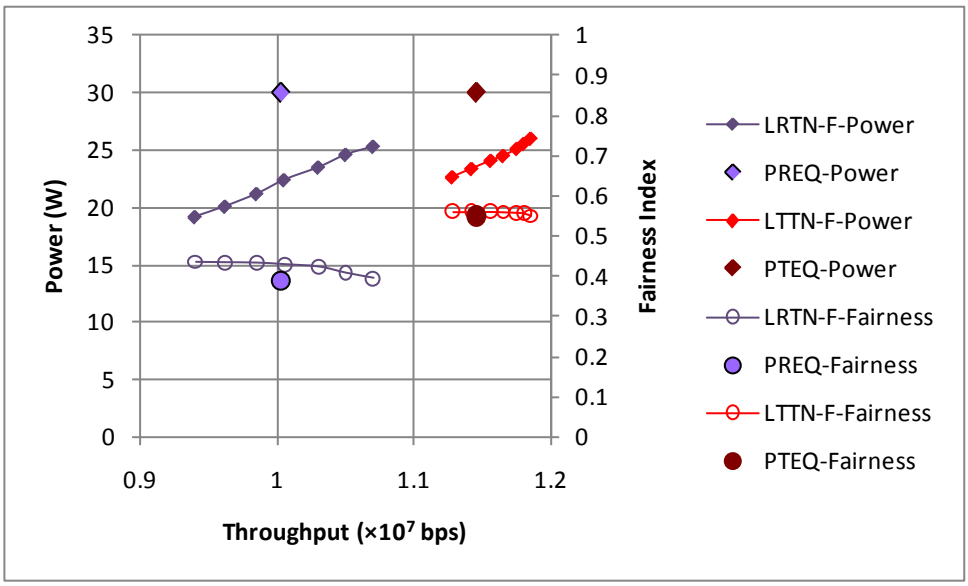

Figure 7.16 Comparison for the NPAG-F variants

In Figure 7.16, it is quite clear that LRTN-F and LTTN-F outperform their 'conventional' counterparts in terms of requiring less power to achieve the same throughput, yet maintain, or just surpass, the fairness index.

LTTN-F achieves higher throughput with the same power compared with LRTN-F. And the LTTN-F achieves a higher fairness index than LRTN-F. The reason is that the THPF and NPAG-F have the same optimisation target of user fairness. Clearly LTTN-F is a better option than LRTN-F, just as LTTN is better than LRTN; in the next section a comparison between LTTN and LTTN-F is considered.

7.3 Performance Comparison between LTTN and LTTN-F

Figure 7.17 shows the comparison between LTTN and LTTN-F plotted in two different ways – against throughput and against power. It is clear from these plots that the two variants are doing exactly what they are designed to:

- LTTN gives improved performance in terms of needing less power for the same throughput, or indeed for achieving higher throughputs than can be obtained with LTTN-F. This is because the NPAG algorithm is optimised for throughput.

- LTTN-F gives much higher fairness index since NPAG-F is optimised for fairness.

This demonstrates that the dominant factor in the algorithms is the NPAG – by choosing the criteria for the game, the overall algorithm can be optimised for those criteria.

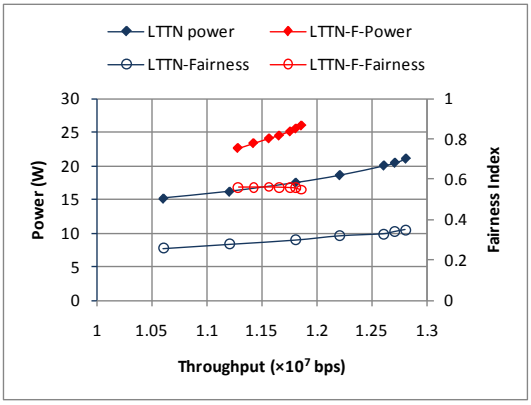

a) Comparison of power and fairness *vs.* throughput

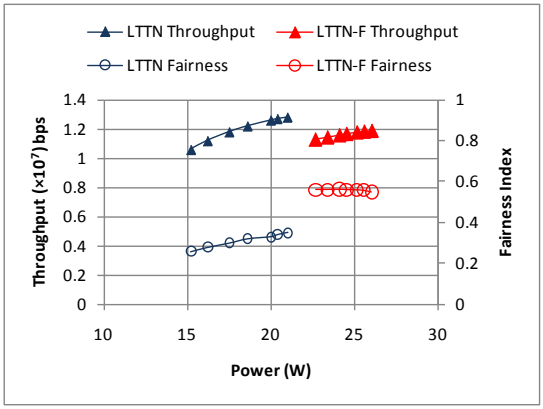

b) Comparison of throughput and fairness *vs.* power

Figure 7.17 Comparison between LTTN and LTTN-F

7.4 Summary

In this chapter, the performance of the combination of all algorithms proposed for radio resource allocation in this thesis is analysed, including relay selection algorithm, subchannel allocation algorithm, and power allocation algorithm. The optimization objects for these algorithms are maximising the system throughput, increasing the user fairness and improving the energy efficiency.

It is quite clear that the LTTN and LTTN-F versions outperform their competitors and that the choice of NPAG or NPAG-F allows the network designer the choice of maximising throughput (or minimizing power) or maximising user fairness. It should be noted that the use of LTTN allows very significant (>50%) reduction in transmission power.

Chapter 8 Conclusions and Future work

This thesis describes research on radio resource allocation schemes in relay based OFDMA cellular networks; the aim of this resource management is to improve the system throughput, user fairness and energy efficiency.

The overall conclusion is that significant power saving can be achieved without affecting capacity but at expense of fairness; fairness can also be improved but this requires more power. By providing different algorithms that are designed for different optimization objects, a "tool box" of approaches is provided so the designer or operator can choose how to optimize the network.

However, a fundamental principle is that matching the data rates on the two hops, improves system power consumption fairness so should always be implemented.

8.1 Specific conclusions

Specific outcomes that have resulted from the work of the author and are reported in this thesis are:

- A two-hop proportional fairness (THPF) algorithm that solves the fair subchannel allocation between direct link users and relay link users. The fairness seen by relay link users and by direct link users is considered, giving a good tradeoff between system throughput and user fairness.
- A load based relay selection (LBRS) algorithm that considers the traffic load of relay link users and direct link users for long-term user fairness. The results reported here show that the LBRS algorithm can achieve better fairness than the traditional relay selection algorithm in typical traffic load distribution scenarios.
- A two-hop power allocation (THPA) algorithm that offers large energy savings by adaptively adjusting the transmission power of the BS and RSs to make the data rate on the two hop links of one RS match each other and

reduce the total transmission power of BS and RSs. The power saving can be of the order of 30%.

- A multi-cell power allocation approach based on game theory that considers co-channel interference. This is designed for throughput improvement and the simulation results show that the system throughput is improved and transmission power is reduced compared with equal power allocation. For the NPAG-F algorithm, if user fairness is chosen as the optimisation target it is shown that the fairness is improved greatly (over that with equal power allocation) with only a small impact on system throughput.
- An assessment of combining the different techniques that show how the network designer can use a combination that is optimized for either throughput or fairness – and with the throughput version, power savings of around 50% are achievable.

8.2 Future work

In this thesis the focus has been on RRM for relay based OFDMA networks and one aspect that has been established is that appropriate techniques can significantly reduce the energy consumption of the wireless part of the network while maintaining acceptable performance for users.

Future work can be done to extend this work in the following aspects:

- All the algorithms can be modified and applied to the non-transparent frame structure.
- The algorithms can be extended to suburban and rural scenarios .
- RRM for different QoS service catgories can be considered as an extension.

Meanwhile, there are other techniques that can improve the performance seen by users, particularly those at the cell edge. One such technique is cooperative relay [85] and another line of approach for further work could be on applying the *principles* of

the methods of relay selection, power allocation and channel selection to cooperative relay networks. In particular, there has been no published work focusing on energy efficiency in cooperative relay networks so this is an area where there is significant potential.

References

[1] W. Xiaodong. "OFDM and its application to 4G," in *Wireless and Optical Communications, 2005. 14th Annual WOCC 2005. International Conference on*, 2005, pp. 69.

[2] A. Kaye, D. George, and M. Eric. "Analysis and Compensation of Bandpass Nonlinearities for Communications," *IEEE Transactions on Communications*, vol. 20, pp. 965-972, Oct. 1972.

[3] IEEE C802.16x-07. "Integrated Relay Architecture for IEEE 802.16m Systems," Nov. 12, 2007.

[4] I. F. Akyildiz and W. Xudong. "A survey on wireless mesh networks," *Communications Magazine, IEEE*, vol. 43, pp. S23-S30, 2005.

[5] Yin and S. Alamouti. "OFDMA: A Broadband Wireless Access Technology," *in Sarnoff Symposium, IEEE*, 2006, pp. 1-4.

[6] F. Kelly. "Charging and rate control for elastic traffic," E*uropean Transactions on Telecommunications*, vol. 8, pp. 33-37, Jan.1997.

[7] R. Pabst, B. H. Walke, D. C. Schultz, P. Herhold, H. Yanikomeroglu, S. Mukherjee, H. Viswanathan, M. Lott, W. Zirwas, M. Dohler, H. Aghvami, D. D. Falconer, and G. P. Fettweis. "Relay-based deployment concepts for wireless and mobile broadband radio," *Communications Magazine, IEEE*, vol. 42, pp. 80-89, 2004.

[8] Xue Jun Li, Boon-Chong Seet, and Peter Han Joo Chong. "Multihop cellular networks: Technology and economics," *Computer Networks,* Vol. 52, pp. 1825-1837, Jun. 2008.

[9] Jerry Sydir. "IEEE 802.16j-06/015: Harmonized Contribution on 802.16j (Mobile Multihop Relay) Usage Models, " Sep. 2006.

[10] Y. Wang, X. Qu, T. Wu, and B. Liu. "Power Allocation and Subcarrier Pairing Algorithm for Regenerative OFDM Relay System," *in Vehicular Technology Conference, 2007. VTC2007-Spring. IEEE*, 2007, pp. 2727-2731.

[11] K.J.Ray Liu, Ahmed K.Sadek, Weifeng Su and Andres Kwasinski. *Cooperative communications and networking*. Cambridge: Cambridge University Press, 2009, pp. 122-126.

[12] V. Genc, S. Murphy, Y. Yang, and J. Murphy. "IEEE 802.16J relay-based wireless access networks: an overview," *Wireless Communications, IEEE,* vol. 15, pp. 56-63, 2008.

[13] Abdulkareem Adinoyi, Lars Berlemann, John Boyer, etc. "IST-2003-507581 WINNER D3.2: Description of identified new relay based radio network deployment concepts and first assessment by comparison against benchmarks of well known deployment concepts using enhanced radio interface technologies. " Internet: www.ist-winner.org, Feb. 2005.

[14] IEEE 802.16's Relay Task Group, Internet: http://wirelessman.org/relay, web date [Dec. 4.2009].

[15] Wireless World Initiative New Radio (WINNER), Internet: www.ist-winner.org, [Sep. 10.2009].

[16] Hui Liu and Guoqing Li. *OFDM-Based Broadband Wireless Networks: Design and Optimization*. Hoboken, New Jersey: John Wiley & Sons, 2005, pp. 13-29.

[17] R.R Moisier and R.G. Clabaugh. "Kineplex, a bandwidth-efficient binary transmission system," *AIEE Transactions*. vol. 76, pp. 723-728, Jan.1958.

[18] R. Chang and R. Gibby. "A Theoretical Study of Performance of an Orthogonal Multiplexing Data Transmission Scheme," *Communication Technology, IEEE Transactions on*, vol. 16, pp. 529-540, Aug. 1968.

[19] Chang Robert W. "Orthogonal Frequency Multiplex Data Transmission System," US Patent Publication number: 3488445. Jan. 1970.

[20] S.B. Weinstein, and P.M.Ebert, "Data transmission by frequency division multiplexing using the discrete Fourier transform," *Communications, IEEE Transactions on*, Vol.COM-19, pp. 628-634, Oct. 1971.

[21] Hirosaki B. "An orthogonally multiplexed QAM System Using Discrete Fourier Transform," *Communications, IEEE Transactions on* vol. COM-29, pp. 982-989, Jul. 1981.

[22] ETS 300 401, "Digital audio broadcasting (DAB); DAB to mobile, portable and fixed receivers," Internet: http://portal.etsi.org/broadcast/dab.asp, Feb, 1995.

[23] Peled A, Ruiz A. "Frequency domain data transmission using reduced computational complexity algorithms," in *Proceeding ICASSP*, 1980: pp.964-967.

[24] Harri Holma, Antti Toskala. *LTE for UMTS - OFDMA and SC-FDMA Based Radio Access*. UK: John Wiley & Sons Ltd, 2009, pp 69-71.

[25] J. Jiho and L. Kwang Bok, "Transmit power adaptation for multiuser OFDM systems," in *Selected Areas in Communications, IEEE Journal on*, vol. 21, pp. 171-178, 2003.

[26] A. J. Goldsmith and C. Soon-Ghee, "Variable-rate variable-power MQAM for fading channels," *Communications, IEEE Transactions on,* vol. 45, pp. 1218-1230, 1997.

[27] IEEE 802.16j-06/026r4, "Baseline Document for Draft Standard for Local and Metropolitan Area Networks part 16: Air Interface for Fixed and Mobile Broadband Wireless Access Systems – Multihop Relay Specification, " Jun. 2007.

[28] IEEE Draft Std P802.16j "Draft Standard for Local and Metropolitan Area Networks--Part 16: Air Interface for Fixed and Mobile Broadband Wireless Access Systems-Multihop Relay Specification," Aug. 2007.

[29] P. Won-Hyoung and B. Saewoong, "WLC25-3: Resource Management Policies for Fixed Relays in Cellular Networks," in *Global Telecommunications Conference, 2006. GLOBECOM '06. IEEE*, 2006, pp. 1-5.

[30] IEEE 80216j-06_013r3, "Multi-hop Relay System Evaluation Methodology (Channel Model and Performance Metric)," Feb. 2007.

[31] 3GPP R1-050676. "Text Proposal: Simulation Assumptions and Evaluation for EUTRA, " June, 2005.

[32] 3GPP R1-050623. "Text proposal: Principles for the Evolved UTRA, " June 2005.

[33] 3GPP2 CR1002 V1.0. "CDMA2000 Evaluation Methodology, " December 2004.

[34] L. Jemin, P. Sungsoo, W. Hano, and H. Daesik, "QoS-guaranteed Transmission Scheme Selection for OFDMA Multi-hop Cellular Networks," in *Communications, 2007. ICC '07. IEEE International Conference on,* 2007, pp. 4587-4591.

[35] K. Doppler, H. Xiaoben, C. Wijting, and A. Sorri, "Adaptive Soft Reuse for Relay Enhanced Cells," in *Vehicular Technology Conference, 2007. VTC2007-Spring. IEEE* 65th, 2007, pp. 758-762.

[36] H. Lei, R. Mengtian, W. Lan, X. Yisheng, and E. Schulz, "Resource Scheduling for OFDMA/TDD Based Relay Enhanced Cellular Networks," *in Wireless Communications and Networking Conference, 2007.WCNC 2007. IEEE*, 2007, pp. 1544-1548.

[37] IEEE 802.16.3c-01/29r4, "Channel Models for Fixed Wireless Applications." July, 2001.

[38] 3GPP R1-091320, “Radio Characteristics of the ITU Test Environments and Deployment Scenarios.” March, 2009.

[39] S. A. AlQahtani and A. S. Mahmoud. "Dynamic radio resource allocation for 3G and beyond mobile wireless networks," *Computer Communications*, vol. 30, pp.41-51, 2006.

[40] V. Sreng, H. Yanikomeroglu, and D. D. Falconer, "Relayer selection strategies in cellular networks with peer-to-peer relaying," i*n Vehicular Technology Conference, 2003. VTC 2003-Fall. 2003 IEEE 58th,* 2003, pp. 1949-1953.

[41] IEEE C802.16e -04/152, "Time first vs. Frequency first allocations in OFDMA mode," Jun. 2004.

[42] Mohsen Guizani. *Wireless communications systems and networks*, New York: Springer, 2004, pp.102.

[43] Mischa Schwartz, *Mobile wireless communications*, Cambridge: Cambridge University Press, 2005, pp. 21.

[44] Sanam Sadr, Alagan Anpalagan, and Kaamran Raahemifar, "Suboptimal Rate Adaptive Resource Allocation for Downlink OFDMA Systems," *International Journal of Vehicular Technology*, vol. 2009, pp. 10, 2009.

[45] L. Venturino, N. Prasad, and W. Xiaodong, "Coordinated Scheduling and Power Allocation in Downlink Multicell OFDMA Networks," *Vehicular Technology, IEEE Transactions on,* vol. 58, pp. 2835-2848, 2009.

[46] Z. Tiankui, Z. Zhimin, F. Chunyan, C. Jie, and S. Lianbo, "Uplink power allocation for interference coordination in multi-cell OFDM systems," in *Communications and Networking in China, 2008*, pp. 716-720.

[47] Z. Dawy, S. Davidovic, and I. Oikonomidis. "Coverage and capacity enhancement of CDMA cellular systems via multihop transmission," in *Global Telecommunications Conference, IEEE*, 2003, pp. 1147-1151.

[48] V. Sreng, H. Yanikomeroglu, and D. Falconer. "Coverage enhancement through two-hop relaying in cellular radio systems," in *Wireless Communications and Networking Conference. WCNC2002. IEEE*, 2002, pp. 881-885.

[49] A. A. N. A. Kusuma and L. L. H. Andrew. "Minimum power routing for multihop cellular networks," in *Global Telecommunications Conference, 2002. IEEE*, 2002, pp. 37-41.

[50] T. Rouse, S. McLaughlin, and I. Band. "Congestion-based routing strategies in multihop TDD-CDMA networks," *Selected Areas in Communications, IEEE Journal on*, vol. 23, pp. 668-681, 2005.

[51] I. Krikidis and J. C. Belfiore. "Three Scheduling Schemes for Amplify-and-Forward Relay Environments," *Communications Letters, IEEE*, vol. 11, pp. 414-416, 2007.

[52] N. Truman Chiu-Yam and Y. Wei. "Joint optimization of relay strategies and resource allocations in cooperative cellular networks," *Selected Areas in Communications, IEEE Journal on*, vol. 25, pp. 328-339, 2007.

[53] Y. N. Yao-Nan Lee, J. C. Jung-Chieh Chen, Y. C. Yeong-Cheng Wang, and J. T. Jiunn-Tsair Chen. "A Novel Distributed Scheduling Algorithm for Downlink Relay Networks," *Wireless Communications, IEEE Transactions o*n, vol. 6, pp. 1985-1991, 2007.

[54] I. Hammerstrom, M. Kuhn, and A. Wittneben. "Channel adaptive scheduling for cooperative relay networks," in *Vehicular Technology Conference, 2004. VTC2004-Fall. IEEE 60th, 2004*, pp. 2784-2788.

[55] Y. Liu, R. Hoshyar, X. Yang, and R. Tafazolli. "Integrated Radio Resource Allocation for Multihop Cellular Networks With Fixed Relay Stations," *Selected Areas in Communications, IEEE Journal on, vol. 24*, pp. 2137-2146, 2006.

[56] L. Xin, E. K. P. Chong, and N. B. Shroff. "Optimal opportunistic scheduling in wireless networks," i*n Vehicular Technology Conference, 2003. VTC 2003-Fall. IEEE 58th, 2003*, pp. 1417-1421.

[57] K. Hoon and H. Youngnam. "An Opportunistic Channel Quality Feedback Scheme for Proportional Fair Scheduling," *Communications Letters, IEEE*, vol. 11, pp. 501-503, Jun. 2007.

[58] M. HU, J.S. Zhang, "Opportunistic Multi-Access: Multiuser Diversity, Relay-Aided Opportunistic Scheduling," *Mobile Networks and Applications,* Volume 9, pp. 435–444, Nov. 2004.

[59] G. Li, and H. Liu, "Resource Allocation for OFDMA Relay Networks With Fairness Constraints," *Selected Areas in communications, IEEE Journal on*, vol. 24, pp. 2061-2069, Nov.2006.

[60] B. Chisung, and C. Dong-Ho, "Fairness-Aware Adaptive Resource Allocation Scheme in Multihop OFDMA Systems," *Communications Letters, IEEE, vol. 11*, pp. 134-136, Feb. 2007.

[61] M. O. Hasna and M. S. Alouini, "Optimal power allocation for relayed transmissions over Rayleigh-fading channels," *Wireless Communications, IEEE Transactions on*, vol. 3, pp. 1999-2004, Nov. 2004.

[62] Q. Zhang, J. Zhang, C. Shao, Y. Wang, P. Zhang, and R. Hu, "Power allocation for regenerative relay channel with Rayleigh fading," in *Vehicular Technology Conference, VTC 2004-Spring. 2004 IEEE 59th*, 2004, pp. 1167-1171 Vol.2.

[63] J. Zhang, Q. Zhang, C. Shao, Y. Wang, P. Zhang, and Z. Zhang, "Adaptive optimal transmit power allocation for two-hop non-regenerative wireless relaying system," in *Vehicular Technology Conference, 2004. VTC 2004-Spring. 2004 IEEE 59th*, 2004, pp. 1213-1217 Vol.2.

[64] G.-D. Yu, Z.-Y. Zhang, Y. Chen, S. Chen, and P.-l. Qiu, "Power allocation for non-regenerative OFDM relaying channels," in *Wireless Communications, Networking and Mobile Computing, 2005. Proceedings. 2005 International Conference on,* 2005, pp. 185-188.

[65] I. Hammerstrom and A. Wittneben, "On the Optimal Power Allocation for Nonregenerative OFDM Relay Links," in *Communications, 2006. ICC '06. IEEE International Conference on*, 2006, pp. 4463-4468.

[66] J. Hee-jin and M. Cheol, "Capacity of Multiuser Diversity with Cooperative Relaying in Wireless Networks," *Communications Letters, IEEE,* vol. 12, pp. 752-754, 2008.

[67] Lin Xiao, Laurie Cuthbert. "Improving fairness in relay-based access networks," in *ACM MSWIM 2008*, Nov. 2008, pp. 18-22.

[68] J. Eatwell, M. Milgate, and P. Newman, Macmillan. "Game Theory," in *The New Palgrave, A Dictionary of Economics*, Vol 2, London and Basingstoke: Palgrave Macmillan, 1987, pp. 460-482.

[69] John von Neumann, and Oskar Morgenstern. *Theory of Games and Economic Behavior*. Princeton University Press, 1944.

[70] A.Alcaide, J.M.Estevez-Tapiador, J.C.Hernandez Castro, and A.Ribagorda. "An extended model of rational exchange based on dynamic games of imperfect information," *Emerging Trends in Information and Communication Security*, Vol.3995, pp.396-408, June, 2006.

[71] A.Alcaide, J.M.Estevez-Tapiador, J.C.Hernandez Castro, and A.Ribagorda. "Bayesian rational exchange," *International Journal of Information Security*. Volume 7, pp. 85-100, Sep. 2008.

[72] E.Palomar, A.Alcaide, J.M.Estevez-Tapiador, J.C.Hernandez Castro. "Bayesian analysis of secure P2P sharing protocols," *Proceeding of the Information Security Workshop*, LNCS, vol.4805, pp. 1701-1717, Nov. 2007.

[73] A.B.MacKenzie, L.Dasilva, and W.Tranter. *Game Theory for Wireless Engineers*. San Rafael, CA: Morgan and Claypool Publishers, 2006.

[74] E.Altman, T.Boulogne, R.EI Azouzi, T. Jimenez, and L.Wyneter. "A survey on networking games in telecommunications," *Computer and Operations Research*, Volume 33, pp.286-311, Feb.2006.

[75] L.Buttyan and J.P. Hubaux. *Security and Cooperation in Wireless Networks*. Cambridge, U.K: Cambridge University Press, 2007.

[76] M.Felegyhazi and J.P. Hubaux. "Game theory in wireless networks: A tutorial," in *EPFL technical report: LCA-REPORT-2006-002*, Feb. 2006.

[77] Klaus Ritzberger. *Foundations of non-cooperative game theory*. New York, USA: Oxford university press, 2002, pp. 7.

[78] D. Goodman and N. Mandayam. "Power control for wireless data," *Personal Communications, IEEE*, vol. 7, pp. 48-54, Apr. 2000.

[79] Saraydar C U, Mandayam N, Goodman D. Efficient Power Control via Pricing in Wireless Data Networks. *Communications, IEEE Transactions on*, Vol. 50, pp. 291-303, 2002.

[80] K. Hojoong and L. Byeong Gi, "Distributed Resource Allocation through Noncooperative Game Approach in Multi-cell OFDMA Systems," in *Communications, 2006. IEEE International Conference on*, 2006, pp. 4345-4350.

[81] Y. Xinmin, W. Tong, H. Jing, and W. Ying, "A Non-Cooperative Game Approach for Distributed Power Allocation in Multi-Cell OFDMA-Relay Networks," in *Vehicular Technology Conference, 2008. IEEE*, 2008, pp. 1920-1924.

[82] Kiyosi Ito, *Encyclopedic Dictionary of Mathematics: The Mathematical Society of Japan*, Second edition, Publisher: The MIT Press, Cambridge, USA, 1993, pp. 331, pp. 1614.

[83] Akira Takayama, *Mathematical economics, Second edition*, Cambridge, UK: Cambridge University Press, 1985, pp. 113.

[84] 3GPP R1-061487. "Uplink Interference Mitigation via Power Control," May. 2006.

[85] IEEE C80216j-06_006r1, "Cooperative Relay in IEEE 802.16j MMR)," May. 2006.